NATIONAL COOPERATIVE
HIGHWAY RESEARCH PROGRAM REPORT 242

ULTRASONIC MEASUREMENT OF WELD FLAW SIZE

TRANSPORTATION RESEARCH BOARD
NATIONAL RESEARCH COUNCIL

NATIONAL COOPERATIVE HIGHWAY RESEARCH PROGRAM
REPORT 242

ULTRASONIC MEASUREMENT OF WELD FLAW SIZE

T. J. JESSOP, P. J. MUDGE, AND
J. D. HARRISON
The Welding Institute
Cambridge, England

RESEARCH SPONSORED BY THE AMERICAN ASSOCIATION OF STATE HIGHWAY AND TRANSPORTATION OFFICIALS IN COOPERATION WITH THE FEDERAL HIGHWAY ADMINISTRATION

AREAS OF INTEREST:

STRUCTURES DESIGN AND PERFORMANCE
GENERAL MATERIALS
MAINTENANCE
• (HIGHWAY TRANSPORTATION)
(PUBLIC TRANSIT)
(RAIL TRANSPORTATION)
(AIR TRANSPORTATION)
(OTHER)

TRANSPORTATION RESEARCH BOARD
NATIONAL RESEARCH COUNCIL
WASHINGTON, D.C.
DECEMBER 1981

NATIONAL COOPERATIVE HIGHWAY RESEARCH PROGRAM

Systematic, well-designed research provides the most effective approach to the solution of many problems facing highway administrators and engineers. Often, highway problems are of local interest and can best be studied by highway departments individually or in cooperation with their state universities and others. However, the accelerating growth of highway transportation develops increasingly complex problems of wide interest to highway authorities. These problems are best studied through a coordinated program of cooperative research.

In recognition of these needs, the highway administrators of the American Association of State Highway and Transportation Officials initiated in 1962 an objective national highway research program employing modern scientific techniques. This program is supported on a continuing basis by funds from participating member states of the Association and it receives the full cooperation and support of the Federal Highway Administration, United States Department of Transportation.

The Transportation Research Board of the National Research Council was requested by the Association to administer the research program because of the Board's recognized objectivity and understanding of modern research practices. The Board is uniquely suited for this purpose as: it maintains an extensive committee structure from which authorities on any highway transportation subject may be drawn; it possesses avenues of communications and cooperation with federal, state, and local governmental agencies, universities, and industry; its relationship to its parent organization, the National Academy of Sciences, a private, nonprofit institution, is an insurance of objectivity; it maintains a full-time research correlation staff of specialists in highway transportation matters to bring the findings of research directly to those who are in a position to use them.

The program is developed on the basis of research needs identified by chief administrators of the highway and transportation departments and by committees of AASHTO. Each year, specific areas of research needs to be included in the program are proposed to the Academy and the Board by the American Association of State Highway and Transportation Officials. Research projects to fulfill these needs are defined by the Board, and qualified research agencies are selected from those that have submitted proposals. Administration and surveillance of research contracts are the responsibilities of the Academy and its Transportation Research Board.

The needs for highway research are many, and the National Cooperative Highway Research Program can make significant contributions to the solution of highway transportation problems of mutual concern to many responsible groups. The program, however, is intended to complement rather than to substitute for or duplicate other highway research programs.

NCHRP REPORT 242

Project 10-13 FY '79
ISSN 0077-5614
ISBN 0-309-03302-0
L. C. Catalog Card No. 81-86215
Price: $8.00

NOTICE

Published reports of the

NATIONAL COOPERATIVE HIGHWAY RESEARCH PROGRAM

are available from:

Transportation Research Board
National Academy of Sciences
2101 Constitution Avenue, N.W.
Washington, D.C. 20418

Printed in the United States of America.

FOREWORD

By Staff
Transportation
Research Board

This report contains the findings of an experimental program with the objective of evaluating the applicability and limitations of ultrasonic procedures currently used to characterize weld flaws. The investigation also included other ultrasonic techniques not in general use but having potential application for determining the dimensions of weld flaws. The report contains recommendations for immediate application and suggests additional research that will be required for long-term improvements in current practice.

There is an urgent need for ultrasonic testing procedures that can be used to measure the dimensions of weld discontinuities with sufficient accuracy to permit evaluation using a fracture-mechanics approach. Most State transportation agencies use the provisions of the American Welding Society Structural Welding Code AWS D1.1 to determine the acceptability of structural welds. These provisions are based on an assumed relationship between the ultrasonic "Indication Rating" and flaw size. Experience has indicated that this relationship may not be valid. Research is needed to advance ultrasonic testing procedures, using equipment presently available, that will permit accurate measurement of the dimensions of flaws common to weldments. These procedures are needed for use in both shop and field inspection of weldments to determine acceptance during construction and for in-service evaluation. Reliable procedures for ultrasonic testing would obviate the costs and delays of unnecessary repairs and reduce the probability that defects that may lead to structural failures will be improperly evaluated.

The objective of NCHRP Project 10-13, "Ultrasonic Measurement of Weld Flaw Size," was to identify or develop, and to validate, ultrasonic testing procedures for accurate measurement of flaw dimensions that will allow fracture-mechanics analysis.

This study was addressed primarily to evaluation of complete joint penetration groove welds containing such planar-type flaws as cracks, incomplete fusion, or incomplete penetration. The investigation also included some consideration of slag inclusions.

An experimental program was carried out on specimens containing a representative spectrum of defects having various dimensions, locations, and orientations. It was shown that AWS D1.1 ultrasonic testing procedures cannot be used to reliably characterize weld defects. Other currently available techniques were investigated, and recommendations for immediate and long-term improvements are included in the report.

A follow-up phase of research is expected to be initiated, in mid-1982, with the objectives of (1) developing recommendations for application of tandem-probe techniques for the characterization of vertical, planar defects and (2) refining the time-of-flight system for sizing through-thickness flaw dimensions.

CONTENTS

ACKNOWLEDGMENTS

The research reported herein was performed under NCHRP Project 10-13 by the Welding Institute, Cambridge, England.

Timothy J. Jessop, Head of Non-Destructive Testing (NDT) Research in the Institute's Engineering Department, was the principal investigator although, during his 16-month absence from the project, John D. Harrison, Head of Engineering Department, acted as principal investigator. Peter J. Mudge, who took over as Head of NDT Research during Mr. Jessop's absence, was responsible for organizing the experimental work during that period under Dr. Harrison's guidance.

Reay Gibson, a Senior Technician in the NDT Research Section, conducted most of the experimental work. Robert B. Floyd, who has since left the Institute, contributed to the early part of the project. John Haugh, Deputy Welding Supervisor in the Institute's Arc Welding Department, was responsible for the manufacture of the welded specimens. Messrs Hayward, Lank, Dobbs and Dargue of The Welding Institute and Mr. Ross of Non-Destructive Testers Limited, England, also assisted with the experimental work.

Sincerest thanks are extended to the American Welding Society for permission to use portions of the Structural Welding Code D1.1-80.

ULTRASONIC MEASUREMENT OF WELD FLAW SIZE

SUMMARY

The research conducted under NCHRP Project 10–13 showed that several invalid assumptions are made in the AWS D1.1 Code which have contributed to the generally unreliable nature of the predictions. There was a tendency for small slag lines to be rejected (requiring repair), whereas more severe defects, such as cracks, were accepted on some occasions. Also, disagreement on acceptance or rejection was often found when different qualified operators were used. However, detection capability appeared to be adequate and a slight variation in equipment had little effect on the results.

The probe movement and time-of-flight techniques for defect through-thickness size measurement were subject to errors, although the time-of-flight tests gave significantly better results. These errors were such that in the case of probe movement up to 0.31 in. (7.9 mm) may have to be added to the measured size in order to be 95 percent sure that the actual flaw size did not exceed the measured value. For the time-of-flight technique the figure was 0.17 in. (4.3 mm). Operator variability increased the errors marginally for the probe movement tests only.

Because of the simplicity of the equipment employed, difficulty was experienced in interpreting the time-of-flight display in some cases. Modifications to the equipment would have to be made to ensure reliable interpretation.

CHAPTER ONE

INTRODUCTION AND RESEARCH APPROACH

PROBLEM STATEMENT

To ensure the integrity of steel highway bridges there is an urgent need for ultrasonic testing procedures that can be used to measure the dimensions of weld discontinuities (flaws) with sufficient accuracy to permit evaluation using a fracture mechanics approach. Most state transportation agencies use the provisions of the American Welding Society Structural Welding Code AWS D.1. *(1)*, referred to hereafter as the Code, to determine the acceptability of such structural welds. These provisions are based on an assumed relationship between the ultrasonic "Indication Rating" and flaw size. Experience indicates that this relationship may not be valid. Research is needed to advance or develop ultrasonic testing procedures, using equipment presently available, that will permit accurate measurement of the dimensions of flaws common to weldments. These procedures are needed for use in both shop and field inspection of weldments to determine acceptance during construction and for in-service evaluation. Reliable procedures for ultrasonic testing will obviate the costs and delays of unnecessary repairs while reducing the possibility of defects, which, being improperly evaluated, may lead to structural failure.

RESEARCH OBJECTIVE AND SCOPE OF PROJECT

The objectives of this study are (1) to quantify the defect assessment performance of the AWS D1.1 procedures and (2) to identify or develop, and to validate, ultrasonic testing procedures that will give the dimensions of flaws with sufficient accuracy to allow them to be analyzed by fracture mechanics.

The tasks necessary to accomplish the objectives include the following:

- Task 1. Undertake a literature survey and use information found where appropriate.
- Task 2. Evaluate the applicability and limitations of AWS D1.1-80 ultrasonic testing procedures for determining the dimensions of flaws in welds. (The AWS D1.1-80 code, effective from January 1, 1980, was used as the source document for this work. It is recognized that this is now superseded by D1.1-81, effective from January 1, 1981, in which detail has been changed.)
- Task 3. Develop procedures that expand or extend available ultrasonic techniques and have a potential for accurate measurements of flaws typically found in structural weldments.
- Task 4. Evaluate the accuracy, precision, reliability and reproducibility of the techniques.
- Task 5. If successful, prepare written procedures and specifications appropriate for use by state transportation agencies for bridge welds.
- Task 6. Prepare a final report that includes research findings and recommendations for possible additional study.

The literature was continually surveyed during the course of the project and the findings are summarized in Chapter Two. A detailed description and assessment can be found in Appendix B.

The experimental work consisted of manufacturing a set of steel specimens containing defects; testing them using the various ultrasonic techniques and procedures; destructively testing some of them to reveal the true size and nature of the defects; and finally assessing the accuracy of the various techniques by comparing the ultrasonic data with measurements from the destructive tests. At this stage, fabrication defects only have been examined and service defects such as fatigue cracks have not been investigated.

RESEARCH APPROACH

This report seeks to comment on the performance of the AWS Code in relation to butt welds in fracture critical members in steel bridges and presents other nondestructive techniques that can be used in conjunction with fracture mechanics assessments of such members.

Four principal methods of nondestructive evaluation (NDE) are used to detect and assess weld defects: magnetic particle testing, dye penetrant testing, radiography, and ultrasonic testing. Of these, only radiography and ultrasonic testing have the ability to detect embedded defects. Although radiography is useful for detection and length measurement, particularly of volumetric defects (e.g., slag inclusions and porosity), ultrasonic testing is generally considered to be the only method which has the potential ability to detect and assess all defect types with sufficient accuracy to interface with a fracture mechanics approach to defect acceptance. This work is concerned with realizing this potential.

Figure 1 shows the essential elements of an ultrasonic test. A beam of energy in the form of pulses of mechanical vibrations (usually in the 2 to 6 MHz frequency range) is launched into the testpiece by means of a piezoelectric transducer. When this beam strikes a boundary, reflection takes place and the reflected beam can be detected by the same, or in some cases a separate, transducer. The nature and size of the returning signal are governed by the nature of the reflector. The electrical pulses to drive the transducer and means of amplifying and displaying the returned signal are provided by a flaw detector set. Figure 2 shows a typical manual ultrasonic test being performed. It should be borne in mind that the foregoing is a very simplistic description: a more comprehensive overview is included in Appendix A.

It is not difficult to appreciate that problems are likely to be encountered in establishing accurate details of embedded flaws from indirect information supplied in the form of reflected ultrasonic pulses. The factors influencing signal parameters are many and varied. First, the performance of the transducer generating the ultrasound is critical if a signal of adequate strength, smooth pulse shape, and uniform energy distribution is to be generated. Furthermore, transducer dimensions control beam characteristics (e.g., size and divergence *(2)*) and variation in contact between the probe and a rough surface can modify beam characteristics *(3)*. Second, the morphology of the flaw, size, overall shape, overall complexity, surface roughness, orientation, and distance from the transducer greatly affect its response. Third, metallurgical effects, especially in complex areas such as weldments, can influence propagation of the ultrasound *(4)*.

The vast majority of ultrasonic tests are conducted manually with relatively simple equipment, so it is not possible to consider these many interrelated variables. Simplifying assumptions are made in order to be able to perform a test (more details are given in Appendix A), which therefore cannot fully account for these effects. The emphasis of current research *(5, 6, 7, 8)* is to quantify the result of such assumptions to establish what errors are likely to occur as a result.

All ultrasonic defect assessment techniques are affected to some degree by the foregoing considerations. Nevertheless, it is possible to reduce measurement errors by choice of a suitable test method.

Specimens

The steel material employed conformed to ASTM A36 (a typical structural grade steel) in thicknesses of ⅜ in. (10 mm), 1½ in. (40 mm) and 3¾ in. (95 mm).

The specimens were produced in one of two ways: using conventional fusion welding processes with bevelled joint preparations and relying on the skill of the welder to introduce the defects desired in a controlled manner; or by the diffusion bonding technique for producing embedded defects of accuately known size.

The following defects were included in the fusion welded specimens: 15 weld metal cracks, approximately 2 in. (50 mm)) long (2c dimension), ranging from ⅛ to ¾ in. (3 to 18 mm) in through-thickness (2a dimension); 13 incomplete fusion defects, all approximately 2 in. (50 mm) long and ranging from 1/16 to 5/16 in. (1.5 to 8 mm) in through-thickness; and 7 slag lines all approximately 2 in. (50 mm) long by ⅛ in (3 mm) in through-thickness. In principle, slag is introduced by inadequate interrun cleaning, incomplete fusion by very low heat input techniques and cracking by either encouraging centerline shrinkage (solidification cracking) or by inducing a brittle fracture through a partially completed weld (referred to as freeze-break cracking). The fusion welded specimens were designed to be similar in all respects to welds found in steel bridges. From previous work *(4)* it can be assumed that

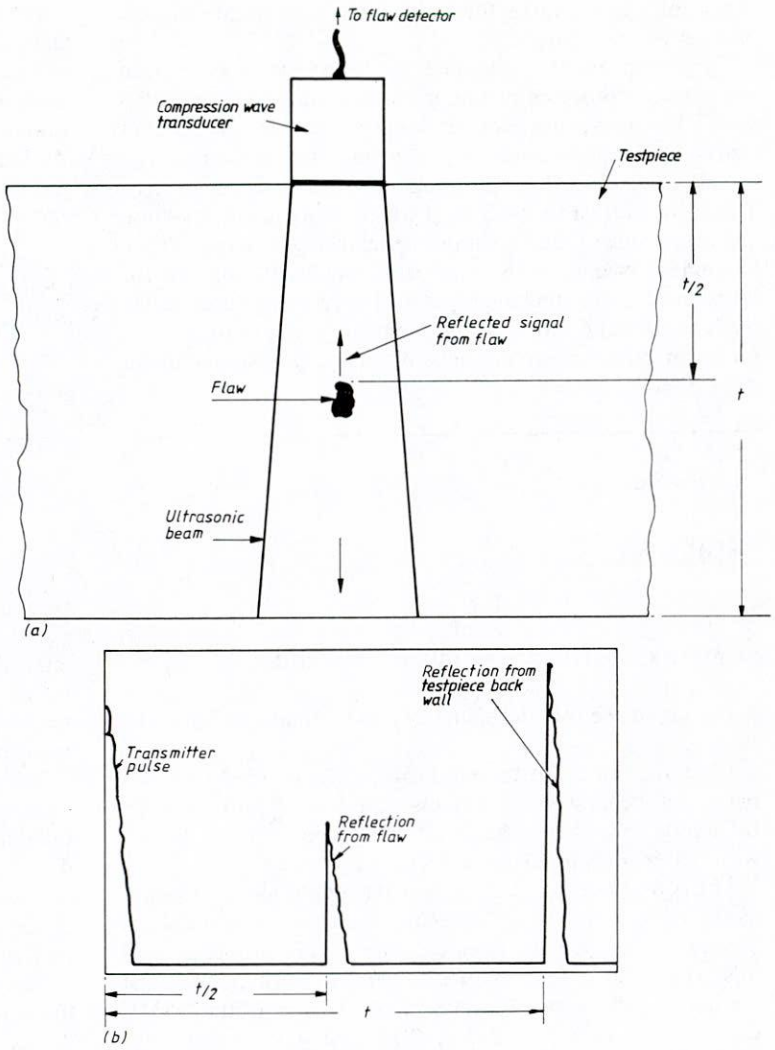

Figure 1. Elements of an ultrasonic test; (a) transducer on testpiece, and (b) CRT display on flaw detector.

different materials (within the ferritic steel range commonly used for bridges) and welding processes (except electroslag welding) would not affect the findings presented in this report.

The diffusion bonding specimens contained eight planar embedded recesses (i.e. of minimal width), all 1-3/16 in. (30 mm) long, ranging from ⅛ to ½ in. (3 to 12 mm) in through-thickness, and at various orientations.

Full details of all the specimens and their manufacture can be found in Appendix C.

Ultrasonic Tests

In the evaluation of AWS D1.1, equipment, calibration, and procedures were all as required by the Code and experimental work was conducted to assess the capability of defect detection and the suitability of the accept/reject levels. In these tests, termed "laboratory" tests, control was exercised over transducer scanning and operator variables. The effects of equipment and operator variability were assessed

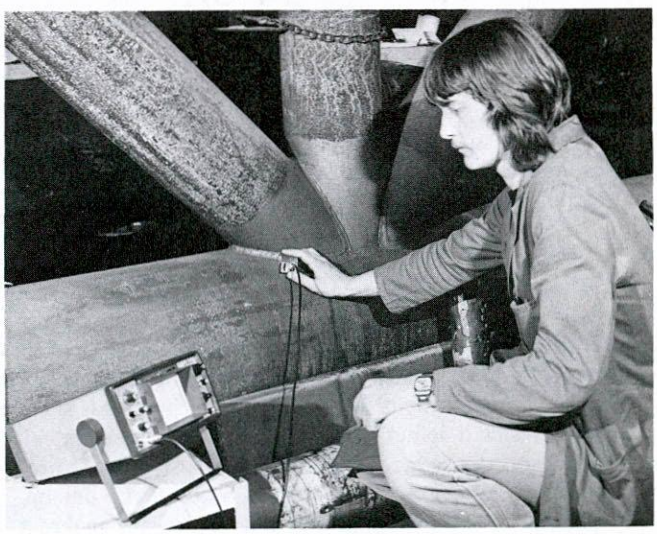

Figure 2. Manual ultrasonic test.

separately. In all cases the procedures appropriate to new bridges were employed.

Two "improved" techniques for defect sizing have been evaluated: "probe movement" and "time-of-flight analysis." The former uses conventional equipment, and a defect size is determined from the way the amplitude of the received signal rises and falls as the ultrasonic beam passes over it. This is in contrast to AWS D1.1 which uses only the position and magnitude of the maximum signal from the defect. Probe movement is commonly used in the United Kingdom for defect measurements being specified in reference documents *(9, 10)* and standards *(11)* and included in the requirements for certification of weld inspectors using ultrasonics under the CSWIP scheme *(9)*.

The time-of-flight technique uses time, rather than amplitude, data and more specialized equipment is necessary to measure the arrival times of signals received from the defect extremities. The accuracy of the technique has been demonstrated previously using essentially laboratory equipment *(5)*. In the current work a simplified version, suitable for shop and site uses, was evaluated.

Both techniques were evaluated with respect to the accuracy with which they could measure defects using controlled, laboratory tests. The effect of operator variability was also assessed.

Full details of the ultrasonic equipment and personnel are given in Appendix D.

CHAPTER TWO

FINDINGS

SUMMARY OF LITERATURE SURVEY FINDINGS

Details of the literature survey can be found in Appendix B.

Literature relevant to this project was divided into two parts: that dealing with problems experienced with the AWS D1.1 code and other codes of a similar type; and that dealing with better techniques for defect assessment.

The AWS code is not alone in using amplitude of response as the main criterion for assessing the severity of a defect. Several instances have been reported where problems with this type of code have been experienced. Perhaps the most glaring example was a round-robin evaluation of the ASME Code *(12)* for ultrasonic testing conducted under the auspices of the PVRC in the United States *(13)* and of the plate inspection steering committee (PISC) in Europe *(6)*. Very large defects were reported in some cases as being acceptable simply because the orientation of the defect was such that only a small response was obtained. As a result of this exercise, the ASME Code Section XI (Inservice Inspection of Nuclear Components) now contains a form of probe movement sizing. A second PISC exercise is now in the planning stage.

Other examples of this sort of problem have been given in papers evaluating AWS procedures *(14)* and in ones comparing results from tests carried out to AWS procedures with those from other test procedures (notably ASME) *(15)*. The inapplicability of an amplitude method, for example, *(16)*, for defect size measurement has been demonstrated *(5)*.

The poor reliability of using signal amplitude as the main arbiter of defect size or "severity" is recognized in many quarters and probe movement sizing techniques seek to overcome this difficulty. However, although amplitude is not used as the basis for the probe movement technique as such, the way in which a defect's shape influences the rise and fall of a signal as a transducer is traversed across it has a profound effect on accuracy. Studies *(5, 8, 17)* have demonstrated that defect size measurement errors are inherent when using such methods and as such they do not offer a panacea for testing inaccuracies. Nevertheless, if these errors can be quantified, a notion of reliability of the tests may be built up from which realistic input data for fracture mechanics calculations may be drawn.

Many more advanced defect assessment methods have been studied on a worldwide basis in an attempt to get more reliable data, but in most cases experimental data have been derived from simple geometric discontinuities rather than real weld flaws (e.g., *(18)*). It should also be noted that some of the techniques studied (e.g. holography *(19)*) would be difficult to apply to shop and site situations.

The ultrasonic sizing techniques chosen for this study were those which appeared to combine an ability to measure real defects with practical applicability. In addition to these the literature search suggests that two additional techniques would be worth evaluating in future studies: (1) the use of electromagnetic-acoustic transducers (EMATs), and (2) signal processing using computer analysis. The former provides a means of generating ultrasound without the use of a piezoelectric-crystal. Oscillation of an AC electrical pulse in a small coil within a magnetic field produces ultrasound at the specimen surface. The coils can be configured to produce different wave modes and beam angles, and no contact with the surface via a coupling layer is required. EMATs are being evaluated for use in the pipeline industry with at least partial success *(20)*. The latter have the advantage that large amounts of data can be simply recorded at the test site and analyzed subsequently off-site. Such equipment is discussed further in subsequent chapters.

EVALUATION OF AWS D1.1-80

Details are included in Appendix E.

Theoretical Considerations

The AWS D1.1 procedures for ultrasonically assessing weld defects are neither suitable nor intended for use in conjunction with fracture mechanics analyses. Like most defect acceptance codes D1.1 is based on a "workmanship"

TABLE 1
ULTRASONIC ACCEPTANCE/REJECTION CRITERIA (TABLE 9.25.3 FROM AWS D1.1-80)

Flaw severity class	Weld thickness and search unit angle										
	5/16 to 3/4	>3/4 to 1-1/2	>1-1/2 to 2-1/2			>2-1/2 to 4			>4 to 8		
	70°	70°	70°	60°	45°	70°	60°	45°	70°	60°	45°
Class A	+10 & lower	+8 & lower	+4 & lower	+7 & lower	+9 & lower	+1 & lower	+4 & lower	+6 & lower	−2 & lower	+1 & lower	+3 & lower
Class B	+11	+9	+5 +6	+8 +9	+10 +11	+2 +3	+5 +6	+7 +8	−1 0	+2 +3	+4 +5
Class C	+12	+10	+7 +8	+10 +11	+12 +13	+4 +5	+7 +8	+9 +10	+1 +2	+4 +5	+6 +7
Class D	+13 & up	+11 & up	+9 & up	+12 & up	+14 & up	+6 & up	+9 & up	+11 & up	+3 & up	+6 & up	+8 & up

Notes:

1. **Class B and C flaws shall be separated by at least 2L, L being the length of the longer flaw, except that when two or more such flaws are not separated by at least 2L, but the combined length of flaws and their separation distance is equal to or less than the maximum allowable length under the provisions of Class B or C, the flaw shall be considered a single acceptable flaw.**
2. **Class B and C flaws shall not begin at a distance less than 2L from the end of the weld, L being the flaw length.**
3. **Flaws detected at "scanning level" in the root face area of complete penetration double groove weld joints shall be evaluated using an indication rating 4 dB more sensitive than that described in 6.19.6.5 when such welds are designated as "tension welds" on the drawing (subtract 4 dB from the indication rating "d").**

Class A (large flaws)
Any indication in this category shall be rejected (regardless of length).

Class B (medium flaws)
Any indication in this category having a length greater than 3/4 inch (19 mm) shall be rejected.

Class C (small flaws)
Any indication in this category having a length greater than 2 in. (51 mm) in the middle half or 3/4 inch (19 mm) length in the top or bottom quarter of weld thickness shall be rejected.

Class D (minor flaws)
Any indication in this category shall be accepted regardless of length or location in the weld.

Scanning levels	
Sound path	Above zero reference, dB
to 2-1/2 (64 mm)	20
> 2-1/2 to 5 (64-127 mm)	25
> 5-10 (127-254 mm)	35
> 10 to 15 (254-381 mm)	45

approach (i.e. a general arbitrary control is kept on the level of quality). It is common practice in workmanship codes to state that planar defects (e.g. cracks and lack of fusion) are not acceptable and that nonplanar defects (e.g. slag inclusions and porosity) are acceptable in small specified quantities. It should be noted that differentiation between these two defect types is readily achieved from radiography, the traditional volumetric inspection method.

The AWS code does not use this approach for ultrasonic testing, but assumes that the defect, irrespective of type, reflects ultrasound in proportion to its effect on the integrity of the weld.

Whether a defect is acceptable or not is determined, first, by establishing its "d" rating based on echo amplitude (obtained by following the procedure laid down in part 6C of the Code), and, second, by referring this value to Table 9.25.3 of the Code (for tension welds in new bridges), as shown in Table 1 of this report. Use of the table permits classification of the defect into Class A (unacceptable under all circumstances), Class D (acceptable under all circumstances), or Classes B and C where defect length is also taken into consideration.

What such classification means in terms of size of defect that is required to be rejected is difficult to determine. Variability of essential parameters from test to test will almost certainly produce the situation whereby the size of defect deemed to be rejectable is not constant, as such variation could change defect response sufficiently to permit different classification. The philosophy behind the AWS Code acceptance criteria is summarized in Figure 3 *(21)* which shows the

accept/reject levels of the Bridge Code Section of AWS D1.1. This depicts the zones in which defects are accepted or rejected on the basis of amplitude of response alone (below and above the hatched zone respectively) and the hatched zone in which acceptability is based on such other factors as length and separation of flaws. These levels are related to the defect through-wall size, expressed as a percentage of the material thickness, which it is assumed will produce a given ultrasonic signal amplitude, depending on angle of incidence, as shown on the left of the figure. The assumed relationship between amplitude, defect percentage through-wall size and increasing material thickness is shown in the figure as a series of diagonal lines. It may be seen that defects of only a very small percentage of the material thickness in through-wall size are expected to be rejected. This very low rejection threshold was derived from the requirement that the ultrasonic testing code should parallel the radiography code in which a sensitivity of 2 percent (of thickness) is required. As can be seen from Figure 3 the ultrasonic code also allows for the fact that achievable radiographic sensitivity (expressed as a % of thickness) tends to increase with increase in thickness.

The process of assessment of a defect by radiography or ultrasonics consists of detection and measurement (or comparison with some standard) to determine whether or not it can be allowed to remain. It would appear logical to specify an ultrasonic procedure that is at least as sensitive as an existing radiographic procedure for detecting defects (i.e. able to detect a defect 2 percent of the wall thickness in through-thickness), and Figure 3 suggests that this is achieved. Nevertheless, there are differences in what the two techniques measure. Radiography gives no information on through-wall extent of defects, and planar (crack or crack-like) defects are less likely to be detected than nonplanar (slag and porosity) defects. Defects are therefore rejected from radiography irrespective of size if they appear crack-like, but whether slag or porosity is rejected depends on its lateral extent.

On the other hand, the assumption that defects reflect ultrasound in proportion to their severity implies an assessment of through-wall size by ultrasonic testing, although very indirectly. There is, however, no requirement for the ultrasonic operator to determine the defect type, acceptance or rejection being solely on amplitude of response with reference to Table 9.25.3 of the Code (see Table 1).

Therefore, slag, porosity, and fusion defects are as likely to be rejected as cracks, which suggests that the ultrasonic flaw rejection criteria are slightly more severe than those of radiography.

To give examples of what the Code sets out to do (referring to Figure 3): for a 0.4-in. (10-mm) thick material, defects greater than 4 percent of the wall, 0.016 in. (0.4 mm) in through-thickness size, would be just rejectable; and for a 3.9-in. (100-mm) thick material, defects smaller than 1 percent of the wall, 0.04 in. (1.0 mm) in through-thickness size, would be just acceptable.

Many theoretically invalid assumptions are made in the formulation of the Code accept/reject levels. The major ones are:

1. Amplitude of response is proportional to defect severity.

2. A unique relationship exists between beam-to-defect orientation and amplitude of response (i.e. if a 90° incidence is equivalent to 0 dB, a 70° incidence would be 6 dB less, a 60° incidence would be 9 dB less, and a 45° incidence would be 11 dB less, see Figure 4).

3. Transducer to defect distance can be allowed for by assuming a 2 dB per inch decay in amplitude after the first inch.

Amplitude of response is often chosen as a parameter worth measuring in an ultrasonic test, but it is important to bear in mind that it is governed by defect type, shape, and orientation; material properties; and transducer-to-workpiece coupling efficiency as well as defect size. Orientation is perhaps the most significant factor when planar defects are involved and, to allow for this, the Code considers that all defects might be in the most serious orientation from a fracture standpoint, which is perpendicular to the direction of stress (in other words, generally a vertically oriented defect), Assumption 2 then comes into play to account for this (since for butt welds it is impossible to get a 90° orientation to a vertical defect, as illustrated in Figure 4). However, the variation of amplitude with orientation is a complex one and heavily dependent on defect size. This is demonstrated in Figure 5, which shows how larger defects exhibit a sharp fall-off in amplitude with misorientation, whereas for smaller defects, the fall-off is more gradual. This effect, which is covered in detail in the literature *(8)*, is not accounted for in the AWS D1.1 Code. The amplitude fall-off rate assumed by the code is more gradual even for the smallest defect (0.21 in. (5 mm)), as shown in Figure 5. The assumption that defects are always vertical will also lead to an overestimation of the severity of defects that are more favorably oriented with respect to the beam (e.g. lack of sidewall fusion).

Coupling variables will also affect amplitude of response. The efficiency of coupling will be affected by the nature of the workpiece surface, the coupling medium used, and the pressure exerted on the transducer. For material thicknesses up to 1.5 in (38 mm) there is only a 2 dB difference between acceptance and rejection. This magnitude of change (less than 25 percent) can easily be brought about by coupling variables alone *(3)*.

The final assumption regarding amplitude decay with distance is invalid because transducers have "near zones" in which the amplitude varies in an unpredictable manner. The length of the near zone is dependent on frequency and piezoelectric crystal size. The value of 2 dB per inch does not correctly describe the theoretical response from small reflectors outside the near zone, which is dependent upon defect size *(16)* and takes no account of attenuation variations which can profoundly affect distance–amplitude relationships *(22)*.

The extent to which these theoretically invalid assumptions have an influence on the practical applicability of the Code can only be judged from experience of using the Code in practice and/or from experimental data.

Experimental Evaluation

Controlled Laboratory Tests

As far as detection capability was concerned in this study, the scanning sensitivity was adequate to detect almost all

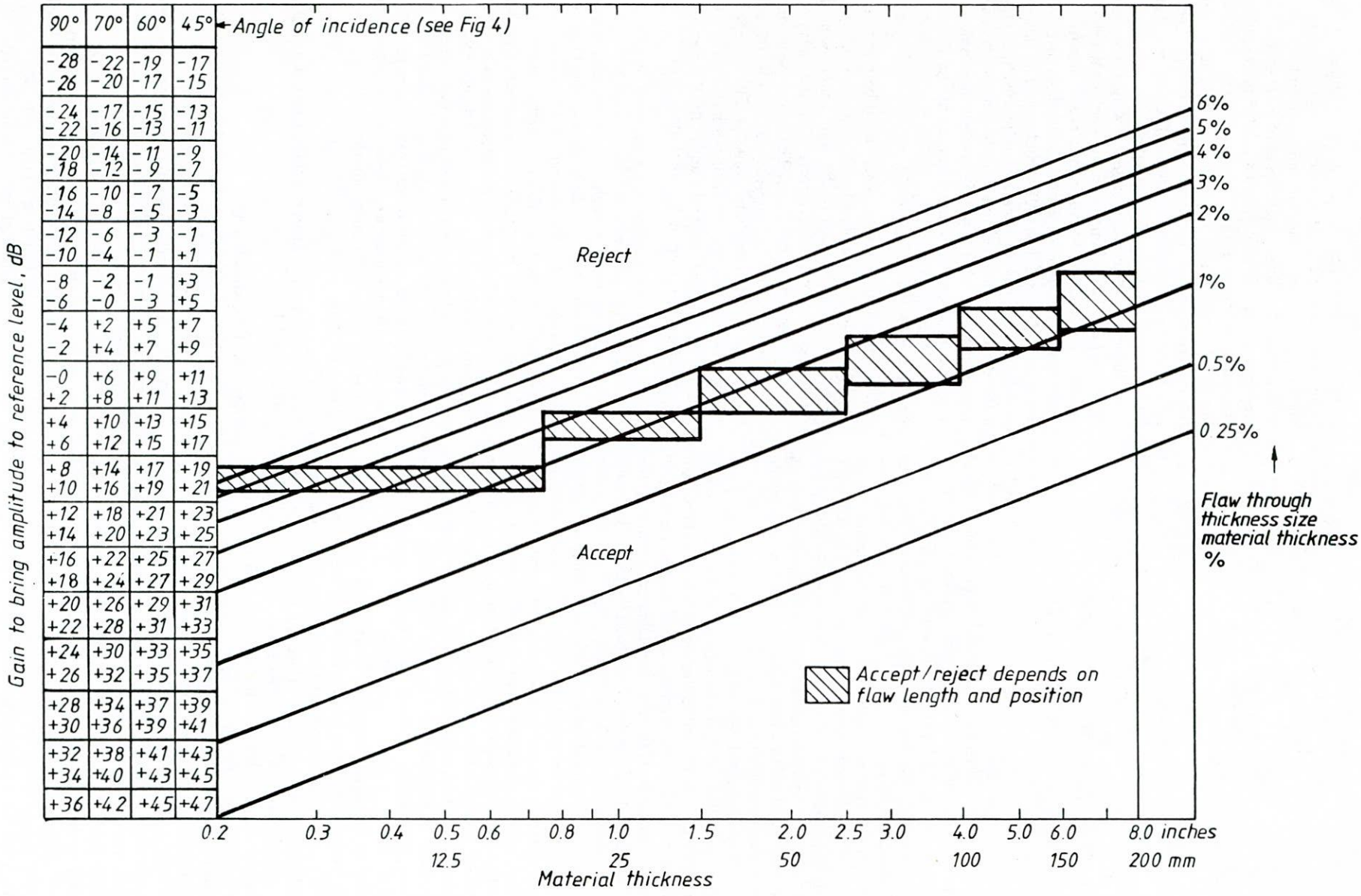

Figure 3. Relationship between material thickness, flaw size, and predicted amplitude of response for AWS D1.1 procedures.

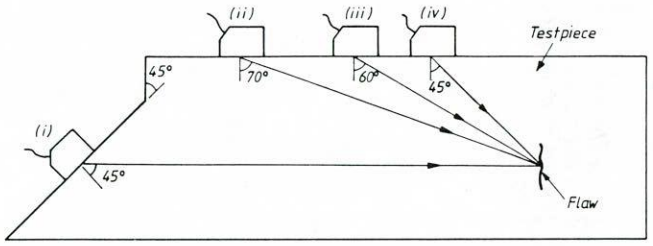

Relative amplitudes of response (assumed by code)

Position	Angle of incidence	Amplitude
(i)	90°	0 dB
(ii)	70°	-6 dB
(iii)	60°	-9 dB
(iv)	45°	-11 dB

Figure 4. Defect orientation relative to ultrasonic beam.

defects, and procedures were sufficient to allow the range of defects studied to be evaluated according to the Code. Out of the 91 tests on the 35 weld defects, on only two occasions were defects not detected and in each of these the flaw was deemed acceptable in other tests. In fact, the scanning sensitivities in all cases were found to be very high, and a large number of small indications were revealed on the CRT screen. Considerable time was involved in evaluating these small reflectors, not associated with the intended defects under study, and all of them were found to be acceptable minor flaws.

The diffusion-bonded defects were easily and reliably detected irrespective of beam-to-defect orientation. Clearly, when the beam was normal to the defect a large echo would be expected as would be the case with a real planar defect. However, the surprising and unanticipated feature of the diffusion-bonded defects was that when the defect was misoriented, strong echoes were still obtained from the defect extremities. Limited previous experience, mainly on smaller diffusion-bonded defects, did not highlight this feature. The extremity signals are thought to arise principally from diffraction effects at the sharp, well-defined edges of these defects. The diffracted signals were much greater in amplitude than those obtained from true planar defects, and, indeed, rendered the diffusion-bonded defects rejectable according to the Code in all cases. Because of this unrepresentative behavior, no further analysis was carried out on these defects.

As far as the suitability of the accept/reject levels is concerned, the experimental results show that the Code allows reliable rejection of incomplete fusion, slag inclusions, and the diffusion-bonded defects. However, the four flaws that were accepted by the controlled laboratory tests were all cracks and, while one was thought to be small and insignificant (defect 2), the other three were vertical cracks of 0.157, 0.197 and 0.354 in. (4, 5 and 9 mm) in depth respectively. This is of considerable concern as it is principally vertical cracks which the Code procedures are intended to detect and reject.

Examination of the overall accept/reject decision for the population of defects studied shows there is a clearly defined transition from a pronounced tendency to accept to a pronounced tendency to reject with increasing defect size at 7.5 percent of wall thickness (see Figure 6). This value would therefore appear to be the effective accept/reject threshold for the AWS D1.1 procedures and indicates that larger defects are accepted than anticipated by Figure 3. (The maximum acceptable defect sizes according to Figure 3 are 2 percent, just under 3 percent, and just under 4 percent of thickness for the three thicknesses of plate studied—3.9 in. (98 mm), 1.5 in. (40 mm), and 0.4 in. (9.5 mm) respectively.) Overall defects greater than 7.5 percent of the wall thickness in size were not reliably rejected (i.e., in 30 percent of cases these were accepted, including vertical cracks). There was no correlation between probability of rejection and absolute flaw size (see Figure E-7, Appendix E).

Furthermore, the greater tendency of the Code procedures to reject the more innocuous slag and obliquely oriented lack of fusion defects rather than vertical cracks means the result is not conservative in a fracture mechanics sense. Whether, in a practical sense, the Code would regard all flaws studied as rejectable cannot be ascertained because it is not known if there are any factors built into the accept/reject levels to allow for the fact that flaws may reflect ultrasonic energy in a manner different from that assumed by the Code.

Operator Variability

Discrepancies were also experienced between the results obtained from the three different operators. Out of the 14 defects used for this part of the study, there was disagreement over acceptance or rejection in five cases (approximately 35 percent of the total). The actual measurements of defect rating varied by, on average, 6.5 dB (the full range being 0 to 21 dB). This magnitude of difference would obviously be extremely critical in borderline cases because, even for the thickest material studied, the difference between acceptance and rejection is only 4 dB.

Equipment Variability

The effect of using a slightly oversize (according to the Code) transducer crystal was small. For the 13 comparative measurements made, the average discrepancy was 2.9 dB (the full range being 0 to 7 dB). Again, this may be significant in view of the small amplitude difference between acceptance and rejection, but not all the discrepancy can be attributed to the transducer size because there was no observable trend to either underestimate or overestimate defect severity. It is suspected that the variations are more likely to stem from coupling and measurement variables, even though precautions were taken to minimize these, and it must be recognized that some such variation is inherent in the performance of ultrasonic tests.

EVALUATION OF IMPROVED TECHNIQUES FOR DEFECT ASSESSMENT

Theoretical Considerations

The Probe Movement Technique

The approach of the AWS D1.1 ultrasonic procedures is to use a single parameter, signal amplitude, to assess defects. To do this is to ignore much of the complexity of the process of interaction of ultrasound with a defect. The probe movement technique attempts to account for the way the sound level rises and falls as a beam of ultrasound is traversed across a defect and from this deduce its size.

Detection of embedded defects relies on reflected signals

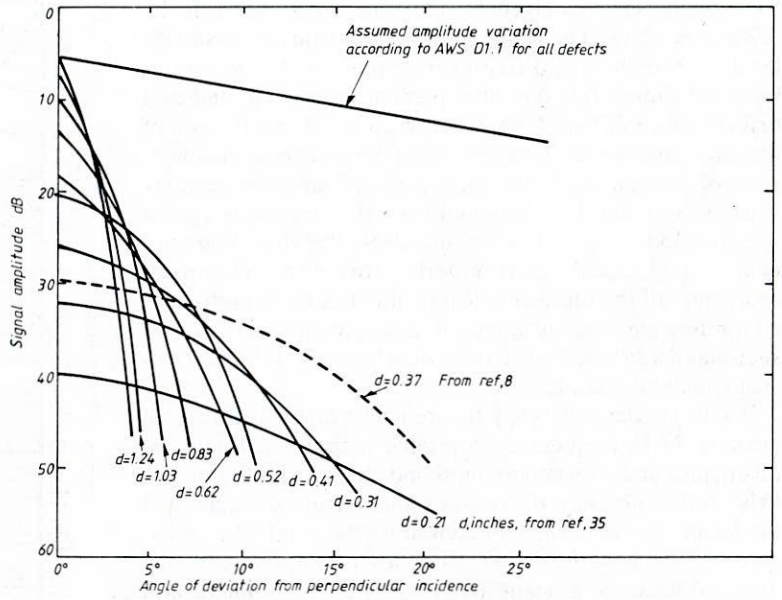

Figure 5. Variation in amplitude with flaw orientation for 2.25-MHz 5/16-in. diameter transducer (d = flat bottomed hole diameter).

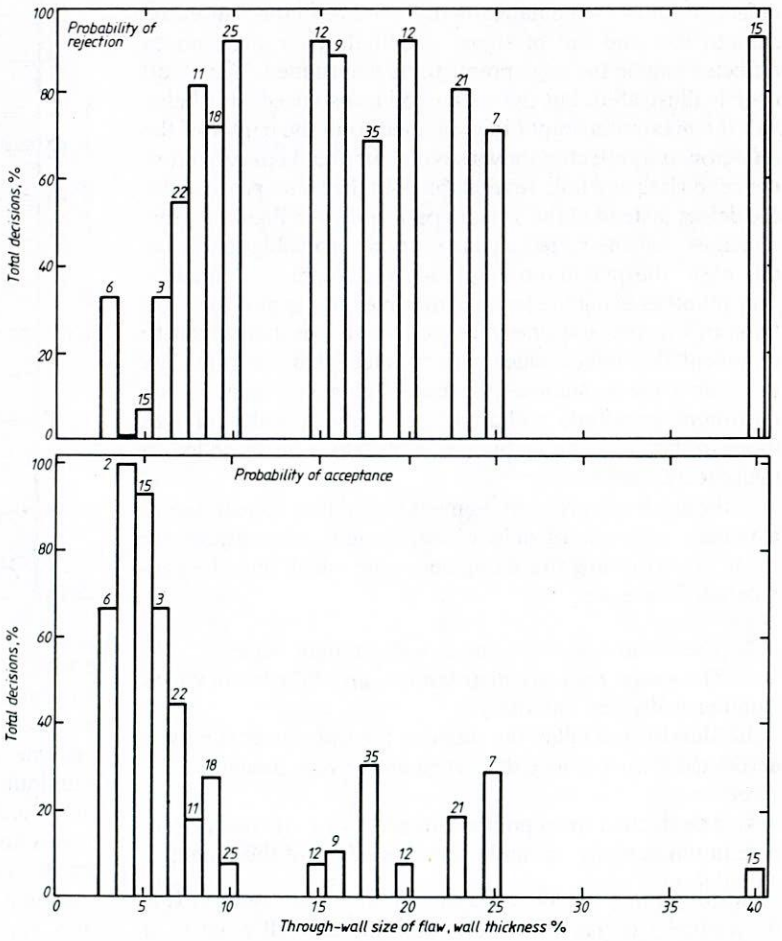

Figure 6. Probability of acceptance and rejection of all defects according to AWS Code with percent wall thickness (all test directions). (Numbers above boxes show sample size.)

from them being received by the transducers as with the AWS procedure. The requirements for adequate sensitivity level for searching and thorough scanning apply equally to both techniques. It is the subsequent assessment of detected defects which differs. It should also be noted that the aim of the technique is merely to determine the location and dimensions of defects. No requirement is placed upon the operator to assess whether flaws detected are within or outside a given specification. The test procedure itself therefore does not contain any accept/reject criteria. However, subsequent evaluation of the ultrasonic test results has to be performed with reference to some standard of acceptance for flaws, so such standards would need to be developed for bridges if this sizing method were to be employed.

It can be demonstrated theoretically that an ultrasonic beam at MHz frequencies is a cone with a small angle of divergence and with maximum sound intensity lying along its axis. Sound pressure decreases radially from the axis, and the beam edge is normally taken to be the point when pressure is 1/10 that at the center (20 dB less). The position of the axis and edges of a beam may be plotted by aiming it at a series of small reflectors at different ranges and interpolating points between these using straight lines. An example of a beam plot is shown in Figure 7, the parallel region being the near zone where little divergence occurs.

How this beam geometry is used to measure the size of defects is shown schematically in Figure 8. In the figure, the smooth rise and fall of signal amplitude over the smooth reflector enable the edge points to be determined. The 20 dB drop is illustrated, but the 6-dB drop is also used, this being half the maximum amplitude obtained from the center of the reflector. If a reflector shows several amplitude maxima (i.e. the echo rises and falls several times as the beam passes over the defect instead of the smooth path shown in Figure 8), this indicates that the reflector has several resolvable facets. In this case, the maximum amplitude technique can be used. This involves using the beam centerline only to plot the positions of the two extreme maxima which are then taken to represent the defect edges. For a defect that has only one resolvable facet, such as the one shown in Figure 8, the maximum amplitude technique gives a zero value of size (point reflector). The technique is therefore best applied to multifaceted defects.

Although these probe movement techniques appear to give a reliable estimate of defect size, several assumptions are made in performing the sizing operation which must be considered. These are:

1. The beam is a simple cone with straight edges.
2. The sound pressure distribution across the beam varies symmetrically and smoothly.
3. The rise and fall of the signal as the transducer is moved across the defect can be discerned on the flaw detector CRT screen.
4. The decibel drop points (either 20 or 6 dB down from maximum) actually coincide with the edges of the defect.

Assumption 1 is only valid in certain circumstances. It is theoretically correct, but normally only a small number of machined reflectors (e.g. four holes in a reference block) are used as datum points for a plot of the beam extending over 6 in. (150 mm). Minor variations in beam shape between these points are not normally noted, which could cause sizing errors. Furthermore, Coffey (*3*) has demonstrated that workpiece surface finish can seriously affect beam shape, increasing roughness and undulations causing beam edges to become more diffuse and beam width to vary with range. Minimum requirements for surface preparation have been proposed to counter this.

Assumption 2 influences the way in which a signal rises and falls when a transducer traverses a defect. This is usually assumed to increase monotonically to a maximum and decay in a similar manner. If it does not, difficulty can be experienced in determination of the extremity points, either 6 or 20 dB below the maximum. However, a check can readily be made on a machined reflector and transducers of substandard performance eliminated.

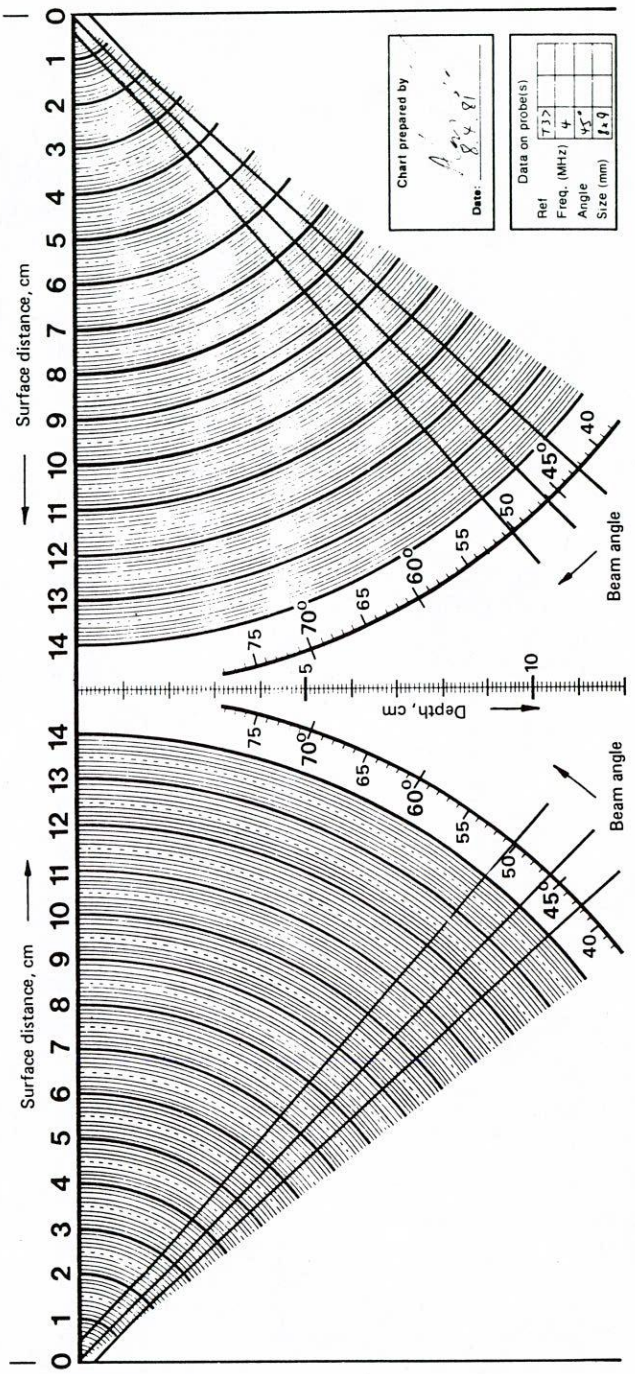

Figure 7. Beam plot for 45° transducer used for probe movement tests, showing –20-dB beam edges.

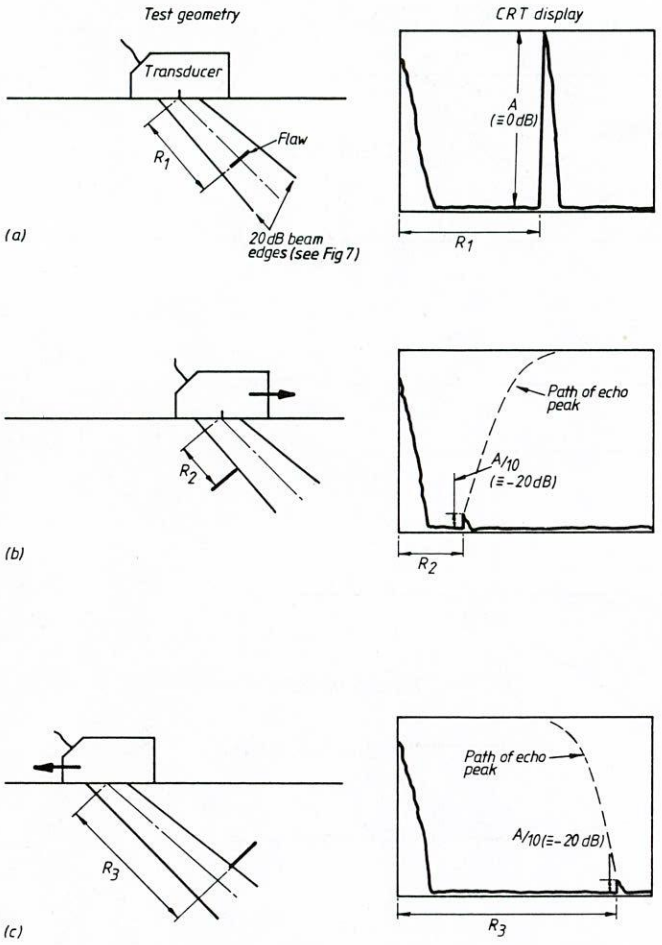

Figure 8. Elements of probe movement technique for flaw sizing; (a) maximum amplitude position, (b) transducer moved forward so lower beam edge coincides with upper edge of flaw, and (c) transducer moved backward so upper beam edge coincides with lower edge of flaw.

Assumption 3 is important for two reasons: (1) with techniques such as the 20 dB drop, echo amplitudes are very small at the extremity points and may be lost in material and electrical noise if high testing sensitivities are required (this limits usable testing sensitivity and can be a problem for investigation of weakly reflecting defects); and (2) real defects that are not simple shapes give rise to more complex signals, containing several maxima and minima, and it may not be possible to determine which points represent the edges of the defect (this causes many real testing problems, not the least of which is establishing whether a series of closely spaced reflectors should be measured as a single flaw or as several discrete parts).

Assumption 4 is affected by theoretical limitations which predict that for a beam impinging on a flaw, as the edge of the flaw is approached, the signal amplitude will decay more quickly than rate of approach to the defect edge. In other words the 20 or 6 dB drop point will always lie slightly inside the defect extremity, suggesting that such methods will always tend to undersize defects slightly.

A variant on the dB drop method is the maximum amplitude technique. This assumes that the response of a rough defect will consist of several maxima and by locating the first and last the defect dimension can be determined. This overcomes some of the problems associated with use of the beam size (maximum points are measured on the beam axis only) and uses the phenomenon of preferential responses from defect tips (as used in the time-of-flight technique discussed next), but is still likely to undersize defects as assumption 4 is still made.

Resolution capability, that is, the ability to determine that two separate, closely spaced reflectors are indeed separate, is an important additional factor. In the simplest example, the maximum amplitude technique cannot be employed unless the equipment is capable of resolving individual facets of the reflector. Opinions differ on the best way to define resolution capability. One approach (*7*) defines a disc-shaped resolution volume in the material (based on the transducer pulse length and beam diameter) within which two or more reflectors cannot be resolved and then goes on to deduce that a defect which can be contained within the resolution volume cannot be sized by probe movement techniques. Whether this is the case in practice must be determined by experimental work. However, using the procedure outlined in Ref. (*7*), the resolution volume for the equipment used in this exercise would be about 0.2 in. (5 mm) in diameter by about 0.06 in. (1.6 mm) thick lying on a plane normal to the beam.

Little rigorous analysis of these individual factors and their effect on sizing performance has been carried out. A rare example is the work of Serabian (*8*) who studied the effect of various parameters of the test systematically. A study conducted by The Welding Institute (*5*) using conventional equipment, which examined the sum of these errors, has demonstrated that an error band of ± a few mm on defects of the same overall size is required to encompass 95 percent of all results, using a statistical approach.

The Time-of-Flight Technique

The principle of this technique is that diffraction effects at the ends of flaws cause secondary signals to be reradiated. These can be picked up by a second transducer so that time of flight from transmitter-to-flaw-to-receiver can be used to position the depth of the flaw tip accurately. If this is done for both ends of the flaw the through-wall size can be measured. This is shown in Figure 9(a) and Figure 9(b) for planar and volumetric flaws, respectively. The main advantage of this method is that flight time and velocity are the only ultrasonic parameters measured, all information on beam size, etc., being ignored.

There are no inherent theoretical limitations to this technique, provided the necessary signals can be detected. As long as signals are of adequate strength and can be resolved, the technique will give accurate results within the measurement errors of the equipment (the instrument available at The Welding Institute can measure time of flight to ±5 ns, which constitutes a negligible measurement error). Even if signals from the upper and lower extremities of a flaw cannot be resolved, the position of the nearer extremity can be defined from one testing surface and repeating the test on the opposite face will give the position of the other edge.

However, two practical difficulties can be encountered. If two resolved indications are obtained, there is no guarantee that they are from the same defect. The indications could be from separate small defects. This suggests the use of a sepa-

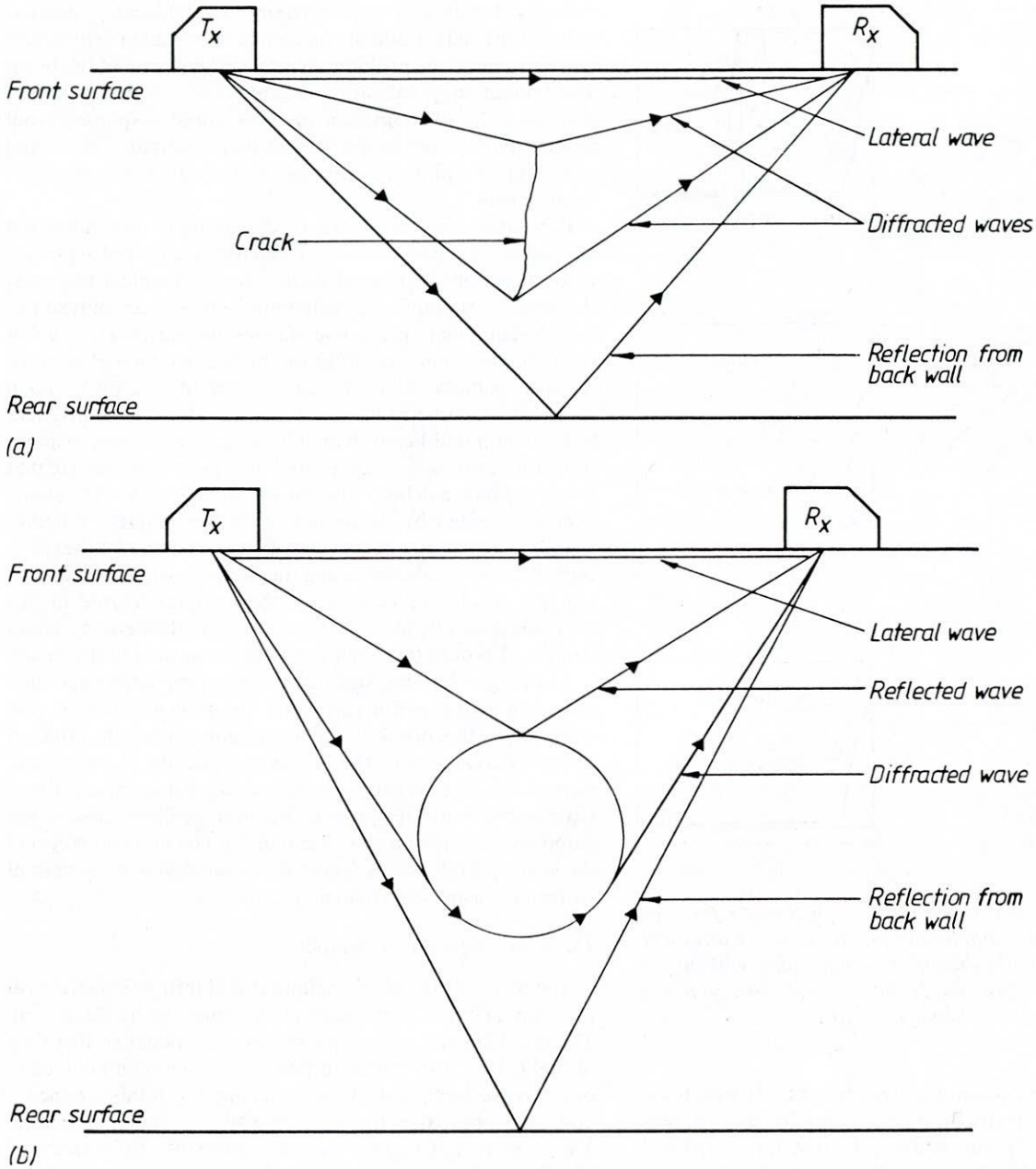

Figure 9. Principle of time-of-flight test; (a) planar defect, and (b) nonplanar defect.

rate technique, probably based on reflection, to confirm that one defect is present.

The second practical difficulty is that, on some occasions, it is unclear as to where on the received indication the time measurement should be taken from. If the interaction at the defect extremity is a complex one, for example if more than one diffraction site is present, the received pulse will not be sinusoidal and the start of it can be ill-defined. In these instances, some operator judgment is necessary and this is a source of error. However, it is unlikely that such errors would exceed one wavelength which, for the transducers employed, is about 0.050 in. (1.2 mm).

Experimental Evaluation

The Probe Movement Technique

Details are given in Appendix F.

Unlike the AWS D1.1 procedures, probe movement tests are not normally conducted to a rigid scheme of scanning pattern and test sensitivity. Certain minimum requirements are usually specified, such as those given in the procedure (see Document F1 at end of Appendix F), but, otherwise, the operator has considerable scope to exercise his judgment while performing the test.

None of the operators had difficulty in detecting the defects by this method. In fact, scanning is often carried out at a maximum sensitivity, limited only by "grass" caused by a combination of electrical and material noise on the base-line of the flaw detector trace. For evaluation of defects so detected the sensitivity is reduced to a suitable lower level. This process enables even weakly reflecting flaws to be found, but each indication is not required to be assessed at high sensitivity as with the D1.1 procedure. The experienced operator judges from the echo characteristics as the beam passes over the defect whether further assessment is necessary.

In the analysis below, the results for the diffusion-bonded defects have been omitted because, as discussed earlier, the responses obtained were not representative of real defects. However, the strong signals received from the defect extremities enable these defects to be measured more accurately than the weld defects.

The principal flaw parameter under study was through-wall depth. Errors between measured and actual depth values from laboratory tests for the weld defects were analyzed statistically to gain a measure of the average and scatter, and the results are given in Table 2. It was found that the trend for the 20-dB drop technique (45° and 60° transducers) was to underestimate flaw size, by on average 0.080 in. (2.0 mm). For these tests the scatterband for 95 percent probability limits was ±0.23 in. (±5.8 mm) either side of the mean. These figures indicate that in order to be 95 percent sure that the actual defect size did not exceed the predicted value, 0.31 in. (7.85 mm) would have to be added to the ultrasonic measurement.

For the maximum amplitude (max. amp.) technique the results were slightly better with a mean error of +0.008 in. (0.20 mm) and a spread of ±0.20 in. (±5.0 mm). For this test, to achieve a 95 percent confidence figure, 0.19 in. (4.8 mm) would have to be added to the ultrasonic measurement. These results are in broad agreement with other work (see Table 3).

No correlation between accuracy and absolute defect size was noted.

Whether these errors are acceptable depends on the acceptance standard in force. This is discussed more fully in the next chapter.

Two sets of check tests were performed by two different qualified operators to establish operator variability. There was a marked difference between the two sets of results (see Table 4): one operator was within the accuracy of the 20-dB drop laboratory tests whereas the other was less precise (95 percent scatterbands of ±0.18 in. (±4.6 mm) and ±0.26 in. (6.6 mm), respectively). This indicates that different results from different operators are likely to be experienced and that an accuracy slightly less than that for the laboratory tests may have to be assumed to ensure that the results for any given operator would be encompassed.

Time-of-Flight Technique

Details are given in Appendix G.

In these tests detection was not considered and effort was put into establishing the accuracy of through-thickness size determinations. For reasons discussed in the previous section, the results of the tests on the diffusion-bonded defects have been omitted from the analysis below. However, these results showed better accuracy than those on the weld defects and are discussed further in Appendix G.

In view of the simplicity of the equipment employed, difficulty was encountered in obtaining a value of size on a "one-time" basis. The difficulty arose from the inability to resolve the signals from the upper and lower extremities: a single complex indication being obtained for most of the defects. However, taking the start point of the received pulse enabled the position of the extremity closest to the test surface to be determined, and repeating the exercise on the opposite surface gave the position of the lower extremity. In this way a through-thickness size measurement was obtained for 18 out of 23 cases in the laboratory tests.

A statistical analysis of the results (see Table 5) revealed that the measurements were significantly more reliable than

TABLE 2
STATISTICAL DATA ON ACCURACY OF DEFECT THROUGH-WALL SIZE MEASUREMENT FOR PROBE MOVEMENT TESTS.

Sizing technique	Transducer angle	Mean error, $\bar{x}$		Standard deviation, σ		95% probability band, $\bar{x} \pm 2\sigma$		Number of measurements
		Inches	(mm)	Inches	(mm)	Inches	(mm)	
Maximum amplitude	45°	+0.088	(+0.20)	0.098	(2.50)	-0.19 to +0.20	(-4.80 to +5.20)	40
20dB drop	45° + 60°	-0.080	(-2.03)	0.115	(2.91)	-0.31 to +0.15	(-7.85 to +3.79)	45
20dB drop	45° only	-0.122	(-3.10)	0.114	(2.89)	-0.35 to +0.11	(-8.88 to +2.68)	24
20dB drop	60° only	-0.032	(-0.81)	0.096	(2.45)	-0.22 to +0.16	(-5.71 to +4.09)	21

TABLE 3
STATISTICAL DATA ON ACCURACY OF DEFECT THROUGH-WALL SIZE MEASUREMENT FOR PREVIOUS PROBE MOVEMENT TESTS FROM REF. *5* (PLANAR DEFECTS ONLY).

Test	Mean error, $\bar{x}$		Standard deviation, σ		95% probability level, $\bar{x} \pm 2\sigma$	
	Inches	(mm)	Inches	(mm)	Inches	(mm)
45° maximum amplitude	-0.047	(-1.2)	0.134	(3.4)	-0.315 to 0.220	(-8.0 to +5.6)
45° 20dB drop	-0.091	(-2.3)	0.102	(2.6)	-0.295 to 0.114	(-7.5 to 2.9)
60° and 70° 20dB drop	-0.106	(-2.7)	0.115	(3.0)	-0.343 to 0.130	(-8.7 to 3.3)

TABLE 4
STATISTICAL DATA ON ACCURACY OF DEFECT THROUGH-WALL SIZE MEASUREMENT FOR PROBE MOVEMENT OPERATOR VARIABILITY TESTS.

Operator	Mean error, $\bar{x}$		Standard deviation, σ		Number of measurements
	Inches	(mm)	Inches	(mm)	
1	-0.037	(-0.95)	0.130	(3.31)	10
3	-0.052	(-1.32)	0.091	(2.32)	11

TABLE 5
STATISTICAL DATA ON ACCURACY OF DEFECT THROUGH-WALL SIZE MEASUREMENT FOR TIME-OF-FLIGHT TESTS.

Test	Mean error, $\bar{x}$		Standard deviation, σ		95% probability level, $\bar{x} \pm 2\sigma$	
	Inches	(mm)	Inches	(mm)	Inches	(mm)
"Laboratory" tests on simplified equipment	-0.041	(-1.03)	0.064	(1.63)	-0.169 to 0.088	(-4.29 to 2.23)
Results from previous Welding Institute Programme (5) with complex equipment	0.02	(0.50)	0.071	(1.80)	-0.122 to 0.161	(-3.10 to 4.10)

the probe movement tests with a mean error of −0.041 in. (−1.03 mm) and a 95 percent probability scatter of ±0.128 in. (±3.26 mm). Again these results are in agreement with other work (see Table 5) and no effect of absolute size was noted.

Because of the difficulties in interpretation, the results for the operator variability tests were limited and insufficient to analyze statistically. However, the results obtained were generally within the error band for the laboratory tests.

It was disappointing that attempts to reduce the complex laboratory-based equipment with proven performance (*5*) to a simple device suitable for site use imposed limitations on performance. However, it is encouraging that when measurements could be made, the accuracy matched that for the complex equipment (see Table 5), suggesting that further investigation of equipment variants based on the time delay principle would be worthwhile. This is discussed further in the next chapter.

CHAPTER THREE

INTERPRETATION, APPRAISAL, APPLICATIONS

GENERAL DISCUSSION

Fitness for Purpose Considerations

The purpose of fracture mechanics is to establish whether a component, or a structure manufactured from a number of components, is capable of withstanding the loading placed on it under any given set of conditions. Within the field there is a wide variety of analyses and approaches, but all seek to relate material fracture properties, stress level, and flaw size. Having knowledge, either measured or assumed, about two

of these enables the third to be determined. For example, for a certain value of material fracture toughness a critical stress for failure can be established for a given flaw size, or a critical flaw size for failure can be calculated on the basis of a known service stress.

In either case, an attempt must be made to determine the actual size of flaw present in the structure if the analysis is to be used to predict its continuing integrity. The requirements of a nondestructive method to provide this information are therefore to be able to detect defects reliably, to be able to measure length and through-wall size (the latter being the most significant dimension from a fracture viewpoint), and to have a known, demonstrable accuracy.

The probe movement and time-of-flight methods only seek to measure defect size. These are incorporated into a testing procedure in which other factors such as scanning patterns, transducer parameters, and so on may be specified, but neither one includes the subsequent step of assessing defect significance. The results from such tests are merely an input into the appropriate fracture calculations. Many standards and codes of construction are now incorporating the option to perform fitness for purpose calculations based on fracture mechanics in addition to the arbitrary standard of workmanship normally specified. This approach has recently been strengthened within the United Kingdom by the issue of a British Standard Published Document giving procedures for the evaluation of the significance of flaws in welds (*32*). In the UK, probe movement techniques would be used in conjunction with this standard, but for many applications it is considered not to be sufficiently reliable; therefore, there is a similar need in the UK to develop more reliable defect sizing procedures.

On the other hand the AWS D1.1 procedures include an assessment of defect "severity." This determination of flaw severity is used in conjunction with design criteria presented in the Code and is also incorporated in the U.S. Department of Transportation's Fracture Control Plan for New Bridges (*24*). However, the assessment of severity is entirely arbitrary from a fracture standpoint because it takes no account of either stress level or material properties and does not measure flaw size. The D1.1 procedures are the basis of a "workmanship" Code, aimed at ensuring a reasonable standard of welder performance by imposing arbitrary defect acceptance levels. Although the use of such a Code should reduce the incidence of defects produced at the time of welding, it cannot be used to determine fitness for purpose of a structure either before or during service.

Therefore any modifications to the defect acceptance system of the Code could only attempt to improve its reliability within the existing framework of a "workmanship" type approach. A completely different system would be needed to achieve a reliable interface with fracture mechanics.

Performance of Test Methods

In the evaluation of the AWS D1.1 Code, the defects studied were detected with a high degree of reliability. However, it cannot be assumed that other types of defect, such as smooth fatigue cracks and transverse cracks, would be found with the same degree of reliability.

The quantitative study of the acceptance and rejection levels of the Code yielded surprisingly consistent results. There was a high probability of defects up to 7.5 percent of the wall thickness in depth being accepted and a relatively high probability, around 70 percent, of larger defects being rejected. In view of the factors affecting signal amplitude, and therefore the accept/ reject decision outlined in Chapter Two, no such trends would have been expected. However, this result is profoundly influenced by the weighting imposed on defect ratings for different wall thicknesses and no correlation was obtained between acceptability and absolute flaw size.

The D1.1 procedures do not therefore meet the requirements of rejecting defects approximately 2 percent of the wall in depth implied by Figure 3, and there is a chance that large defects will be accepted. This is potentially serious because there is a tendency to accept vertical cracks (which are always badly oriented with respect to the ultrasonic beam) and reject the less significant slag and obliquely oriented lack of fusion defects.

On the other hand, the closely controlled procedure simplifies performance of the test, which is always of benefit in the field. This approach should bring benefits of reproducibility of test results so that a uniform quality of inspection may be maintained, but in practice this is not so. The results revealed a significant number of discrepancies from repeated tests. This suggests that the inherent variability of parameters in actually performing a test cannot be eradicated by close specification of a test procedure.

When an ultrasonic technique or other NDE method attempts to measure defect size, the measurements will always be subject to errors of some magnitude. When attempting to use defect size data obtained from NDE in fitness for purpose analyses the errors should be known and accounted for. The best way of accomplishing this is to ascertain the amount of error likely to occur (from experimental data and past experience) and make an adjustment to the NDE measured value so that an estimate of defect size is obtained with an acceptable degree of confidence. Defining "an acceptable degree of confidence" will depend on the application, and, ideally, there would be probabilistic aspects to the fitness for purpose considerations which could be interfaced with statistical data (such as that presented here) from NDE experiments. There may be cases where apparently large errors in the NDE measurements can be tolerated if the maximum allowable defect size (from fracture mechanics calculations) is very large. On the other hand, in very critical applications or where poor design or materials selection has resulted in small defects being critical, a heavier reliance may have to be placed on the NDE results, with a high order of accuracy being desirable.

In this work, the level of accuracy to be expected from two types of ultrasonic sizing techniques has been quantified. The probe movement technique, which would be the simpler to apply immediately to bridges in the United States, gave inferior results to the time-of-flight technique, which needs a better definition of equipment requirements before it can be introduced to bridge testing applications.

The probe movement tests showed that up to 0.31 in. (7.85 mm) would have to be added to the ultrasonically measured through-thickness size to give a prediction about which one could be 95 percent confident that the actual defect size would not exceed the prediction. The same figure for the time-of-flight tests was 0.169 in. (4.29 mm).

Clearly the figure for the probe movement technique would cause problems on thinner plate (i.e. about ⅜ in. (9.5 mm) and less), but may be quite adequate in thicker plate if the design and materials selection are satisfactory and defect tolerance is high. However, as previously highlighted, there may be circumstances where better accuracy is desirable and, in such cases, the time-of-flight approach would have advantages. This technique has been proven in the laboratory (*5*), but, unfortunately, attempts in this work to apply a simple, portable equipment were not wholly successful from the point of view that difficulties were experienced in interpreting the display in some cases. However, when a defect could be measured, accuracies similar to those using the complex laboratory-based equipment were obtained. Therefore, further work to optimize equipment requirements for shop and site testing would be worthwhile.

POSSIBLE IMPROVEMENTS TO AWS D1.1-80

The ultrasonic equipment requirements, calibration of equipment, and sensitivity are all adequate to ensure that, assuming the operator carries out the test in the prescribed manner, defects which are required to be detected will be found. The main difficulties lie in the areas of the acceptability or otherwise of defects and the variations experienced from operator to operator.

Because AWS D1.1 is such a widely used code and people in the bridge fabrication industry are generally very familiar with it, it is considered that changing completely to another existing ultrasonic testing code (none of which has demonstrably better reliability than AWS D1.1) would create more problems than it solves. It is therefore suggested that attempts be made to improve the Code within its existing framework. One area in which immediate improvement could be made is in the removal of at least some of the invalid assumptions in the Code. In this respect, three actions should be considered: (1) minimize external factors (i.e. those other than the defect) which influence amplitude of response; (2) apply more appropriate distance/amplitude correction factors than the present 2 dB per inch; and (3) avoid the rigid relationship between amplitude and beam-to-defect orientation implied by the Code.

With respect to item (1), steps to ensure a consistent surface quality (not mentioned by the Code), and hence coupling, could be taken. The degree of flatness, smoothness, and cleanliness required could be stipulated. Also variations in coupling characteristics between the calibration block and the testpiece can be accounted for as is done in ASME V. Another factor influencing coupling characteristics (and hence amplitude of response) is the pressure exerted on the transducer. This could be controlled by employing some scanning or jigging arrangement.

To satisfy item (2), it would be a straightforward step to employ a distance/amplitude correction (DAC) curve as is the case in ASME V. This requires machined holes in a representative calibration block to be examined at different depths so that a true picture of the attenuation within the material emerges.

With respect to item (3), the present emphasis on 70° transducers is unwarranted in view of the rapid fall-off of amplitude with increasing beam-to-defect misorientation. It can be seen from Figure 5 that by the time a 20° misorientation is reached (i.e. a 70° transducer examining a vertical defect), direct reflection amplitude is very low for all defect sizes. In these circumstances, when reliance for detection has to be placed on favorably oriented facets of the defect, a 45° transducer would be just as good as a 70° one. Furthermore a 45° transducer has the advantage of shorter range and a narrower beam. There should also always be a requirement to scan with a beam that is normal to the prepared edges of the weld.

The fact that some vertical planar defects were erroneously accepted by the Code demonstrates that an angle beam transducer gives a low amplitude of response from these defects. To overcome this, it is strongly recommended that more extensive use be made of the pitch and catch (or tandem probe) test configuration (see Figure 10) for the reliable detection and identification of vertical planar defects. This relies on detecting the strong specular reflection from a vertical defect, but in the Code it is only specified for testing of electroslag and electrogas welds where the fusion faces are

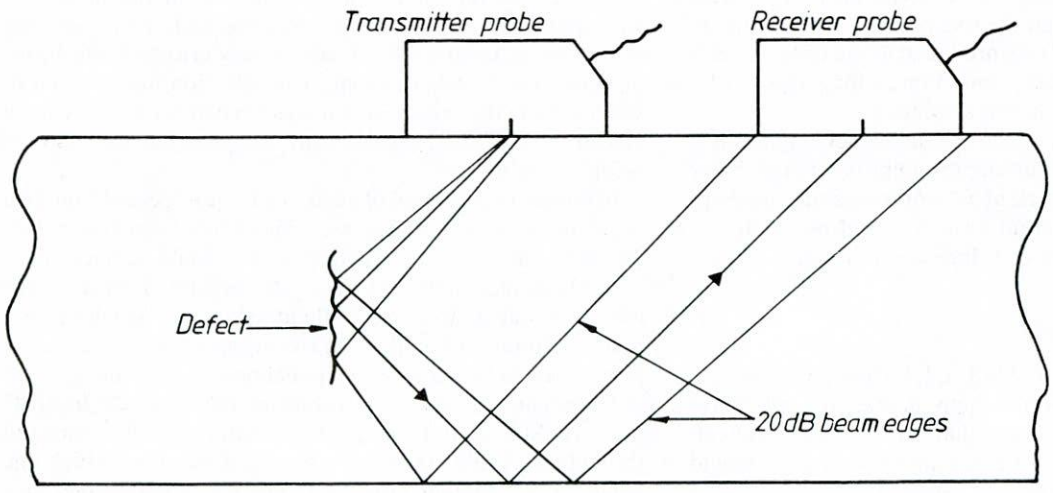

Figure 10. Pitch and catch (or tandem probe) test configuration.

perpendicular to the plate surface. However, in order to be able to size defects in this manner within the existing Code framework, some experimental work to establish amplitude values for typical defects would be necessary.

To avoid the erroneous rejection of small (i.e. much less than the beam diameter) nonplanar defects (which leads to unnecessary repair) is more difficult because it is difficult to distinguish them from small planar defects. Supplementary radiography may provide assistance if the weld geometry is favorable, but ultrasonic techniques, based on computerized flaw signature analyses, are still under development. Such techniques could therefore only be considered as longer term objectives.

The problem of operator variability will be reduced to some extent by the measures to ensure a uniform pressure on the transducer discussed above. However, in addition it is recommended that a national system be developed for qualifying ultrasonic operators, which involves hands-on tests on real defects.

A national NDE operator qualification scheme was started in the United Kingdom in 1969 (*25*) and has certainly helped in alleviating some of these problems. Such an approach has enabled a nationally recognized standard to be developed (within the UK) for operator competence in the major nondestructive test methods, which not only provides a demonstrable consistent minimum quality of operator (unlike the more specific, employer-oriented ASNT training schedules), but also provides employers with a reliable guide to the suitability of operators within their employ.

POSSIBLE IMPROVEMENTS TO PROBE MOVEMENT SIZING

The sources of error in probe movement sizing have been considered, and they stem largely from insufficient knowledge of the ultrasonic beam shape and lack of information on the interaction of ultrasound with complex defects. It is here that a conflict exists. To gain more reliable results a more complex test method is required, which is capable of assimilating more data from the test than a manual operator is capable of observing from a conventional CRT screen. On the other hand, a more complex test implies more equipment, which is bulkier, heavier, consumes more power, and generally hampers the maneuverability of the operators in getting to the test site.

Nevertheless, if the error bandwidth presented in Chapter Two is to be reduced, a means of organizing the data more effectively by means of some display, coupled with mechanical means of measuring transducer probe position reliably is required. Such devices as the Danish Welding Institute's P-scan (*26*), the CEGB's B-scan (*27*), and Accuscan (*5*) adopt this approach. Similarly, The Welding Institute is currently acquiring a computerized testing system (*28*) and a P-scan unit to investigate the improvements that can be made to sizing methods both in the laboratory and in the field. These will incorporate a real time display of data in correct spatial positions within the weld and the recording of all information for subsequent analysis. It is only with such equipment that the probe movement technique can be stretched to give accuracies up to its theoretical limit.

POSSIBLE IMPROVEMENTS TO TIME-OF-FLIGHT SIZING

Developments currently being pursued in relation to the time-of-flight technique are connected with adapting the necessary equipment so that it may be used readily on site. It is clear that a simple system, such as that used in the current work, is not sufficient for reliable measurement of all weld flaws, so more sophisticated equipment is required. From experience gained in the present work, it will be possible to specify more closely the equipment requirements to ensure accurate results and still be compatible with site testing situations. Again the essential features are: recording of all data collected and a better understood display from which the operator may make reliable measurements of flaws. The use of microprocessor techniques is increasing for such systems because this provides the only realistic means of handling the large amounts of data which these tests can generate very rapidly.

The equipment developed in previous work (*5*) incorporates computing techniques for enhancing relevant signals and displaying the data. Figure 11 shows a typical elevation plot of an embedded defect revealed by time-of-flight tests using this system. Signals from the defect extremities are shown as light and dark fringes from which, with a little interpretation, through-thickness size can be established.

CHAPTER FOUR

CONCLUSIONS AND SUGGESTED RESEARCH

CONCLUSIONS

A total of 35 embedded weld flaws, including cracks, incomplete fusion and slag lines, were manufactured in mild steel butt welds in thicknesses of 0.4, 1.5 and 3.9 in. (9.5, 40 and 98 mm). Eight diffusion-bonded defects were also manufactured in the thinner plates. These were all ultrasonically tested using AWS D1.1-80 ultrasonic procedures for assessing flaw severity, and using probe movement and time-of-flight techniques for measurement of defect through-wall size. Twenty-three of the weld defects were subsequently sectioned so that their true size could be measured and an evaluation of the three techniques carried out. The conclusions that can be drawn from this work are as follows:

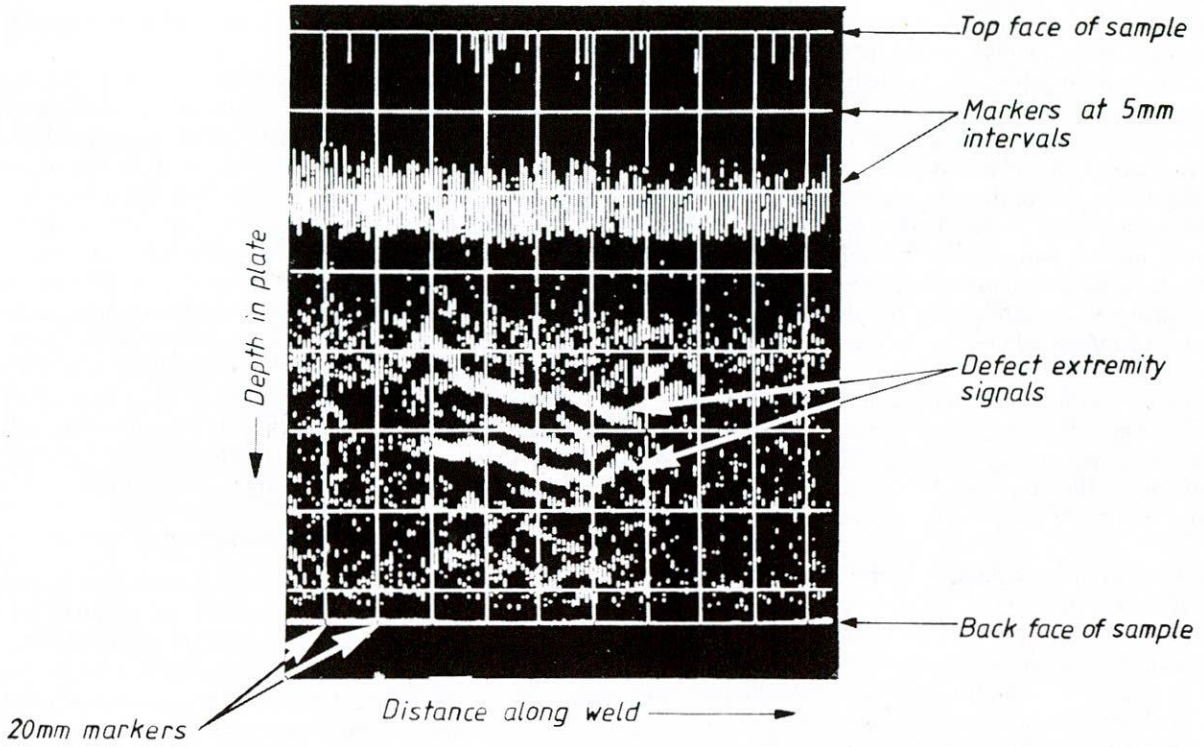

Figure 11. Side elevation display from time of flight test (from Ref. 5).

1. The AWS D1.1 Code procedures were adequate for reliable defect detection.

2. In many cases, the flaw severity predicted by the Code did not correlate well with the true defect. There was a tendency to reject slag inclusions and accept cracks, even up to 0.35 in. (9 mm) in through-thickness size. There was little indication that the Code actually achieved what it apparently set out to do, and the fact that several false assumptions were made in the formulation of the Code will obviously have contributed to this.

3. Defects less than 7.5 percent of wall thickness in size are likely to be accepted by the Code and larger flaws stand a 70 percent chance of rejection.

4. Variation in results between different operators showed that operator variability with the Code was a major factor. There was disagreement between three operators on acceptance or rejection of a defect in 35 percent of cases.

5. The AWS D1.1 procedures do not, and are not intended to, interface with fracture mechanics assessments but some improvements may be possible within its existing framework.

6. Probe movement tests provided a measure of weld flaw size in all cases, but errors were obtained. These were such that up to 0.31 in. (7.9 mm) would have to be added to the measured size in order to be 95 percent sure that the actual flaw size did not exceed this value. This is in general agreement with other work.

7. The time-of-flight technique also gave a measure of weld flaw size but, in some cases, difficulty was encountered in interpreting the display of the simplified equipment used in this work. However, when a size measurement was obtained (i.e. for 18 out of the 23 defects destructively tested), the results were substantially more accurate than the probe movement test results with the comparative figure for 95 percent confidence being 0.17 in. (4.3 mm) to be added to the measured value. This is in general agreement with other work.

8. Operator variability for the probe movement technique was shown to be significant. Factors of slightly more than the 0.31 in. (7.9-mm) figure quoted above may have to be added to take account of this.

9. Operator variability for the time-of-flight technique was, on limited evidence, shown to be within the errors of the main tests.

10. The diffusion-bonded defects gave ultrasonic responses that were not representative of those from real defects, so the results are not included in the above conclusions. Analyzed separately, more accurate results were obtained than for the respective tests on weld defects. This highlights the danger in using artificial reflectors to demonstrate ultrasonic testing performance.

11. From the results of this work it was not possible to prepare written procedures and specifications, but it was recognized that this was an ambitious objective for the study. However, possible improvements to the AWS D1.1 Code have been suggested and further work, discussed in the following, may yield more accurate results that can form the basis of new procedures.

POSSIBLE FURTHER RESEARCH

AWS D1.1

This work has provided valuable experimental data to quantify the limitations of these procedures. There are two

main areas where further work will be valuable. First, to avoid vertical planar defects being underestimated, the pitch and catch technique should be evaluated and verified experimentally to enable it to be incorporated into the existing framework of the Code. Second, means of distinguishing ultrasonically between planar and nonplanar defects when they are small should be evaluated when techniques are sufficiently developed.

Probe Movement Techniques

It may be that the current level of accuracy of this technique is considered to be inadequate. If this is the case, improvements can be sought in either or both of two ways: transducer development (in the form of focussed beams) or transducer arrays; and other equipment development to provide the operator with less ambiguous information on which to base a measurement. Focussed transducers have the advantage of a narrow sound field and hence better resolution; and arrays of transducers have the advantage that a wide range of scanning angles can be employed simultaneously.

With respect to other equipment, a mechanized scanning frame would substantially reduce scanning, coupling, and measurement variables and could also provide the necessary indexing of transducer position so that defect displays can be produced with appropriate handling of the ultrasonic data and combining with the transducer position data. The computerized P-scan equipment produces displays in this way (see Ref. *26*), and these provide the operator with a more objective basis on which to make a probe movement estimate of defect size. Such equipment is currently being evaluated experimentally for measuring defects in gas pipeline girth welds. The outcome of this work should be studied before any decision is made to develop the probe movement technique for bridge inspection. Despite the foregoing possibilities for improving accuracy, the theoretical limitations remain.

Time-of-Flight Technique

It was found in this work that an attempt to take laboratory-based equipment with proven accuracy and reduce it to a simple device suitable for site use resulted in a reduction in performance. This stemmed from a difficulty in interpreting the simple, untreated display in some cases, but when a measurement could be made, the results were as accurate as the laboratory-based equipment.

There is therefore a need to optimize the equipment requirements to enable the technique to be used on site reliably. Such an exercise would be worthwhile in view of the accuracy of measurement achievable. It is believed that some improvement to resolution coupled with signal enhancement would be required. This could be accomplished using shorter pulse transducers and signal averaging. Computer techniques may be necessary, and these have the advantage that relevant data can be recorded at the site of the test on portable equipment for subsequent playback and analysis off-site.

Other Techniques

Whatever sizing technique is envisaged, it is likely that a computer technique in some form will be necessary to accomplish quantitative and objective data collection and assessment.

The literature survey revealed several techniques that are under investigation by other workers; for example, spectroscopy, synthetic aperture focussing, and holography. These all involve digitization of the unrectified ultrasonic waveform and computer treatment and analysis.

By the end of 1981, The Welding Institute will be commissioning a computerized system that will have sufficient flexibility to study the above techniques, and any other of the more complex mathematical analyses, by selection of appropriate software.

RECOMMENDATIONS

Immediate

The AWS D1.1 ultrasonic testing procedures should be altered to remove some of the inherent invalid assumptions. Ensuring constant coupling characteristics, making a proper assessment of material attenuation, and considering a wider range of transducer angles than the currently used 70° angle are all recommended.

A national system of qualifying ultrasonic operators, based on "hands-on" tests, should enable the reduction of operator variability.

Short term

Provision should be made in the Code for more reliable rejection of vertical planar defects. This can be accomplished by the pitch and catch test configuration, but a short project would be necessary to collect the necessary amplitude data for the technique to be applied within the existing code framework.

Experimental work may also be necessary to determine testpiece surface requirements for ensuring constant coupling characteristics discussed above.

Long term

It is considered that the time-of-flight technique offers sufficient advantages for defect sizing to be studied further. From this work and other experience, a system can be designed which should optimize the requirements for both accuracy and site applicability. Such a system should then be evaluated both in the laboratory and in field trials.

Other techniques for sizing and for defect diagnosis should be kept under surveillance and evaluated at such a time when they are sufficiently developed.

REFERENCES

1. *Structural Welding Code—Steel,* AWS D1.1-80, American Welding Society (1979).
2. KRAUTKRÄMER, J., and KRAUTKRÄMER, H., "Ultrasonic Testing of Materials." 2nd Ed. Springer Verlag, Berlin (1969).
3. COFFEY, J. M., "An Experimental Study of the Effects of Surface Finish, as Produced by Hand Grinding, on Ultrasonic Inspection." Central Electricity Generating Board, *Report No. NW/SSD/RR/85/79* (1979).
4. MUDGE, P. J., "Effect of Metallurgical Features of Welds in Ferritic Steel on Ultrasonic Testing." Part 3 of Welding Institute Project "Size Measurement and Characterisation of Weld Defects by Ultrasonic Testing." (To be published).
5. JESSOP, T. J., ET AL., "Size Measurement and Characterisation of Weld Defects by Ultrasonic Testing, Part 2 Planar Defects in Ferritic Steel," *Welding Institute Report 3527/10/80,* (1980). (A copy of this report was made available to NCHRP, Jan. 1981).
6. Reports of the Plate Inspection Steering Committee (PISC) Exercise, Commission of the European Communities, *Nuclear Science and Technology Series Report No. EUR 6371,* Vol. 1-V Luxembourg (1979).
7. COFFEY, J. M., "Quantitative Assessment of the Reliability of Ultrasonics for Detecting and Measuring Defects in Thick-Section Welds." Paper presented at IMechE Conference, "Tolerance of Flaws in Pressurised Components," London (May 1978).
8. SERABIAN, S., "Reliability of Ultrasonic Weld Interrogation Methods." University of Lowell, Mass., *Report No. DOT-RC-92014* (June 1980).
9. "Procedures and Recommendations for the Ultrasonic Testing of Butt Welds." 2nd Ed. Publ., The Welding Institute, Cambridge (1971).
10. "Handbook on the Ultrasonic Examination of Welds." *International Institute of Welding Doc. 115/IIW—527-76. Publ.,* The Welding Institute, Cambridge (1977).
11. *British Standard: BS 3923,* "Methods for Ultrasonic Examination of Welds: Part 1: Manual Examination of Fusion Welds in Ferritic Steels." British Standards Institution, London (1978).
12. American Society of Mechanical Engineers, Boiler and Pressure Vessel Code, Section V (1980).
13. BUCHANAN, R. A., and HEDDEN, O. F., "Analysis of the Ultrasonic Examination of PVRC Weld Specimens 155, 202 and 203 by Standard and Two Point Coincidence Methods." *WRC Bulletin* (Feb. 1980) p. 257.
14. GILMOUR, R. S., "Ultrasonic Testing of Welds Using AWS D1.1-72." *Testing, Instruments and Control, 10* (8) (Aug. 1973) pp. 9–16.
15. MCGAUGHEY, W. C., "Ultrasonic Examination of Welds: Comparison of ASME and AWS Procedures." Materials Evaluation (Feb. 1972), pp. 44–48.
16. KRAUTKRÄMER, J., "Determination of the Size of Defects by the Ultrasonic Impulse Echo Method." *British J. Applied Physics, 10* (6) (June 1959) pp. 240–245.
17. KATO., ET AL., "Estimation of Weld Defects through Ultrasonic Testing." *Welding Journal* (Nov. 1976) pp. 946–953.
18. WÜSTENBERG, H., ET AL., "Experiences with Flaw Size Estimation by Ultrasonic Holography with Numerical Reconstruction." *Proc.* Conf. Non-Destructive Evaluation in the Nuclear Industry, Salt Lake City (Feb. 1978).
19. FLORA, J. H., HOLT, A. E., and BROPHY, J. W., "Defect Characterisation with Computerised Acoustic Holography." Conference on Periodic Inspection for Pressurised Components, IMechE, London (1979).
20. FORTUNKO, C. M., and SCHRAM, R. E., "Ultrasonic Non-Destructive Evaluation of Butt Welds using Electromagnetic Acoustic Transducers." (Paper to be published).
21. SHENEFELT, G. A. Private Communication, AWS D1.1 Code Committee for Ultrasonic Testing.
22. SERABIAN, S., "Influence of Attenuation on the Weld Interrogation Distance—Amplitude Curve." *Materials Evaluation, XXXIV (12)* (Dec. 1976) pp. 265–274.
23. PD 6493. "Guidance on Some Methods for the Derivation of Acceptance Levels for Defects in Fusion Welded Joints." BSI London (1980).
24. HARTBOWER, C. E., "A Proposed Fracture Control Plan for New Bridges with Fracture Critical Members." Vol. 1., *Report: Structural Engineering Series No. 5,* prepared by Bridge Division, Office of Engineering, Federal Highway Administration, Washington DC (1978).
25. YOUNG, J. G., "CSWIP—The British Scheme for Assessment of Proficiency of NDT Personnel." *Materials Evaluation, 30* (12) (Dec. 1972) pp. 18A–23A.
26. NIELSEN, N., "P-scan System for Ultrasonic Weld Inspection." *British Journal* of NDT *23* (2) (Mar. 1981) pp. 63–69.
27. HARPER, H., ET AL., "A portable B-Scan Ultrasonic Flaw Detector." *Central Electricity Generating Board Report No. NW/SSD/RR/8/78* (1978).
28. DUNCUMB, A. C., and MUDGE, P. J., "Specification for a Computerised Ultrasonic Test System." (To be published).
29. SILK, M. G., and LIDINGTON, B. H., "Defect Sizing using an Ultrasonic Time Delay Approach." *British Journal* of NDT, *17* (2) (1975).
30. CHARLESWORTH, J. P., LIDINGTON, B. H., and SILK, M. G., "Defect Sizing using Ultrasonic Flaw Diffraction." *Proc.,* 1st European Conference on NDT, Mainz 24-26 April 1978, Publ. DGZFP, Berlin.
31. DE STERKE, A., "Advancements in the Technologies for Mechanised Ultrasonic Testing." Plenery Lecture, 8th World Conference on NDT, Cannes (1976).
32. RENSMERY, M. E., and GROTHUES, H. L., "Automated Data Processing for ASME Section XI Requirements using the SUTAR System." Paper presented at ASNT

National Fall Conference Denver (Oct. 1978) pp. 171–181.
33. MUDGE, P. J., "Ultrasonic Time of Flight Measurements of Fatigue Pre-Crack Depth in Fracture Toughness Specimens." In "The Measurement of Crack Length and Shape During Fracture and Fatigue," Ed. Beevers C.J. *Publ. EMAS Ltd.*, Halesowen, UK (1980).
34. BABOROVSKY, V. M., ET AL., "Schlieren and Computer Studies of The Interaction of Ultrasound with Defects." *Non-Destructive Testing, 6* (4) (Aug. 1973) pp. 200–207.
35. MEYER, H. J., "Probability of Detecting Planar Defects in Heavy Wall Welds by Ultrasonic Techniques According to Existing Codes." Paper presented at meeting of IIW Commission V. Copenhagen (1977).
36. JONAS, P. G., and SCHAROSCH, D. L., "Ultrasonic Inspection of Butt Welds in Highway Bridges." State of California Division of Highways, Materials and Research Dept., *Research Report CA-HY-MR-6210-1-72-36*.
37. Test method CRB 115.01 Ultrasonic Inspection of Butt Welds, Country Roads Board, Victoria, Australia.
38. SHENEFELT, G. A., "Ultrasonic Testing—Requirements of the AWS 1969 Building Code and Bridge Specifications," *Welding Journal* (May 1971) pp. 342–349.
39. SILK, M. G., "Defect Sizing using Ultrasonic Diffraction." *British Journal NDT* (Jan. 1979) pp. 12–15.
40. DOYLE, P. A., and SCALA, C. M., "Crack Depth Measurement by Ultrasonics: a Review." *Ultrasonics, 16* (4) (July 1978) pp. 164–169.
41. LUMB, R. F., "Defect Sizing—The State of the Art." Paper presented at Conference, "Tolerance of Flaws in Pressurised Components," *Institution of Mechanical Engineers*, London 16-18 May 1978.
42. ADLER, L., ET AL., "Flaw Size Measurement in a Weld Sample by Ultrasonic Frequency Analysis." *Materials Evaluation, 35* (1977) p. 44.
43. FREDERICK, J. R., ET AL., "Improved Characterisation of Discontinuities in Thick Walled Pressure Vessels." *Proc.*, IMechE Conf: Periodic Inspection of Pressurized Components, London 8-10 May 1979.
44. MUCCIARDI, A. N., ET AL., "Signal Processing for In-Service Inspection." *EPRI Report No. NP 1421* (May 1980).
45. PARKINSON, G. J., and WILSON, D. M., "Non-Contact Ultrasonics." *British Journal NDT* (July 1977) pp. 178–184.

APPENDIX A

OVERVIEW OF CURRENTLY APPLIED NDE METHODS

INTRODUCTION

The advantages of nondestructive inspection methods to assess the quality of construction of a manufactured structure or component and to ensure its continuing integrity during service are self-evident. This implies the application of a medium which will in some way delineate discontinuities or flaws without materially altering the component itself. The use of such techniques is particularly important when embedded flaws (i.e. not visible to the naked eye) are likely to exist; for example, in weldments. The essential criterion which determines the choice of an inspection method is the change in response to the interrogating medium between sound and flawed regions, caused by the consequent difference in physical properties, which must be large enough to be observed by the inspector. Only if this condition is fulfilled will a flaw be detected.

REVIEW OF NDE METHODS

The principal test methods in use may be divided into two types: those which can only detect surface breaking or near-surface flaws and those which can also detect deeply embedded flaws. Commonly used methods sensitive to surface defects include dye penetrant testing, magnetic particle testing (for ferrous materials), eddy current testing (also for ferrous materials), and visual inspection. The detection and assessment of embedded defects on the other hand require an interrogating medium sensitive to discontinuities and also capable of penetrating the material, which is invariably opaque to light. Penetration is achieved by the use of electromagnetic radiation (X- or γ-rays) or mechanical elastic waves (ultrasound). Eddy current testing may also be used to detect embedded flaws in nonferrous materials to a limited extent.

X- and γ-rays are normally beamed through a component and flaws revealed by images on a photographic film resulting from differential absorption of the rays in the flawed region. Essentially, a shadow picture is formed of the flaws. This technique can reveal detailed information about the lateral extent of the defects detected in a direction perpendicular to the X-ray beam. However, the method is relatively insensitive to thin defects not oriented parallel to the beam, and no information on defect depth dimension or through-wall extent is presented directly on the radiographic image. In some cases measurement of the density of the images on the film may yield details of defect through-wall size, but this is generally qualitative, may be unreliable, and is not normally carried out.

Ultrasonic testing relies on the fact that discontinuities will produce reflections in some way related to their size and shape and is therefore the only nondestructive test technique in common use which has the capability both to detect and to

measure the size (especially the depth, or through-wall dimension) of embedded and surface flaws. As the depth dimension is normally the overriding factor in determining the severity of the flaw, this capability of ultrasonic testing has been exploited and the technique is now extensively employed to measure defect sizes in a wide range of industries.

PRINCIPLES OF ULTRASONIC TESTING

Ultrasonic testing relies on the generation of pulses of ultrasonic frequency elastic waves in the material under test. Megahertz (MHz) frequency waves combine good directional properties with adequate penetration, 2–6 MHz usually being employed for manual tests. Conventionally, these are generated by a piezoelectric transducer which is energized by a flaw detector unit. This unit also contains amplification circuitry and a CRT for display. The waves can propagate through solid materials and exhibit the four principal properties of wave motion (i.e., they undergo reflection, refraction, diffraction and interference). The basic theory of generation and propagation of ultrasonic waves has been summarized by Krautkrämer (*2*). Detection of flaws or discontinuities is achieved because the boundary between the regions which offer differing resistance to the passage of sound (acoustic impedance) acts as a site for partial reflection of the sound energy, enabling its presence to be detected.

DEFECT ASSESSMENT BY ULTRASONICS

General Considerations

The techniques invariably used for defect location and sizing have been developed from these principles, employing ray diagrams to locate sources of ultrasonic reflection from discontinuities in conjunction with knowledge of the ultrasonic beam size or signal amplitude for size measurement (*9, 10*). A schematic view of a typical test arrangement is shown in Figure 1 of the main report. The pulse of ultrasound reflected from a flaw is displayed on a CRT screen where the horizontal axis represents distance from the transducer to the flaw and is calibrated in inches (or mm). The vertical axis represents signal amplitude normally measured by comparison with a standard reflector, differences being recorded in decibels (dB) or as a percentage.

This conventional A-scan display of the ultrasonic signals is virtually the only form of presentation used by ultrasonic technicians in the field, and invariably such technicians perform a test manually (i.e., the ultrasonic transducer is scanned across the workpiece surface by hand and signals appearing on the ultrasonic flaw detector's CRT screen are interpreted and recorded in writing by the operator when deemed significant).

Amplitude Assessment Methods

For defect detection purposes the sensitivity or gain level of the ultrasonic system is crucial. In many cases an amplitude threshold level is employed so a high gain can be used, but very small signals, such as those arising from material or electrical noise, are not required to be recorded and investigated. An extension of this philosophy is to use a rigid regime of amplitude threshold levels as a basis for acceptance or rejection of detected flaws. This is particularly highly developed in the United States where ultrasonic testing procedures of the AWS (*1*) and ASME (*12*) codes require strict adherence to an amplitude based acceptance/rejection scheme for defects.

The AWS code takes amplitude assessment one stage further in that signal amplitude is used directly as a measure of a defect's severity and therefore a correlation with defect size is inferred. This is similar to the DGS (distance, gain, size) system developed by Krautkrämer (*16*) in which echo amplitudes from defects are compared with responses from flat bottomed hole reflectors of known size.

Probe Movement Methods

The ASME code method of defect size measurement (*12*) is partially dependent on amplitude compared with a threshold level, but also makes use of the way an echo from a defect rises and falls as the probe is traversed across it. This requires some knowledge of the shape of and energy distribution within the ultrasonic beam produced by the probe, which always has a finite width. Such probe movement techniques, as they are generally called, are in widespread use in the United Kingdom where they are detailed in the relevant British Standard Specification (*11*). In conjunction with this it is usual practice to determine the dimensions of the ultrasonic beam on an appropriate test block (*10*). The probe movement (decibel drop) sizing methods are preferred in the UK as the view is widely held that the amplitude maxima of signals reflected from a defect (of which there may be several) are likely to bear only a limited correspondence to the defect's overall size. This aspect is discussed further in Chapter Two.

The complexity of the propagation of ultrasound through metals having a microstructure which is not homogeneous over short distances, and the interaction of ultrasound with defects of unknown shape and form, cannot be fully accounted for in a manual test because of the limited amount of information that even a trained operator can reasonably be expected to comprehend and interpret from the flaw detector screen at any one time. Assumptions are therefore made which simplify the test: such as rectilinear propagation of the ultrasound enabling ray diagrams and geometric plots of the test to be used, although in many instances this condition is not satisfied; simple reflection of sound from defects, which does not account for diffraction, scattering, interference, and wave mode conversion effects; and probe beam and pulse characteristics that are assumed to vary in a simple manner, which does not take account of variations in beam shape with range and due to surface roughness. It would appear that considerations such as these could account for wide variations in estimated defect size compared with true defect size observed in recent studies of probe movement methods (*5*) and methods relying at least partially on amplitude (*6*).

DEVELOPMENTS OF DEFECT SIZING TECHNIQUES

As ultrasonic measurements of the through-wall size of defects are invariably the source information for determination of the integrity of a component, whether this is in a qualitative manner to satisfy the requirements of some arbitrary code principally designed to ensure good workmanship or as an input to a fitness for purpose assessment based on

fracture mechanics, the accuracy of such measurements is highly important if integrity is to be reliably maintained.

Time of flight

The improved accuracy of the time-of-flight method has been well demonstrated (*5, 29, 30*), and this reflects the practical advantages in using a parameter that can be measured very accurately (i.e. time) to size defects instead of relying on ultrasonic beam parameters and reflection patterns from defects which are, at best, difficult to quantify.

Specialized Techniques

It should be noted, however, that "novel" methods of defect sizing such as time of flight, spectroscopy and others have not been used to any great extent outside the laboratory. The requirements of shop and site inspection for ease of access and variability of components to be inspected have greatly militated against implementation of new techniques and development of more sophisticated mechanized or automated test systems for general use. Although many automated ultrasonic systems have been developed (*31*), their use is almost entirely restricted to highly specialized applications (e.g. inspection of nuclear pressure vessels) or where components of identical geometry are inspected (e.g. inclusions and lamination checks in plate and strip mills or inspection of pipeline girth welds). It has, however, long been recognized that errors incurred by manual measurements of probe location during a test and reliance on the subjective interpretation of echoes appearing on the flaw detector screen could significantly affect the accuracy and reliability of defect detection and measurement. On the other hand, studies comparing the performance of a manual operator with more sophisticated test methods (*5*) indicate that assumptions inherent in sizing procedures used play a far more significant role in introducing errors of measurement than operator error. Furthermore, it is difficult to simulate the wealth of experience of defect diagnosis from ultrasonic signals built up by an operator over a period of time by a fixed signal analysis algorithm in an automated recording system.

In this context it is worthy of note that the systems that have been used to some extent in the field have all assisted the operator rather than attempted to replace him. The instruments concerned, notably the Danish Welding Institute's P-scan (*21*), the CEGB's B-scan (*27*) (see Figure A-1), and Southwest Research Institute's SUTAR system (*32*), all provide a means of measuring probe position and a display in which the information is more highly organized to allow the operator to make a better judgment.

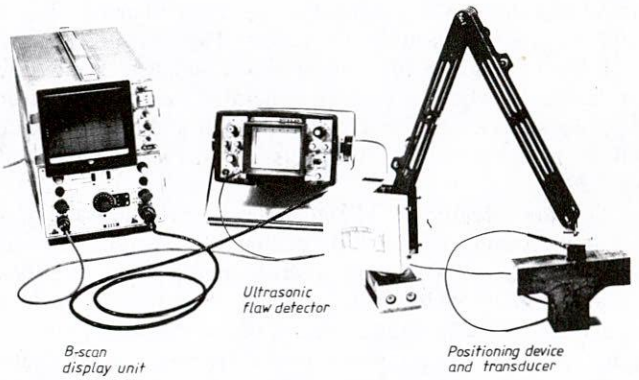

Figure A-1. B-scan equipment.

APPENDIX B

LITERATURE SURVEY

An assessment of literature relevant to the program was carried out throughout the duration of the work in order to provide background information on, and development of, the AWS Code, similar codes which also rely on amplitude of ultrasonic signals for defect assessment, and other size measurement techniques. Sources searched were The Welding Institute's Weldasearch computerized data retrieval system, the Compendex system, also available through The Welding Institute's computer, the nondestructive testing information retrieval system administered by the NDT Centre at the Atomic Energy Research Establishment, Harwell, England, and the NDT Information Analysis Center (NTIAC) operated by Southwest Research Institute in the United States.

A principal consideration was to examine factors affecting the performance of various sizing methods.

PROBLEMS ASSOCIATED WITH USE OF AMPLITUDE FOR DEFECT ASSESSMENT

General Considerations

The amplitude of an ultrasonic signal reflected from a defect is an easily measured parameter and would be expected to convey useful information about the nature of the reflecting site. For this reason it has been used as the basis for AWS (*1*) and ASME (*12*) inspection procedures and for the DGS method pioneered in Germany (*16*), which is in widespread use on the Continent of Europe.

However, to use echo amplitude directly to estimate defect size or severity leads to extreme difficulties because of the complexity of production of the reflected echo. Variations in amplitude can arise from a variety of sources:

1. *Nature of the interface at a discontinuity*—The production of a reflected signal relies on acoustic mismatch or difference in acoustic impedance at a boundary (*2*). This gives rise to transmitted and reflected components of the incident wave, and it is normally the reflection that is collected and displayed. For a free surface of a solid (e.g., the edge of a metal plate), almost total reflection will occur. This will also apply to an air or gas filled crack. However, if a flaw is filled with solid (e.g., a slag line or an oxide filled crack), the transmitted component of the incident wave can be significant (*33*) with a consequent drop in intensity of the reflected wave.

2. *The reflection process*—The transmission and reflection of sound at discontinuities, previously described, only applies to the theoretical situation of plane waves at normal incidence to infinite planar surfaces. When a flaw has a finite size, smaller than the wavefront, and the wave is not at normal incidence, the behavior of the reflected wave is no longer simple. Baborovsky et al. (*34*) demonstrated by practical and theoretical studies that no fewer than 14 different wave trains were scattered or reflected by a surface breaking slit from a single incident shear wave. Similarly, the diffraction effects, whereby sound is generated over 360° as if from a point source, observed for both planar and volumetric defects, have been used as the basis for other sizing techniques (*5, 29*).

3. *Flaw orientation and roughness*—From the assumption that ultrasound propagates rectilinearly, thereby allowing ray diagrams to be used to predict sound paths, it is evident that the angle which a flaw plane makes with an incident beam will influence the direction of the reflected pulse and therefore will affect detection. An investigation by Meyer (*35*) carried out on smooth machined slots of different sizes showed clearly the great effect of orientation on amplitude of reflected signal, the result being given in Figure 5 of the main report. Echo amplitude is not only highly sensitive to angle of incidence, but this dependence increases as defect size becomes greater. This is almost certainly due to a lesser tendency for large defects (in relation to the ultrasonic wavelength) to behave as diffraction sources reradiating sound over 360°. In addition, a study by Coffey (*7*) which also included defect surface roughness as a parameter indicated a reduction of signal amplitude with increasing roughness at normal incidence but a lesser rate of fall in amplitude with increasing angle of incidence for rough defects as opposed to smooth slots. Recent work at The Welding Institute (*5*) has corroborated these findings on the effect of roughness. Indeed it appears that defect roughness has a major controlling influence on the reflected signal amplitude. Echoes received only arise from small, favorably oriented areas on the crack surface rather than from the major plane of the crack itself, which confirms that the echo amplitude bears little or no relation to the dimensions of the major plane of a crack but is wholly dependent on small facets of the surface.

Influence of AWS D1.1 Procedural Requirements

In addition to the considerations previously given, which are associated with the physics of ultrasound, some of the stipulations of the AWS Code also affect test performance. A strict testing procedure is laid down (Section 6c), with an acceptance/rejection criterion for any defect based principally on its amplitude of response. Section 9.25.3 of the Code states: "Ultrasonically tested welds are evaluated on the basis of a discontinuity reflecting ultrasound in proportion to its effect on the integrity of the weld." Table 9.25.3 (see Table 1) of the Code sets out the amplitude threshold levels for acceptance/rejection for different probe angles and plate thicknesses.

This procedure was developed from recommendations resulting from studies carried out on behalf of AWS. Many details of current procedures are outlined in the report of investigations carried out by the California Division of Highways into ultrasonic inspection methods for welds in bridges (*36*). The test procedure has gained wide acceptance within the United States and elsewhere (*37*). The philosophy behind the AWS Code test method was outlined by Shenefelt (*38*) shortly after its introduction, and the same principles apply to the current version (*1*). One of the main factors which has influenced the development of the rigorous AWS Code procedure is the view that: "In order to attain consistent results in ultrasonic weld testing, it is necessary that a consistent procedure be used" (*38*). Although this is generally accepted, the tendency within the United States has been to structure testing procedures so the operator is constrained by rigid scanning, sensitivity, and accept/reject requirements, which in practice allow little latitude for the use of judgment based on experience when assessing defects. This is true of both the AWS (*1*) and ASME (*12*) ultrasonic inspection requirements, the two major codes used within the United States, and is in sharp contrast to practice within the United Kingdom. In the UK, the usual procedure is to establish a suitable test method for the job using recommended test methods outlined in British Standards (*11*) or similar documents (*9, 10*), but these are only guidelines for good practice and do not prevent procedural variations being incorporated to meet the demands of the testing situation or to aid defect diagnosis.

Transducer specification has a profound effect on test resolution. Coffey (*7*) estimates that range resolution is no better than one quarter the ultrasonic pulse length, measured in inches (mm) in the material under test, which is dependent on transducer frequency and level of damping. Similarly, lateral resolution is equal to one-half the beam width, which is principally dependent on transducer frequency and crystal size. The requirement to use relatively large transducers in the 2.0–2.5 MHz range would indicate that both lateral and range resolution will be less than the optimum attainable with smaller crystals and higher frequencies.

Efficiency of coupling between the ultrasonic probe and surface has been shown to vary markedly with changes in surface finish (*3*) with consequent variations in actual test sensitivity. This will change the apparent sensitivity used to assess a defect's "d" rating. There is no precise requirement for surface finish given in the Code.

The "2 dB per inch" correction for material attenuation is also a source of error in estimating "d" ratings. Experimental and theoretical work on the nature of DGS and DAC curves (*16, 22*) has shown that the slope of such curves is highly dependent on attenuation and cannot be represented by a simple correction factor.

Performance of Defect Assessment Techniques Based on Amplitude

A comprehensive systematic study of the foregoing effects has been undertaken by Serabian (*8*) who concluded that the inherent problems associated with the use of signal amplitude, either directly or indirectly, to evaluate flaws impose severe limitations on the attainable accuracy of such methods. The developments of amplitude independent sizing methods and the use of computing techniques to extract more information from the available signal are advocated.

Certainly programs aimed at establishing the effectiveness of amplitude-based techniques have yielded disturbing results. Results of the Plate Inspection Steering Committee (PISC) exercise in Europe (a subsidiary of the PVRC ultrasonic testing assessment program) were presented in two principal ways: the probability of defect detection by the procedures used and the probability of rejecting correctly an unacceptable defect according to the code in force (ASME Section XI) (*6*). It was shown that a crack would require to have a through-wall size of 2.4 in. (60 mm) for an 85 percent probability of detection (the limiting value) at the 95 percent confidence level if the PISC procedure (based on ASME XI) were used. Other types of defects, notably cluster defects, showed even poorer probabilities of detection. Similarly, crack-like defects were required to be 2.8 in. (70 mm) deep to be correctly rejected by the procedure in 85 percent of cases at the 95 percent confidence level (again the limiting value).

Additionally so called "alternative procedures" were also employed during the PISC exercise. These consisted of a variety of specialized manual and automated methods developed for inspection of nuclear plant components and exhibited a significant overall improvement on the PISC procedure. For crack-like defects, detection probability reached 95 percent for a defect through-wall size of 2.0 in. (50 mm) and probability of correct rejection, again for crack-like defects, was 95 percent for a through-wall size of 0.7 in. (18 mm). In addition, for the PISC procedure, there was poor correlation between estimated and actual defect size. Errors were smaller for the alternative procedures. Other studies of accuracy of techniques based on amplitude, specifically related to AWS D1.1 (*14, 15*), again showed a poor correlation between defect size estimated by the method stipulated and actual size.

OTHER DEFECT SIZING METHODS

The other principal method of sizing defects is to use echo signal amplitude indirectly, monitoring the way this rises and falls as the transducer is traversed over a defect (*9, 10*). Some of the inherent complications of the reflection process continue to apply to these "probe movement" methods and their use does not completely eradicate sizing errors. Again, Serabian (*8*) has attempted to quantify the effects of flaw size, orientation, roughness, etc. on the detection and measurement process. It is clear that the large number of interrelated variables which will potentially affect the test result, together with the almost infinite variety of possible flaw morphologies, will give rise to detection problems and measurement errors. Nevertheless, a measurement of defect through-wall size is obtained, and recent work (*5, 17*) has been aimed at quantifying the magnitude of errors involved so error tolerance levels can be generated. This approach enables the size measurements so obtained to be used reliably as an input to fracture mechanics.

However, the error magnitude of ± a few millimeters obtained from the previous studies can lead to considerable variations in fracture assessment and ways of improving accuracy have been sought. Problems of ensuring reproducibility of results with amplitude-based methods (*38*) prompted Silk and his colleagues to investigate time-of-flight methods for defect measurement. These largely overcome the problems associated with amplitude measurement, and their accuracy has been demonstrated (*5, 29, 30, 33, 39*). In recent reviews of defect sizing methods Doyle and Scala (*40*) and Lumb (*41*) conclude that time-of-flight methods of defect measurement offer great potential for improving measurement reliability.

Other methods for defect measurement which have been researched include maximum amplitude (*8*) (note: this is not the same technique as the one referred to elsewhere in this report), spectroscopy (*8, 42*), synthetic aperture focussing (*43*), and holography (*18, 19*)—but none of these is yet suitable for use in the field as a general inspection tool and they have not been thoroughly evaluated on real defects. However, as indicated in Appendix A, the use of computing techniques is becoming more widespread in equipment for field use (*26, 32*), and in some cases highly complex mathematical analyses are incorporated in such instruments (*44*). Another avenue currently being explored is that of using electromagnetic generation of ultrasound instead of a piezoelectric element. This gives greater control over the resulting ultrasonic beam, and it enables wave modes to be generated which cannot be excited by a piezoelectric crystal. Some work has been performed within the UK in this area (*45*), but wider applications are currently being sought in the US (*20*).

APPENDIX C

RESEARCH SPECIMENS

GENERAL DESCRIPTION

The results of ultrasonic examinations of welds are critically dependent on the nature of the joint under test and the form of defects present. In a program such as this where techniques and procedures are being studied with respect to a particular type of joint (i.e., structural welds in bridges), it

is highly desirable that the specimens used represent as closely as possible the conditions prevailing in such joints.

To this end, all welded specimens produced were manufactured from equivalent grades of steel to those used in the United States for structural steelwork. Welding processes were representative of those widely used for welding bridge structures, namely shielded metal arc (SMA) (also known as manual metal arc (MMA)), and submerged-arc (SAW). Surface finish was typical of that found in structural weldments (i.e., hand grinding of weld caps produces a rippled, uneven finish which cannot be adequately simulated by machining), and defects introduced for study were, where possible, "natural" flaws. It should be noted that all defects introduced were intended to be representative of fabrication defects only. Fatigue cracks were not included.

A total of 17 welded specimens were produced in three thicknesses of steel plate in which 35 defects were manufactured. In addition three further specimens were manufactured by diffusion-bonding with a total of 8 shallow square slots of known size incorporated into the bond face to simulate planar defects. This enabled interim conclusions to be drawn from the program during its execution without the need to destroy specimens.

MATERIAL

A recent study (*4*) has shown that minor microstructural variations between different grades of ferritic carbon and low alloy steel have little effect on ultrasonic behavior. Nevertheless microstructural and compositional changes do affect welding metallurgy and can influence the form of defects produced in the weld. It was therefore decided to use steels conforming to ASTM Grade A36, a typical structural grade. Table C-1 gives the chemical composition requirements for A36 steels, and Table C-2 (a and b) gives chemical analyses of the three plate thicknesses used for these investigations. These were conducted at The Welding Institute and were obtained using a direct reading spectrograph after remelting a through-thickness sample to minimize the effect of local compositional variations.

It can be seen that these plates fall within the A36 specification with the exception that the 3.9-in. (98-mm) plate had a lower silicon level than specified. This one variation would not be expected to influence metallurgical properties sufficiently to affect ultrasonic testing.

WELDING

Welding was carried out entirely in a conventional manner using the SMA and SAW processes, except where these needed to be modified to introduce the required flaws. Details of the welding process and weld preparations for the specimens are given in Table C-3, and an example of the process record sheets (for J204) is given in Figure C-1 and Figure C-2. Four types of defect were included. These were:

1. *Slag lines*—Linear inclusions produced by insufficient interrun cleaning.
2. *Lack of fusion*—both sidewall and interrun, produced by using low power metal inert gas (MIG) welding to deposit the required area of defect. This method effectively casts metal into the joint with no fusion of the metal below because of insufficient heat input.
3. *Solidification cracking*—Produced by submerged-arc welding using a condition to give a deep, narrow weld bead, the shrinkage stresses on cooling causing the bead to rupture along the center line.
4. *Freeze-break cracking*—produced by partially welding the joint, cooling it, and fracturing it in a brittle manner through the ligament of weld metal. The two halves are then fitted together and the weld completed.

All mechanisms except freeze-breaking produce entirely natural flaws that are highly desirable for demonstration of the capabilities of ultrasonics. Furthermore, their location and dimensions can be closely controlled during the welding operation. Freeze-break cracks are not natural as they are brittle failures, and such crack morphologies would not be expected to be found in welds. Nevertheless, it is otherwise difficult to produce cracking greater than one weld pass in depth; therefore this method was used for the larger cracks. For example, solidification cracking is only likely to exist within one bead under most circumstances.

Further details of the manufacture of controlled defects for weld testing purposes are given in the Document C1, "Making defective welds," which is appended.

On completion the weld caps of all specimens were ground by hand to leave a generally flat surface, and all were radiographed to establish whether the intended defects had been produced successfully. All appeared satisfactory except that only one defect was clearly defined in specimen J201. (The original radiographs are available if required.)

TABLE C-1
ASTM A36 CHEMICAL COMPOSITION REQUIREMENTS.

Plate thickness	Element, wt%				
	C (Max.)	Mn	P (Max.)	S (Max.)	Si
To 3/4in. (19mm) inclusive	0.25	-	0.04	0.05	-
Over 3/4 to 1½in. (19 to 38mm) inclusive	0.25	0.80-1.20	0.04	0.05	-
Over 1½ to 2in. (38 to 64mm) inclusive	0.26	0.80-1.20	0.04	0.05	0.15-0.30
Over 2½ to 4in. (64 to 102mm) inclusive	0.27	0.85-1.20	0.04	0.05	0.15-0.30

TABLE C-2(a)
CHEMICAL COMPOSITION 0.4-IN. (10-MM) PLATE.

Element, wt%																
C	S	P	Si	Mn	Ni	Cr	Mo	V	Cu	Cb	Ti	Al	B	Pb	Sn	Co
0.24	0.021	0.007	0.26	0.76	0.02	0.01	0.01	<0.01	0.02	<0.005	<0.005	0.050	<0.0005	<0.01	<0.01	<0.01

TABLE C-2(b)
CHEMICAL COMPOSITION 3.9-IN. (98-MM) AND 1.5-IN. (40-MM) PLATE.

Sample	Element, wt%																
	C	S	P	Si	Mn	Ni	Cr	Mo	V	Cu	Cb	Ti	Al	B	Pb	Sn	Co
3.9in. (98mm) plate	0.24	0.022	0.027	0.07	1.02	0.05	0.03	0.01	<0.01	0.02	<0.005	0.004	0.016	<0.0005		<0.01	0.02
	0.23	0.020	0.027	0.07	1.01	0.05	0.03	0.01	<0.01	0.02	<0.005	0.005	0.018	<0.0005		<0.01	0.02
	0.25	0.038	0.011	0.02	1.04	0.06	0.03	0.01	<0.01	0.02	<0.005	<0.003	0.010	<0.0005		<0.01	<0.01
1.5in. (40mm) plate	0.15	0.016	0.012	0.23	0.90	0.02	<0.01	<0.01	<0.01	0.01	<0.005	<0.003	0.029	<0.0005		<0.01	<0.01
	0.15	0.016	0.012	0.21	0.89	0.02	<0.01	<0.01	<0.01	0.01	<0.005	<0.003	0.030	<0.0005		<0.01	<0.01
	0.15	0.015	0.012	0.22	0.90	0.02	<0.01	<0.01	<0.01	0.01	<0.005	<0.003	0.033	<0.0005		<0.01	<0.01

TABLE C-3
WELDING DETAILS.

Specimen number	Plate thickness		Welding process	Preparation	Root gap		Root face		Preparation angle degrees (total)
	Inches	(mm)			Inches	(mm)	Inches	(mm)	
J201	3.9	(98)	SAW	Double V	0.16	(4)		0	65
J202	3.9	(98)	SAW	Double V	0.16	(4)		0	65
J203A	3.9	(98)	SAW	Double V	0.16	(4)		0	65
J203B	3.9	(98)	SAW	Double V	0.16	(4)		0	65
J204	3.9	(98)	SAW	Double V	0.16	(4)		0	65
J205A	3.9	(98)	SAW	Double V	0.16	(4)		0	65
J205B	3.9	(98)	SAW	Double V	0.16	(4)		0	65
J206	3.9	(40)	SAW	Double V	0.16	(4)		0	65
J207	3.9	(40)	SAW	Double V	0.16	(4)		0	65
J208	3.9	(40)	SAW	Double V	0.16	(4)		0	65
J209A	3.9	(40)	SAW	Double V	0.16	(4)		0	65
J209B	3.9	(40)	SAW	Double V	0.16	(4)		0	65
J210	3.9	(40)	SMA	Double V	0.16	(4)		0	50
J211	0.4	(9.5)	SAW (2 passes)	Square butt	0.16	(4)	-	-	-
J212A	0.4	(9.5)	SMA	Single V	0.06	(1.5)	0.06	(1.5)	70
J212B	0.4	(9.5)	SMA	Single V	0.06	(1.5)	0.06	(1.5)	70
J213	0.4	(9.5)	SMA	Single V	0.06	(1.5)	0.06	(1.5)	70

NB. All submerged arc welded specimens (except J211) have SMA root pass.

DIFFUSION BONDING

The diffusion bonding process produces a joint between two flat clean surfaces by the application of heat and pressure. The joint is made entirely in the solid state by, as the name implies, diffusion of voids away from the interface to eliminate the boundary between two pieces of material, leaving a single component. No macroscopic deformation is observed during bonding. This process required a high standard of surface preparation of the joint surfaces, which are butted together prior to the joint being made. It is therefore apparent that a shallow groove cut in one of the joint surfaces will leave a void in the subsequent bond. This has been exploited to produce totally embedded reference reflectors of known size for ultrasonic calibration purposes, and further details are given in Document C2, "Diffusion bonded test blocks for ultrasonic testing," which is included at the end of this appendix.

Three specimens were produced by this method for use in the program to provide a set of known reference defects with which other results might be compared in the interim without destroying specimens. Two of these were square butt joints, but the third contained a bond angled at 30° to the thickness direction of the plate to simulate inclined fusion boundary defects.

All defects were in the form of square slots 0.005 in. (0.13 mm) deep and milled into one of the joint faces. Their form on completion of the joint is therefore that of a rectangular planar defect. Details of the specimens and defect dimensions are given in Table C-4.

SPECIMENS

The range of specimens produced enabled the capabilities of the AWS Code ultrasonic techniques plus the other methods used to be investigated on a variety of cracks and non-crack-like flaws. Furthermore, the thicknesses used, 0.4, 1.5 and 3.9 in. (9.5, 40 and 98 mm) enabled a range of the specified AWS Code procedures to be included in the study and the effect of thickness on the accuracy of other methods to be examined.

A complete description of all the specimens used in this program is given in Table C-5. This includes details of defects intended to be produced during welding. A description of the actual defects and sectioning procedures is given in the following.

THE WELDING INSTITUTE

SUBMERGED ARC

WELDING RECORD SHEET

PROCEDURE No. J204

NAME OF WELDER EILEEN8 JOB No. 3625

DATE OF WELDING 15·10·79 P.W.LAB REF. 5345

Welder to record information when boxes ticked.

✓	WIRE TRADE NAME	Boc. MOREX			
✓	BATCH No.'s	um 8617			
✓	FLUX TRADE NAME	Boc.			
	QUANTITY USED	✓	WIRE Boscrod S1	✓	FLUX 450
			SLAG WEIGHT		
✓	SKETCH ELECTRODE CONFIGURATION, EXTENSION, ETC.				
✓	POWER SOURCERS AND WELDING HEAD ESAB 800				
✓	ROOT RUN PROCESS AND CONSUMABLES MMA 4mm 7018				
	FLUX BURDEN DEPTH				
	SLAG DETACHABILITY				

SKETCH ☐

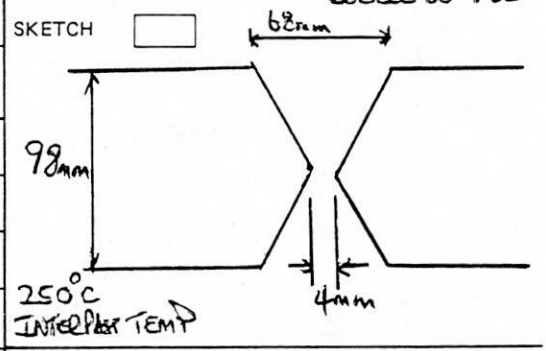

ELECTRODE CONFIGURATION

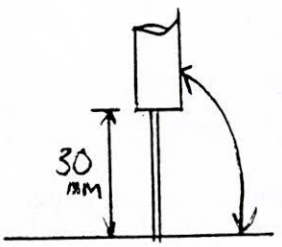

	RUN No.	MMA 1–20	21	39	40–142
✓	ELECTRODE No.		1 →		
✓	WIRE DIA.	4 mm	4 mm →		
✓	CURRENT AC DC + DC -	AC 151 Amps	DC+ 400 Amps →		
✓	ARC VOLTAGE		26 →		
✓	TRAVEL SPEED		839 mm/min	510 mm/min →	
	ENERGY INPUT				

	ADDITIONAL INFORMATION REQUIRED
	DEFECTS OBSERVED
	REPAIRS CARRIED OUT
✓	WAS FORM PW1 (REQUEST FOR WELDING SERVICES) OR PW3 (PROCEDURE) FOLLOWED? YES ✓ NO ☐ IF NOT, STATE CHANGES
	WERE NDT STANDARDS ACHIEVED? IF NOT, STATE WHY

P.W. LAB. INSPECTION.

Signed: [signature]

INSPECTED BY: [signature] SATISFACTORY FOR RELEASE ✓

Date: 15·10·79

Form no. P.W.6

Figure C-1. Process record sheet for welding of specimen J204 (welding conditions).

TABLE C-4
DETAILS OF DIFFUSION-BONDED SPECIMENS.

Specimen number	Plate thickness		Joint preparation	Planar defect sizes	
	Inches	(mm)		Inches	(mm)
J251	0.4	(9.5)	Square edge	1.2 x 0.1	(30 x 3)
				1.2 x 0.2	(30 x 6)
J252	1.5	(40)	Bevel edge*	1.2 x 0.1	(30 x 3)
				1.2 x 0.2	(30 x 6)
				1.2 x 0.5	(30 x 12)
J253	1.5	(40)	Square edge	1.2 x 0.1	(30 x 3)
				1.2 x 0.2	(30 x 6)
				1.2 x 0.5	(30 x 12)

*30° from vertical

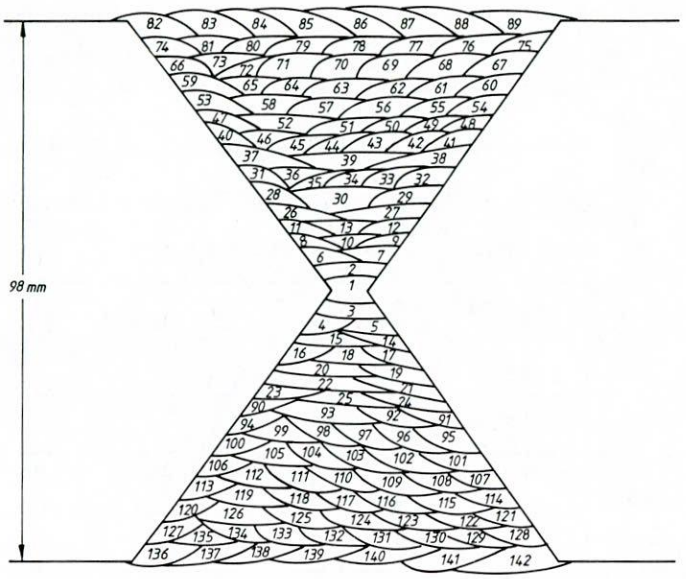

Figure C-2. Process record sheet for welding of specimen J204 (welding sequence).

Each specimen was clearly marked with its individual number, and reference points were identified according to the requirements of the Code, Section 6.19. Surfaces A and B were marked—A being marked with a Y—and on both surfaces a center line was scribed on the ground weld cap, this representing x = 0. This enabled distance along the weld to be measured (from end y) and identification of the surfaces A+, A−, B+ and B−, the distance x being measured from the scribed center line.

SURFACE FINISH FOR TESTING

All specimens had an as-rolled plate surface finish with the weld caps hand-ground smooth, producing a smooth, but rippled, finish. Studies by Coffey (*3*) have indicated that a minimum requirement for surface finish for components to be ultrasonically tested is a short range roughness better than 125 μin. CLA (3.2 μm Ra) and a medium range waviness such that a gap greater than 0.020 in. (0.5 mm) cannot be present beneath a 2 in. (50 mm) long straight edge placed anywhere on the surface.

Assessment of roughness of the specimens using a comparator gauge indicated that they were all well within the limit given above, but waviness was more difficult to quantify. To do this a stylus attached to a linear displacement transducer was scanned across the specimen and the output plotted on an x-y recorder to produce a trace of the vertical displacement of the stylus tip. Line scans were taken every 0.4 in. (10 mm) over the weld area, both perpendicular and parallel to the weld centerline. The results for J204 are shown in Figure C-3 and Figure C-4, respectively. Only three areas on perpendicular scans and no areas on parallel scans were found to be outside the above requirements. The surface was therefore considered suitable for testing according to these criteria, and surfaces of other specimens gave very similar results.

However, these surface criteria were determined with the miniature probes commonly used in the UK in mind, which have a contact surface area in the region of 0.3 in.^{2} (60 mm^2). Contact areas or probes meeting AWS D1.1 Section 6.15 requirements may have a contact area of 1 in.^{2} or more (greater than 645 mm^2) and, consequently, a smaller degree of waviness can be tolerated if coupling is to be maintained. Difficulties were experienced on occasions in maintaining coupling during tests to AWS procedures on these surfaces, which are not atypical of those expected on a site weld.

SECTIONING

After completion of the ultrasonic tests most of the specimens were sectioned to reveal actual dimensions of the defects present. This was done in two ways. First, a brittle fracture technique was used for defects of a simple shape. This involves determination of a defect's location from radiographic and ultrasonic data and cutting a full width slice containing it from the specimen. A shallow V notch is then milled in the surface of the slice directly above the position of the defects to act as an initiator, and the block is cooled in liquid nitrogen to ensure brittle behavior, thus ensuring minimal deformation. The sample is then fractured in a three-point bend loading mode. In most cases the fracture takes place directly through the defect so that its morphology and size can be measured.

Second, more complex defects and those not suitable for brittle fracture (such as some horizontal lack of fusion or those whose position has not been so closely defined by nondestructive tests) were revealed by progressive sectioning. This involves isolating a block containing the defect and then taking transverse sections (perpendicular to the x = 0 line) every 0.2 in. (5 mm). This enables the detail of the defect's cross-section to be clearly seen, and morphology along its length can be determined by interpolation between

TABLE C-5
SPECIMEN DETAILS.

Specimen			Intended defects			
Number	Dimensions		Defect number	Type	Size requested	
	Inches	(mm)			Inches	(mm)
J201	13.8 x 13.8 x 3.9	(350 x 350 x 98)	1	Solidification crack	2 x 3/16	(50 x 4)
			2	Solidification crack		
			3	Solidification crack		
J202	11.8 x 13.8 x 3.9	(300 x 350 x 98)	4	Slag line	2 x 1/8	(50 x 3)
			5	Slag line		
			6	Slag line		
J203A	1.3 x 13.8 x 3.9	(160 x 350 x 98)	7	Freeze-break crack	2 x 3/8	(50 x 9)
J203B	5.5 x 13.8 x 2.9	(140 x 350 x 98)	8	Freeze-break crack		
J204	11.8 x 13.8 x 3.9	(300 x 350 x 98)	9	Lack of fusion	2 (50mm) long, depth uncertain	
			10	Lack of fusion		
			11	Lack of fusion		
J205A	6.3 x 13.8 x 3.9	(160 x 350 x 98)	12	Freeze-break crack	2 x 3/8	(50 x 9)
J205B	5.5 x 13.8 x 3.9	(140 x 350 x 98)	13	Freeze-break crack	2 x 3/16	(50 x 4)
J206	13.8 x 13.8 x 1.4	(350 x 350 x 40)	14	Solidification crack	2 x 3/16	(50 x 3)
			15	Solidification crack		
			16	Solidification crack		
J207	13.4 x 13.8 x 1.5	(340 x 350 x 40)	17	Slag line	2 x 1/8	(50 x 3)
			18	Slag line		
			19	Slag line		
J208	9.8 x 13.8 x 1.5	(250 x 350 x 40)	20	Freeze-break crack	2 x 1/4	(50 x 6)
			21	Freeze-break crack	2 x 3/8	(50 x 9)
J209A	4.9 x 13.8 x 1.5	(125 x 350 x 40)	22	Freeze-break crack	2 x 1/4	(50 x 6)
J209B	4.7 x 13.8 x 1.5	(120 x 350 x 40)	23	Freeze-break crack	2 x 3/8	(50 x 9)
J210	13.6 x 13.8 x 1.5	(320 x 350 x 40)	24	Lack of fusion	2 (50mm) long, depth uncertain	
			25	Lack of fusion		
			26	Lack of fusion		
J211	5.9 x 11.8 x 0.4	(150 x 300 x 9.5)	27	Freeze-break crack	2 x 3/16	(50 x 4)
J212A	11.8 x 11.8 x 0.4	(300 x 300 x 9.5)	28	Lack of fusion	2 (50mm) long, depth uncertain	
			29	Lack of fusion		
			30	Lack of fusion		
J212B	11.6 x 11.8 x 0.4	(295 x 300 x 9.5)	31	Lack of fusion		
			32	Lack of fusion		
			33	Lack of fusion		
J213	9.8 x 11.8 x 0.4	(250 x 300 x 9.5)	34	Slag line	2 (50mm) long, depth uncertain	
			35	Lack of fusion		
J251	5.9 x 7.9 x 0.4	(150 x 200 x 9.5)	36	Square slot	1.2 x 1/8	(30 x 3)
			37	Square slot	1.2 x 1/4	(30 x 6)
J252	8.7 x 7.9 x 1.5	(220 x 200 x 40)	38	Square slot	1.2 x 1/8	(30 x 3)
			39	Square slot	1.2 x 1/4	(30 x 6)
			40	Square slot	1.2 x 1/2	(30 x 12)
J253	8.7 x 7.9 x 1.5	(220 x 200 x 40)	41	Square slot	as for 38	
			42	Square slot	as for 39	
			43	Square slot	as for 40	

the defect on each of the slices. Note that 0.2 in. (5 mm) is the thinnest slice which can be conveniently handled.

In both cases all parts of the specimen were stamped and reference points for dimensions scribed on before cutting, so that positions of defects in the various sections could be related to the original datum points. Sectioning method defects found and their sizes are given in Table C-6. Examples of defects are shown in Figures C-5 through C-9.

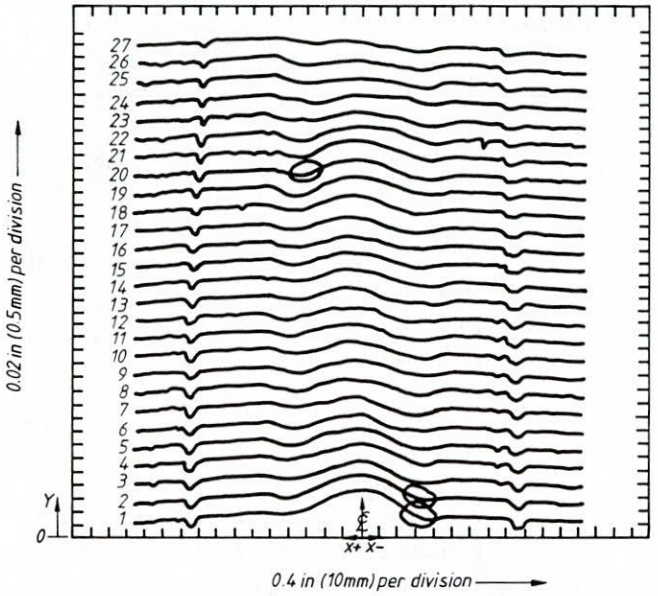

Figure C-3. Surface finish of specimen J204. Scans perpendicular to weld centerline. Ringed areas show a gap of greater than 0.5 mm under a 50-mm straight edge.

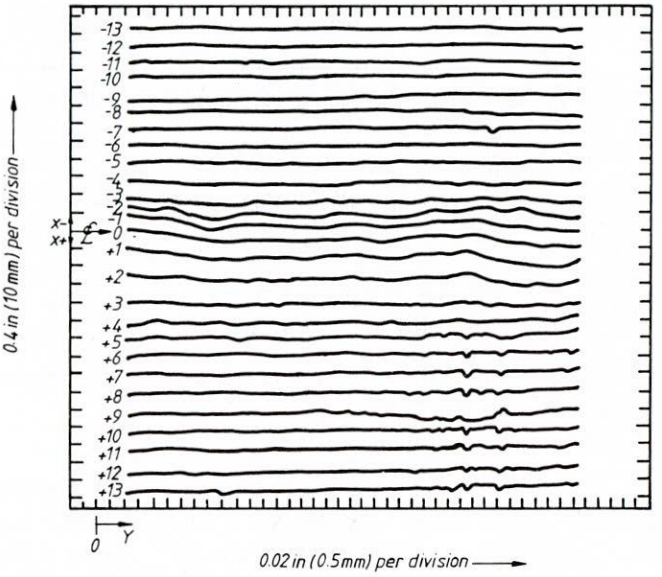

Figure C-4. Surface finish of specimen J204. Scans parallel to weld centerline.

Figure C-5. Macrosection of solidification cracks, defect 1. (Enhanced by magnetic particle inspection.)

TABLE C-6
SECTIONING AND DEFECTS REVEALED.

Specimen	Defect number	Sectioning* method	Defect revealed	Size length x depth x width+	
				Inches	(mm)
J201	1	S	Solidification cracks	2.2 x 0.5 x 0.1 1.1.x 0.3 x 0.1	(56 x 12 x 2) (28 x 7 x 2)
	2	Not sectioned	Not confirmed radiographically		
	3	Not sectioned	Not reliably confirmed ultrasonically		
J202	4	F	Slag line	2.0 x 0.1 x 0	(51 x 3 x 0)
	5	F	Slag line	2.0 x 0.1 x 0	(52 x 3 x 0)
	6	S	Slag line + short crack	2.2 x 0.20 x 0.12	(55 x 5 x 3)
J203A	7	F	Freeze-break crack	1.81 x 0.2 x 0	(46 x 5 x 1)
J203B	8	S	Freeze-break crack	2.1 x 0.3 x 0.1	(52.5 x 8.5 x 2)
J204	9	Not sectioned	Many small reflectors present in specimen. Retained for further study		
	10	Not sectioned			
	11	Not sectioned			
J205A	12	F	Freeze-break crack	2.2 x 0.4 x 0	(55 x 9 x 0)
J205B	13	F	Solidification crack	1.8 x 0.2 x 0	(45 x 4 x 0)
J206	14	F	Solidification crack	2.0 x 0.1 x 0	(52 x 3.5 x 0)
	15	F	Solidification crack	1.9 x 0.1 x 0	(47 x 3 x 0)
	16	F	-	-	-
J207	17	F	Slag line	2.0 x 0.2 x 0	(52 x 4 x 0)
	18	F	Slag line	2.0 x 0.2 x 0	(52 x 4 x 0)
	19	F	Slag line	2.3 x 0.2 x 0	(58 x 4 x 0)
J208	20	F	Freeze-break crack	1.9 x 0.2 x 0	(49 x 4 x 0)
	21	F	Freeze-break crack	2.0 x 0.3 x 0	(50 x 7 x 0)
J209A	22	F	Freeze-break crack	2.0 x 0.3 x 0	(51 x 7 x 0)
J209B	23	F	Freeze-break crack	1.9 x 0.4 x 0	(49 x 9 x 0)
J210	24	F	Lack of fusion	2.1 x 0.3 x 0.2	(54 x 8 x 4)
	25	F	Lack of fusion	2.0 x 0.1 x 0.2	(52 x 3 x 6)
	26	F	Lack of fusion	2.2 x 0.2 x 0.1	(56 x 6 x 3)
J211	27	F	Freeze-break crack	2.1 x 0.2 x 0	(54 x 4 x 0)
J212A	28	Not sectioned			
	29	Not sectioned			
	30	Not sectioned			
J212B	31	Not sectioned			
	32	Not sectioned			
J212B	33	Not sectioned			
J213	34	F	Slag line	1.9 x 0.1 x 0	(48 x 2.5 x 0)
	35	F	Lack of fusion	2.0 x 0.1 x 0.3	(50 x 1.5 x 7)
J251	36	Not sectioned			
	37	Not sectioned			
J252	38	Not sectioned			
	39	Not sectioned			
	40	Not sectioned			
J253	41	Not sectioned			
	42	Not sectioned			
	43	Not sectioned			

* Method of revealing defects - S = sectioned
F = freeze break

+ "Width" indicates lateral extent for volumetric defects and lateral distance between extremities for non-vertical planar defects.

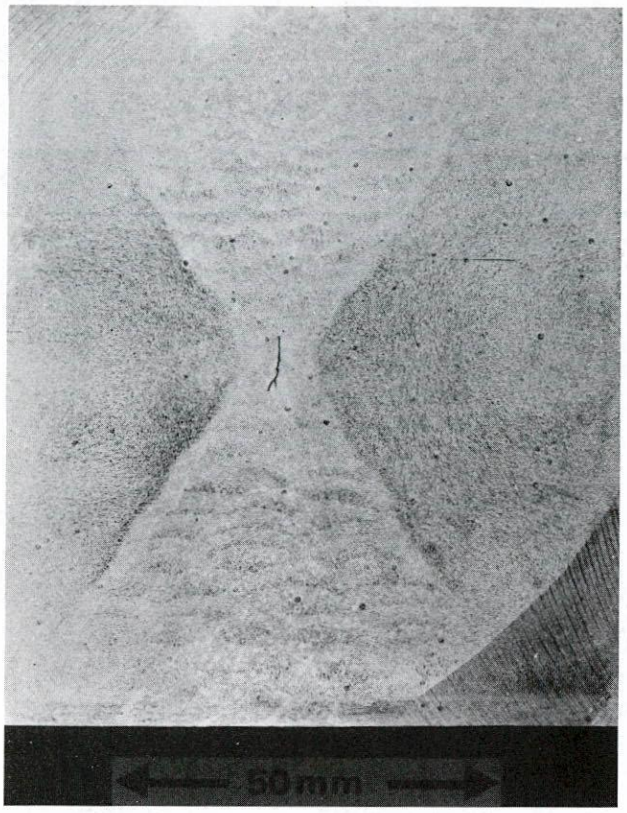

Figure C-6. Macrosection of freeze-break crack, defect 8. (Enhanced by magnetic particle inspection.)

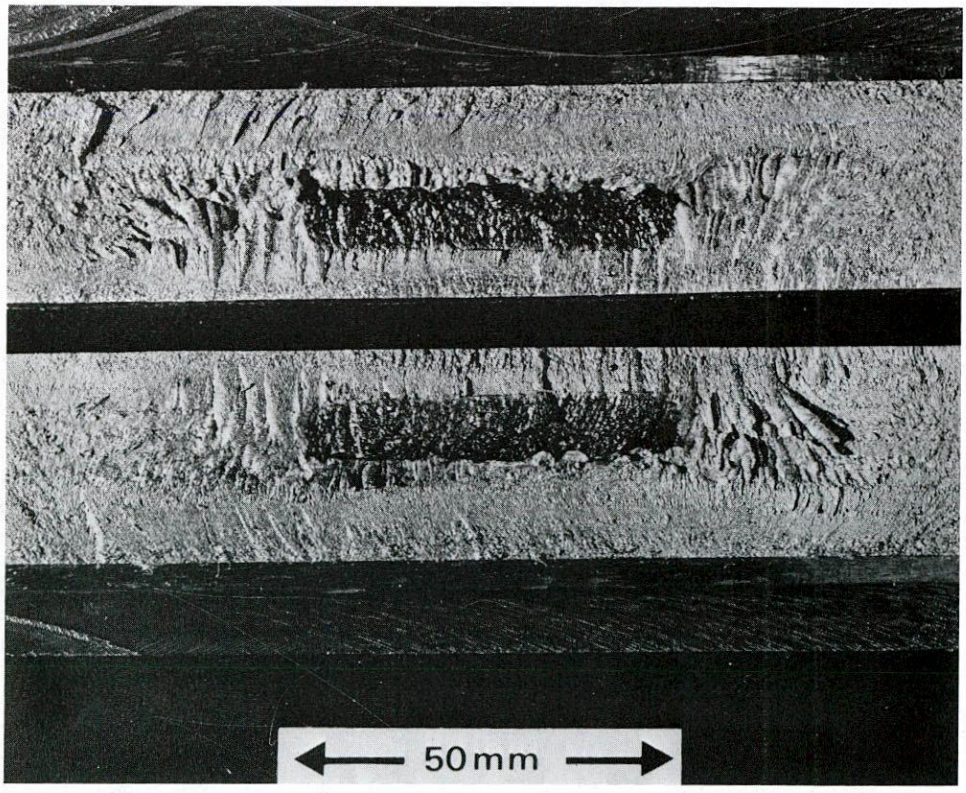

Figure C-7. Fracture surfaces revealing freeze-break crack, defect 29.

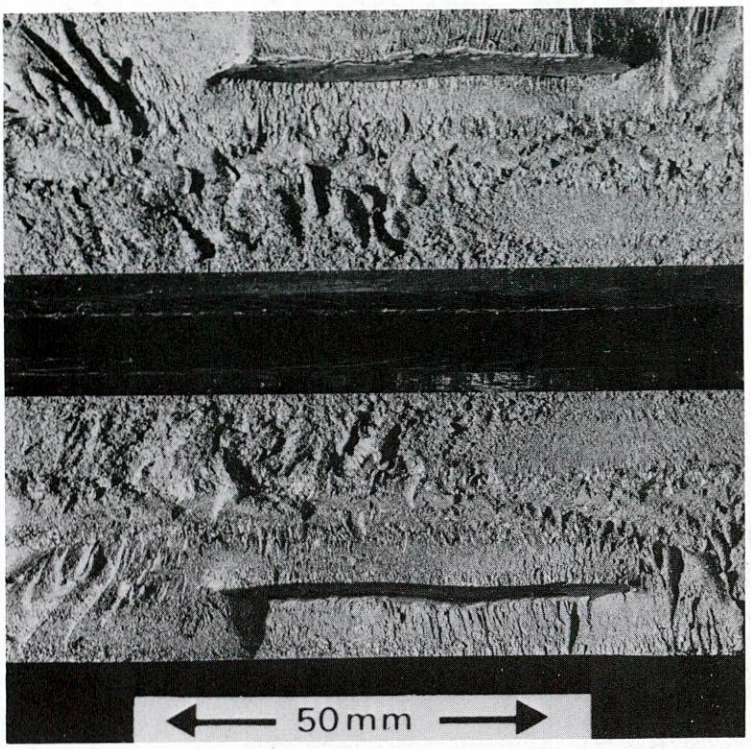

Figure C-8. Fracture surfaces revealing lack of fusion, defect 25.

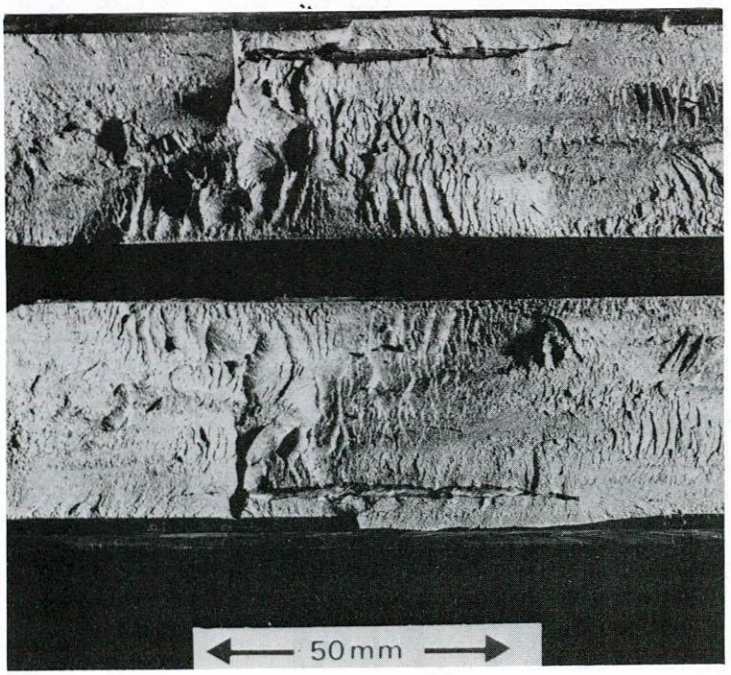

Figure C-9. Fracture surfaces revealing slag line, defect 17.

Making defective welds

by J Haugh, Tech(CEI) and T J Jessop, BSc(Eng), ACGI, MWeldI

An article with an identical title to this was published in the *Research Bulletin* in 1974.[1] The author described methods which were being used at that time to produce weld defects in a controlled and reproducible manner for research into the significance of defects, and for training of non-destructive testing (NDT) operators. He stated that: 'fabricators, recalling problems which they have experienced in reducing defects in their own products, are amused that the Institute has perhaps had greater problems in making defects to order.' This still applies today, but the requirements for welds containing defects have become more stringent and a wider range of materials has been studied. This article reports recent work in this area.

In August 1976 the Institute embarked upon a major programme to study the interaction of ultrasonic energy with real defects in ferritic steel weldments. It was hoped that this would provide data to enable the accuracy and reliability of defect characterisation by ultrasonic testing to be improved. It is clear that the quality of the defective specimens produced for such a programme is of vital importance. All types of defect were required and, since defect size was to be studied as a variable, some control over defect dimensions was necessary.

The project is continuing,[2] although most of the specimens have now been manufactured. Publicity for the project brought several requests from Research Members for the supply of specimens containing defects, and consequently activity in this area has been considerable. Most specimens have been made from structural or pressure vessel steels but, more recently, stainless steel defective specimens have been ordered for both internal projects and for a Research Member.[3]

In discussing defective specimens it is important to define the type of method used to produce the defect. The most satisfactory source of specimens is structures and fabrications which were intended for service but were found to be unacceptably defective. Unfortunately, it is rarely economically feasible for structures to be scrapped: repair of the defects is generally undertaken. However, there have been cases where specimens have been obtained in this way; for example lamellar tearing was so extensive in one particular vessel that it was donated to The Welding Institute for research purposes! The best alternative is to create, in the laboratory specimen, the conditions necessary for the required defect to form naturally. This is the approach most often adopted. The third possibility, when neither of the above methods is successful, is to simulate the defect as closely as possible.

Mr Haugh is in the Arc Welding Department and Mr Jessop is Section Head of Non-Destructive Testing Research in the Engineering Department.

GENERAL CONSIDERATIONS

Defective specimens have been made in various dimensions and thicknesses: typically in the range 150 × 150 × 12mm thick to 500 × 500 × 80mm thick. The upper limit is set generally by the necessity to move the specimen about the laboratory for the various operations during manufacture. The number of defects per specimen usually ranges from one to four depending on size.

Defective specimens have also been manufactured in the form of circumferential pipe welds (typically 150mm diameter by 19mm wall). These specimens present an additional difficulty in view of the lack of access from the reverse side, and because of the narrow weld preparation.

The submerged arc (SA) or manual metal arc (MMA) welding processes are normally used for plate specimens. In pipe specimens, MMA, tungsten inert gas (TIG) or metal inert gas (MIG) processes are used. TIG weld runs are also used where necessary to protect the defect from being fused into the molten pool of the following passes of MMA, SA or MIG using normal welding currents.

The size of the defect requested may vary, but 50mm long is usual for all types. The width and through thickness alter according to the type of defect. The various tolerances on size are indicated

Typical sizes and tolerances of defects.

	Size, mm	Tolerance	
		Length,* mm	Through thickness, mm
Slag inclusions	50 × 2	±1	±1
Porosity	50 × 5	±2	$\pm^{4}_{1}$
Incomplete penetration	50 × 1.5	±1	±1
Lack of fusion	50 × 5	±1	±1
Solidification crack	50 × 5	±1	±2
Brittle fracture crack	50 × 8	±1	±1
HAZ crack	Not determined		

**Generally controlled by mechanical trimming* (e.g. *grinding*).

in the Table. All weld metal defects can be controlled in the longitudinal dimension by mechanical trimming (*e.g.* grinding) before the covering runs are completed. Control of the through thickness dimension relies on controlling the penetration of the covering passes.

DEFECTS

Slag inclusions

The welding processes which are prone to slag inclusions are MMA, MIG and SA. Slag inclusions can be found in any position in a welded joint and in practice slag defects in a weld usually are scattered. The size of these defects varies: sometimes they occur as small particles (Fig. 1) and sometimes as a continuous line (Fig. 2).

A slag line can be produced at any position in the weld and would generally be made about 50mm long with a cross sectional dimension of ~2mm. This is inserted by welding to the point where one end of the defect is to be located, and restarting the weld pass ~54mm further on. Adjacent passes can be completed as normal, leaving a recessed volume of ~54 × 7 × 3mm into which powdered slag is placed, where it fuses as the temperature is raised during subsequent passes. Small TIG weld runs are made on either side of the slag until a bridging run can be placed to cover the defect.

This area must be covered by 4–5mm of weld metal using a low current before conventional welding procedures can continue. Protection of the defect is also ensured by placing subsequent weld passes such that the weld bead overlaps the defect rather than being placed directly on top of it.

Porosity

Porosity is one of the most difficult defects to control as any attempt to cover the defect can result in the porosity being drawn into the covering weld bead. To introduce porosity, a cavity of similar size and depth to that required for a slag inclusion defect is prepared. Methods which can then be employed include:

1 Using MIG welding with CO_2 shielding – porosity can be introduced by reducing the shielding gas flow by ~50%.

The amount can be controlled to some extent by increasing or decreasing the gas flow. An example of porosity introduced by this method is shown in Fig. 3.

2 Using SA welding with damp or insufficient flux – the amount is determined primarily by the dampness.

3 MMA welding – among several techniques, use of iron powder electrodes on low current will give some porosity but not to the extent attained by method 1. Use of a low hydrogen electrode with an arc slightly too long is another possibility, but controlling the amount of porosity is difficult.

4 TIG welding with reduced gas shielding and strips of black mild steel as a filler – good control can be achieved.

Once the porous section has been filled, welding is completed as for slag inclusions.

Incomplete penetration

Incomplete penetration to the root face in a close butt weld preparation is a possible defect in sub-

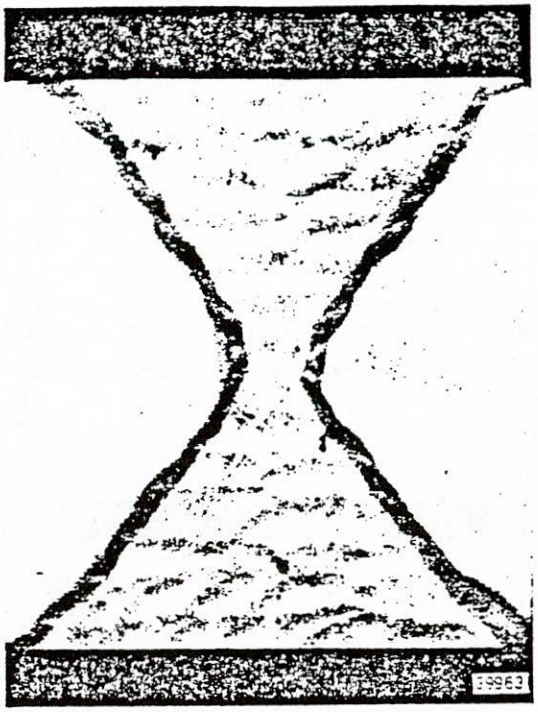

1 Scattered small slag inclusions. 45mm plate.

2 Slag line defect. 45mm plate.

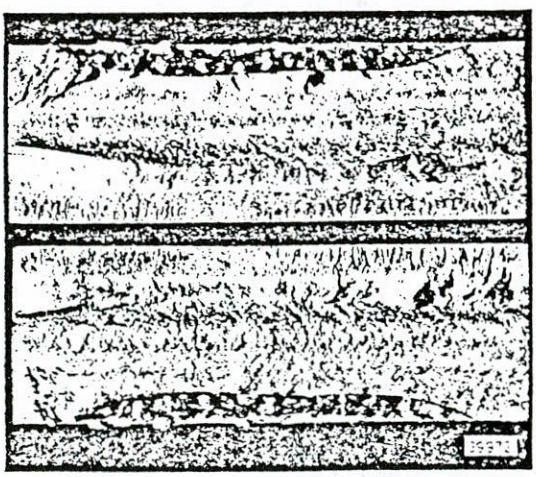

3 Coarse porosity in root area. 39mm plate.

merged arc welding where the root face is likely to be 5 to 6mm deep. The defect can be produced by using any of the techniques mentioned previously (in a SA joint preparation) with a condition to give a known depth of penetration. The weld is built up with MMA welding until sufficient weld metal is deposited to hold back the penetration of subsequent submerged arc welding passes. Approximately 4mm of weld metal would be required. An example is shown in Fig. 4.

For smaller root faces (1.5–2mm), small TIG weld runs are deposited prior to the normal root run, to ensure that full penetration does not take place. Approximately 2–3mm depth of filler is required in this case, and great care must be taken to avoid lack of fusion in the root area.

4 Incomplete root penetration, 40mm plate.

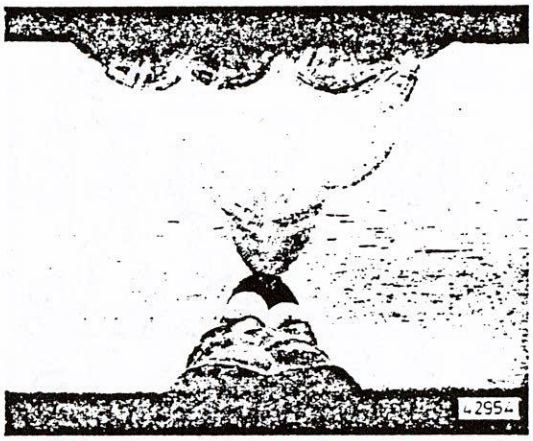

5 Incomplete penetration with associated lack of sidewall fusion in stainless steel.

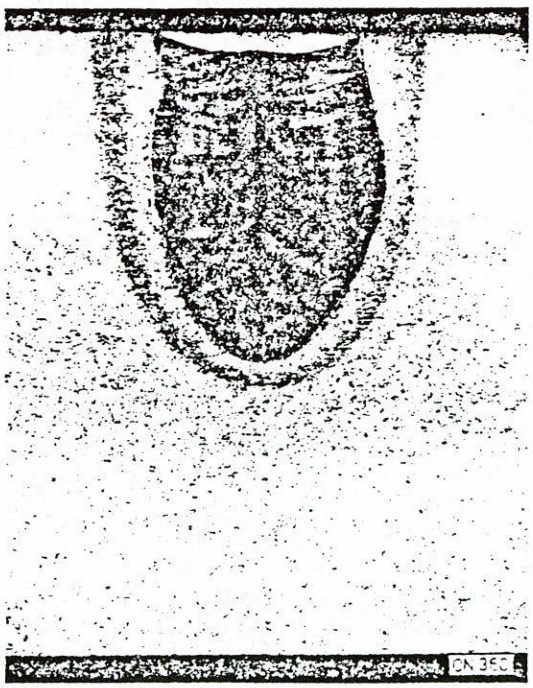

6 Natural solidification crack, 18mm plate.

Lack of fusion

Preparation for the defect is similar to that required for slag inclusions, the size of the prepared area being determined by the size of defect required. The defect is produced by TIG welding using a larger filler wire (approximately double the size of that used for the bulk of the weld), and a continuous feed into the molten pool. It is necessary to ensure that there is sufficient heat only to melt the filler and not enough to fuse it into the prepared surface area. The edges are fused properly all around the defect. Incomplete penetration with associated lack of sidewall fusion is shown in Fig. 5.

Cracking

Solidification method

Solidification cracks will occur naturally when a SA weld run with a large depth to width ratio is deposited in an appropriate groove (Fig. 6).

A suitable welding condition is 700A, 25V and 800 mm/min. A 6mm deep, 5mm wide groove is employed at the desired position in the weld, or, in the root of a close butt preparation, a maximum included angle of 55° and a root face of approximately 9mm are required. The latter is necessary to avoid burn through at this high current.

The weld run needs to be 100mm long to ensure a 50mm long defect, in view of the time taken to reach the maximum welding speed.

Heat affected zone (HAZ) cracking

Hydrogen induced HAZ cracking can be produced by using the opposite of what is normally considered to be good welding practice. For example, cracking can be promoted by welding with damp rutile electrodes over an area on the sidewall where the crack is required. A hardenable steel (EN8) is used normally for that side of the weld with no preheat while the defect is being produced. Of all defects, the manufacture of hydrogen cracks is probably the least reliable and controllable.

Brittle fracture method

This method can be used only for cracks in the root area. The specimen is partially welded where a crack is required. This is normally not more than 50mm long with a weld thickness of 8mm. The weld is notched and the whole specimen is cooled in dry ice. It is then fractured in three point bending. The crack faces are subsequently matched and welded in the normal way after TIG runs along the edge of the crack to ensure control of penetration. A radiograph of a completed specimen containing such a defect is shown in Fig. 7.

Weld metal hydrogen cracking ('chevron' cracking)

An example of this type of defect is shown in Fig. 8. The cracks have a characteristic orientation and when they appear in successive weld beads on a longitudinal section they form a 'chevron' pattern.

The phenomenon has been studied in detail[4,5] and a method has been devised for producing this type of defect reliably in the laboratory.[4]

This involves using submerged arc welding with damp flux and a water quench between runs.

7 Radiograph of a crack produced by the brittle fracture method.

CONCLUDING REMARKS

Production of defects to order will never be an exact science, and some tolerance is inevitably necessary. Whilst slag inclusions, incomplete penetration, lack of fusion, and solidification cracks can all be produced with reasonable certainty and to a close tolerance, porosity and other types of cracks are less predictable.

There is scope for future work in the production of HAZ cracks, and it is hoped that future NDT projects will encompass this area.

8 Chevron cracks.

Acknowledgements

The authors gratefully acknowledge the assistance of Mr C Eileens, who produced many of the welded specimens.

References

1 Gregory E N: 'Making defective welds'. *Welding Institute Research Bulletin* 1974 15 (7) 199–204.

2 Jessop T J *et al:* 'Size measurement and characterisation of weld defects by ultrasonic testing. Part 1 Non-planar defects in ferritic steel'. Welding Institute Report Series.

3 Private communication with Röntgen Technische Dienst bv, Rotterdam.

4 Tuliani S S: 'A metallographic study of chevron cracks in submerged arc weld metals'. CEGB Research Report R/M/R234, May 1976.

5 Wright V S and Davison I T: 'Chevron cracking in submerged arc welds'. Paper 38, Welding Institute Conference 'Trends in steels and consumables for welding', November 1978.

Diffusion bonded test blocks for ultrasonic inspection

by P. M. Bartle, AIM, MWeldI

Diffusion bonding offers the opportunity to produce test blocks with machined 'defects' completely buried within homogeneous material. Such blocks could greatly enhance the value of ultrasonic inspection by allowing the ready demonstration and close definition of its capability to a degree at present difficult, if not impossible, to achieve. Diffusion bonded test blocks would have application in equipment calibration (defect sizing), operator training, and as structural or component replicas.

PRODUCTION OF DIFFUSION BONDED BLOCKS

Diffusion bonding is a process[1] whereby two clean, well-machined surfaces are heated while held together (under a pressure below the bulk yield stress at the bonding temperature) in a protective environment so that a bond may form across the original interface, Fig. 1. The bond forms as a result of microdeformation of surface asperities and the solution, by the parent metal, of the residual oxide and contaminant layers. In many bonds the original interface cannot be detected when sections are examined under an optical microscope.

Thus, for test blocks, 'defects' can be machined into one or both of the surfaces to be bonded, the plane of which can be inclined at any suitable angle to the final external surfaces. The shape and surface finish of the defects can be tailored to suit requirements. Diffusion bonding should be applicable to most inorganic materials and, therefore, the block material should eventually be a matter for users' choice. It is envisaged, however, that blocks will initially be produced in mild steel.

CALIBRATION (SIZING) BLOCKS

For equipment calibration purposes simple rectangular blocks which contain suitable arrays of defects could be produced to supplement the normal BS 2704:1966 or IIW specification machined calibration blocks. These are basically adequate for calibrations relating to defect position (including time base calibration), but leave a good deal to be desired in respect of defect sizing (amplitude calibration). Defects could be 'ideally' positioned within blocks so that no problems were encountered as a result of back or side wall reflections, the detection of more than one defect at one time, or near field effects.

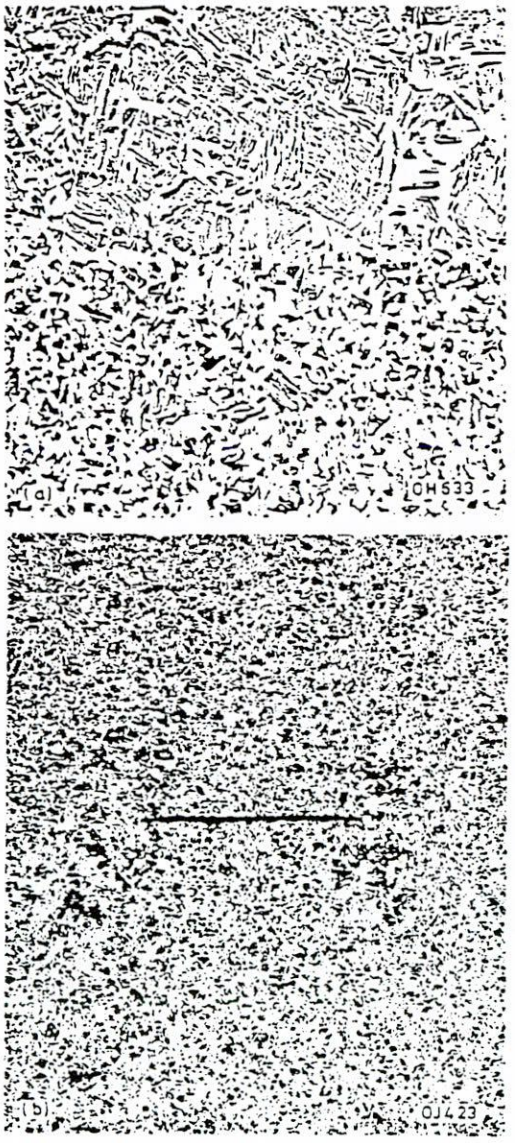

1 Diffusion bond: (a) interface between two mild steel samples revealed only by change of grain structure: etched in nital (50), (b) section through defect: etched in nital (10)

Mr Bartle is a Principal Scientific Officer in the Institute's Process Operation and Control Department.

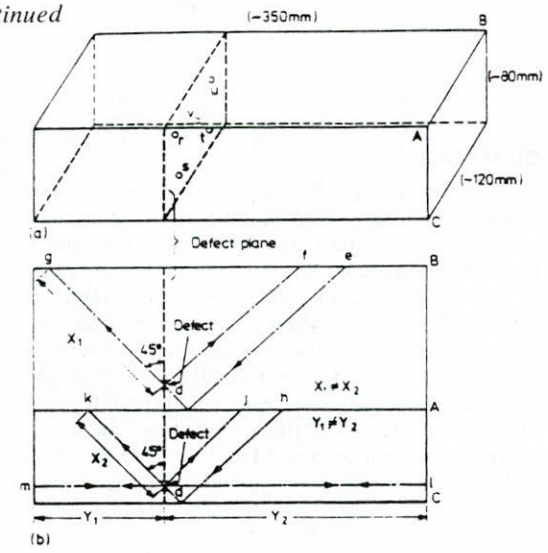

2 Calibration block with 'defects' perpendicular to main axis: (a) arrangement of defects r, s, t, u, v, (b) basic transmission and reflection, single and paired probe beam paths (edf, edg, hdj, hdk, ldl, ldm, mdm)

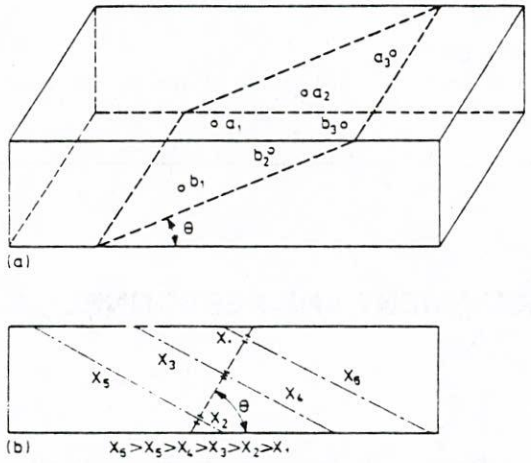

3 Calibration block for single angled probe work: (a) arrangement of three 1mm diameter defects (a_1, a_2, a_3) plus three 2mm diameter defects (b_1, b_2, b_3), (b) basic beam paths X_1 to X_5 (normal θ values 45°, 65°, and 70°) Note: θ in (a) is exceptionally shallow to show layout of defects

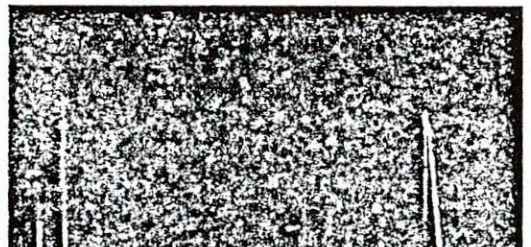

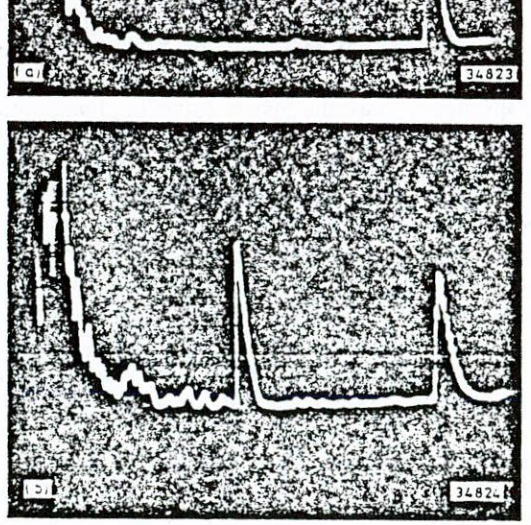

4 Oscillograph traces obtained during ultrasonic examination of diffusion bonded test block (normal probe): (a) beam passing through bond clear of defect (back wall echo only), (b) beam partially on defect (defect and back wall echoes)

Alternatively, defects could be positioned to encounter these difficulties so that their effect on equipment response could be checked. The blocks would be suitable either for calibrating signal amplitudes in relation to defect area, or for use as reference blocks to compare signal amplitudes with those from other testpieces which require examination.

For the calibration approach blocks containing five defects perpendicular to the main axis are visualised, Fig. 2, the defects having diameters of 1, 2, 2·8, 4, and 5·7mm. A suitably designed single block of this type could be used for size calibration with normal probe techniques, angled probe transmission, and tandem probe work. The 1mm diameter defect serves to check size resolution, but the other four have area ratios of 1, 2, 4, and 8 for amplitude calibration. By offsetting the plane of the defects from the centre of a rectangular instead of square cross-section block, calibrations for two surface-to-defect distances could be produced. Having used the above blocks to obtain a basic size calibration, blocks for single angle probe work, containing defects of two sizes (1 and 2mm diameter), could be used for check tests (assuming a repeat full calibration proves unnecessary). For single angled probe work, both ideally and nonideally positioned defects could be included in the same block, Fig. 3, but for defects perpendicular to the main axis, separate blocks would probably be advisable to avoid excessive block sizes. (Blocks of the order of 80 × 120mm section × 350mm long are currently envisaged.)

The same blocks could be used for reference purposes, or separate reference blocks could be produced with defect diameters (as opposed to areas) in fixed ratios. At present the defects in reference blocks are flat-bottomed drilled holes. Although such blocks are in essence simple, drilling narrow, relatively deep, flat-bottomed holes is difficult and the blocks are not suitable for transmission probe use.

Normally for calibration purposes defects would have flat surfaces to give strong reflections and well-defined signals, Fig. 4, but, to establish equipment response more fully, defects with hemispherical or mottled surfaces could be produced. Additionally the production procedure allows blocks to be produced with defects either close to, or well below, the surface for more detailed checking of equipment capabilities.

TRAINING USES

These calibration and reference blocks would be invaluable for initial operator training. They would need to be supplemented with similar blocks which contained larger defects and also with blocks of perhaps less regular shape with defects of size, orientation, and position not revealed to the operator until he had completed his inspection. For training purposes several forms of defect surface should be employed. It is expected that blocks with known artificial defects would be used in conjunction with testpieces containing real defects, e.g. weld defects, but where the defect dimensions have been determined by ultrasonic sizing and radiography (where appropriate) rather than premachining.

Document C2 Continued

It must be remembered that the use of blocks for training purposes will prove satisfactory only if they are employed as part of a well-founded course.

COMPONENT REPLICAS

When applying ultrasonic inspection in practice it is important to know where geometric features of a structure or component cause difficulties: for example, some parts of some tubular assemblies are difficult to inspect. If the validity of ultrasonic inspection for suspect joints can be demonstrated, both confidence in and usefulness of the technique are enhanced. In many situations it would be possible to diffusion bond replicas with specific-sized defects suitably spaced and oriented to allow the value of ultrasonic inspection to be checked. Such replicas would also be very valuable for planning and improving inspection procedures.

SUMMARY

Diffusion bonding offers a method of producing size calibration, reference, training, and replica blocks which contain sized defects of specified position, orientation, and surface finish. Eventually these blocks could be produced in the materials (or material combinations) of the users' choice. They would supplement calibration blocks to BS 2704:1966 or IIW specifications, and might replace current flat-bottomed hole type reference blocks. The value of diffusion bonded blocks is currently being investigated and the author would welcome comments or enquiries from Members.

REFERENCE

1 Bartle, P. M. 'Introduction to diffusion bonding'. *Metal Constr.*, **10** (5), 1969, 241-4.

APPENDIX D

DETAILS OF ULTRASONIC TEST EQUIPMENT AND PERSONNEL

EQUIPMENT

The requirements of the testing program were such that equipment did not need to conform to the AWS D1.1 specifications given in Section 6.15 of the Code, in every test; for example, a wide variety of different transducers was used in the probe movement tests. However, to maintain a degree of consistency throughout the pulse-echo tests, the same ultrasonic flaw detector was used. This was a Krautkrämer USM2M portable flaw detector which complied with Section 6.15 of the Code, the performance being checked according to Code procedures. This type of unit is widely used as a site testing tool.

Tests conducted in accordance with D1.1 procedures were performed using the flaw detector, previously described, in conjunction with an Aerotech "gamma" series 2.25-MHz, ¾-in. (19-mm) diameter compression wave (0°) transducer and three Krautkrämer "WB" series transducers having ¾-in. (19 mm) square transducer elements and operating at 2.25 MHz. The three transducers produced beams of 45, 60, and 70°, respectively. These parameters satisfy the requirements of Section 6.15. An assessment of performance is given in the following.

The "WB" transducers were loaned to The Welding Institute by the American Bridge Division of the US Steel Corporation for use on this project. They were said to be typical of transducers currently employed on bridge structures in the United States.

The effect of using a transducer outside code requirements was explored using an Aerotech "gamma" series transducer of 2.25 MHz and crystal size 1 in. (25 mm) x ¾ in. (19 mm) (outside specified dimensions) in conjunction with Perspex (lucite) wedges to produce 45, 60, and 70° shear wave beams. In all other respects this transducer met Code specifications.

Probe movement tests were conducted using the same flaw detector but a variety of minature angle transducers was used. These are given in Table D-1. Compression (0°) probes were used for preliminary examination of weld and plate for inclusions and laminations.

Equipment for time-of-flight tests is somewhat different from that used for pulse-echo testing. The equipment is shown in Figure D-1. At present, there is no standard specification for such equipment. The probes are a pair of Panametrics 0.5 in. (12.5-mm) diameter transducers, operating at 2.25 MHz, attached to Perspex (lucite) wedges which give 45° compression waves in steel. These are used because they are the fastest travelling bulk wave mode and the received signal is the first observed, thereby avoiding confusion with other reflections and slower moving mode-converted signals. A complete description of the equipment is given in Document G1 (which is included at the end of Appendix G).

Reproducibility of testing conditions is extremely difficult to achieve when tests are performed manually. To overcome this a scanning device was employed for all 'laboratory" pulse-echo tests (i.e., those not involving assessment of operator variability). This ensured that measurement of probe position could be made reliably, thereby reducing the possibility of errors, and coupling between the transducers and specimen surface could be maintained at a virtually constant level, again reducing signal amplitude variations from this source. This device is shown in Figure D-2.

Light oil couplant was used throughout.

TABLE D-1
ULTRASONIC TRANSDUCERS USED FOR PROBE MOVEMENT TESTS.

Welding Institute serial number	Transducer and Type	Angle	Nominal frequency, MHz	Crystal size	
				Inches	(mm)
T33	Krautkrämer MWB45	45°	4	0.3 x 0.4	(8 x 9)
T34	Krautkrämer MWB60	60°	4	0.3 x 0.4	(8 x 9)
T20	Wells-Krautkrämer MAP 45	45°	2	0.3 x 0.4	(8 x 9)

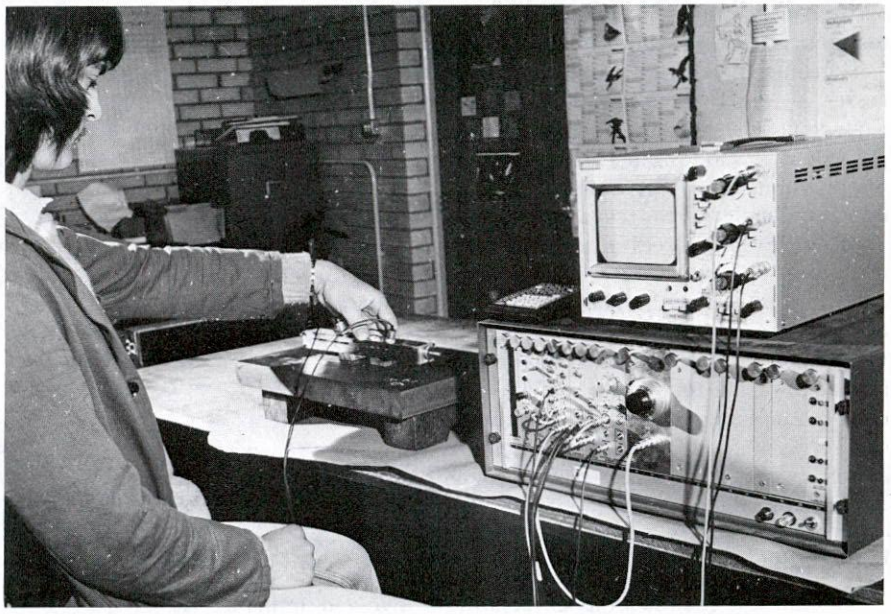

Figure D-1. Time-of-flight equipment—general view.

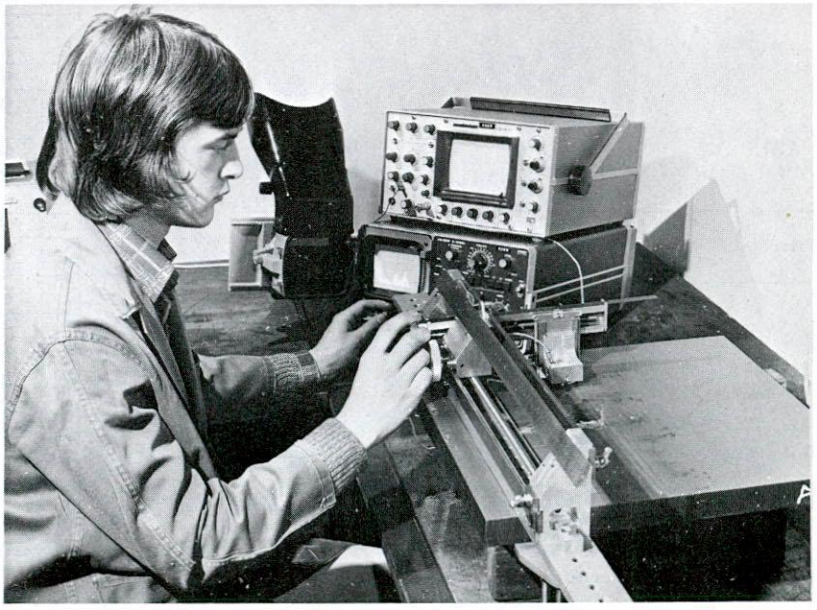

Figure D-2. Scanning device.

Assessment of Equipment Performance

The performance of the flaw detector used for all pulse-echo tests was checked in accordance with Section 6.17 of the Code, using the procedures presented in Section 6.22. Figures D-3 and D-4 show examples of completed forms E9 and E10 from the Code Appendix E, indicating that the unit conforms to Code requirements.

Transducers that were required to conform to Section 6.15 of the Code did so. In addition, the three Krautkrämer "WB" series transducers were subjected to a characterization procedure by the NDTA Centre, CEGB, England, and results are shown in Figures D-5, D-6 and D-7 for the 45, 60, and 70° probes, respectively, which also indicate satisfactory performance. The Aerotech transducer also met the Code requirements except those relating to crystal size.

Transducers used for probe movement tests were not assessed in terms of the requirements of Section 6.15 of the Code, but The Welding Institute's probe characterization procedure was followed. This is based on the UK Electricity Supply Industry (ESI) Standard 10-92 for assessment of miniature angled shear wave probes.

All angle transducers used were deemed satisfactory by this procedure and all were, in addition, subjected to a characterization test by the Harwell NDT Centre as described above. These also indicated satisfactory performance.

At present, there are no similar means of checking performance of the time-of-flight equipment directly, but this can be determined by checking the accuracy of measurement of a series of known reference defects. Accuracy on a range of defects from ⅛-in. to 1½-in. (4 to 40 mm) deep was always better than ±0.020 in. (0.5 mm) after calibration.

PERSONNEL

The relevant qualifications of technicians involved in this study are given in Table D-2. It should be noted that there is no recognized certification procedure for the time-of-flight equipment because it is not a standard test method.

TABLE D-2
OPERATOR QUALIFICATIONS.

Name	Employer	CSWIP qualification grade held*
R. Gibson	The Welding Institute	3.1 and 3.2 butt welds in plate and pipe
J.A.E. Dobbs	The Welding Institute	3.6, plate, pipe and nozzle welds
D.H. Dargue	The Welding Institute	3.1 and 3.2 butt welds in plate and pipe
M.L. Ross	Non-destructive Testers Ltd	3.6, plate, pipe and nozzle welds

* CSWIP = Certification Scheme for Weldment Inspection Personnel (See reference 25)

Ultrasonic Unit Certification

Ultrasonic unit KRAUTKRAMER Date 20. Sept. 1979
Model USM2M Serial no. NPT 1
By T. J. JESSOP
Search unit
Size ¾" DIA Type AEROTECH ASNT Level N/A
Frequency 2.25 MHz

TABULATION CHART

No.	a dB Diff.	b dB Reading	c % Scale	d Correct dB	e dB Error
1	0				
2	6	6	58	8.8	-2.8
3	12	12	74	12.7	-0.7
4	18	18	78	18.2	-0.2
5	24	0/24	81	23.9	+0.1
6	30	20/4	83	23.7	+0.3
7	36	0/30	83	29.7	+0.3
8	42	20/10	82	29.8	+0.2
9	48	20/16	80	36.0	0
10	54	0/36	83	35.7	+0.3
11	60	20/22	83	41.7	+0.3
12	66	20/28	80	48.0	0
13	72	20/34	80	54.0	0
14	78	20/40	90	59.0	+1
15	84	from 0/36			
16	90	40/2	92	40.8	+1.2
17	96	40/8	80	48.0	0
18	102	40/14	80	54.0	0
19	108	40/20	80	60.0	0
20	114	40/26	82	65.8	+0.2
21	120	40/32	85	71.5	+0.5
22	126	40/2	90	41.0	+1
23	132	from 20/16			
24	138	40/36	107	73.5	+2.5
25	144				
26	150				

Find the largest range of consecutive dB error "e" values whose sum is equal to or less than 2 dB such that no consecutive combination within that range exceeds 2 dB.

In order to find the acceptable vertical linearity of the unit, subtract one from the number of error values considered in the range above and multiply the remainder by 6. This dB value is the acceptable dB range of the equipment.

In order for the unit to meet the minimum requirements of 6.17.2, this range shall not be less than 60 dB.

Total qualified range 11 dB to 75 dB = 64 dB Total error 2 dB

Form E-9

Figure D-3. Completed form E9.

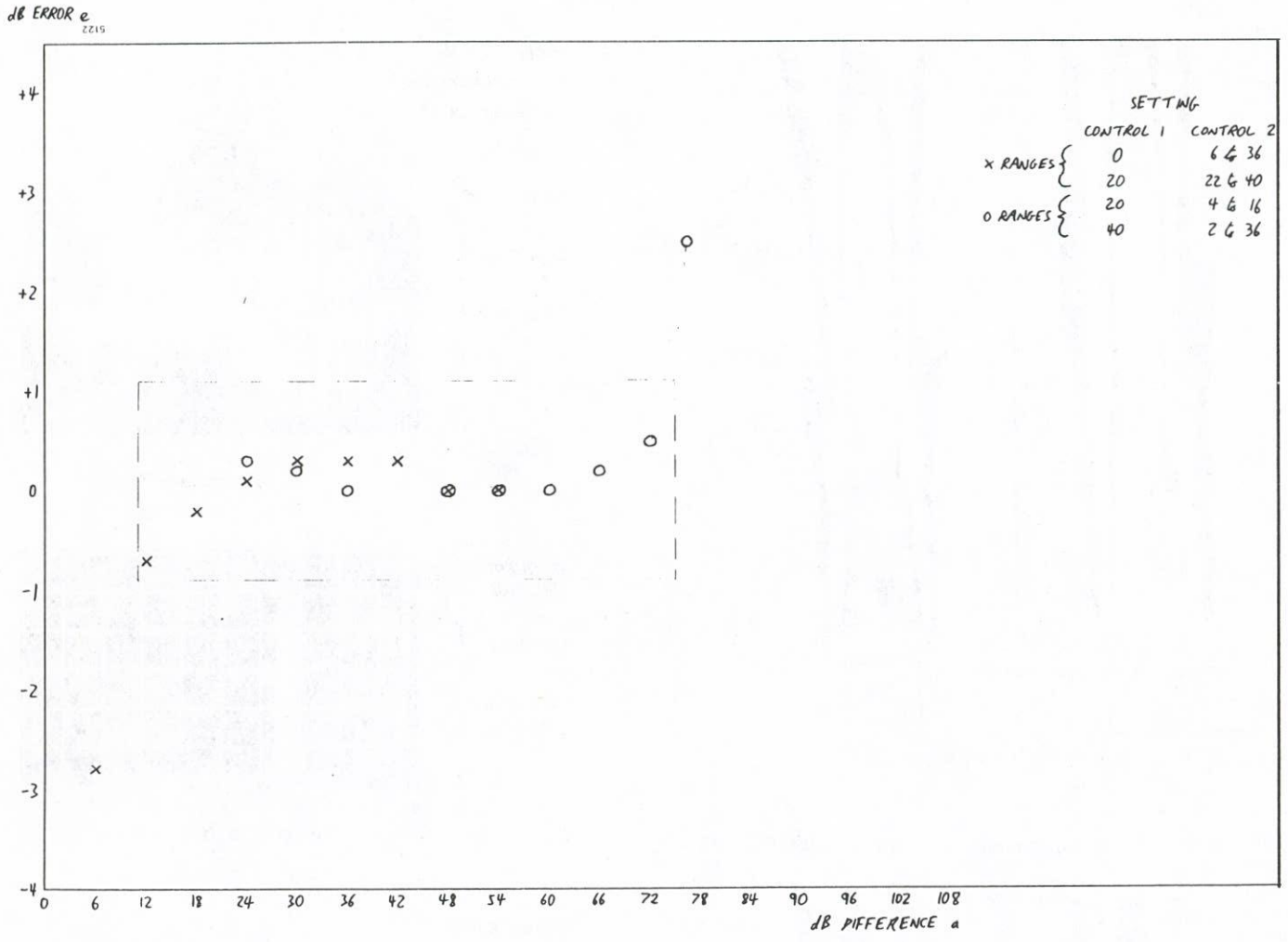

Figure D-4. Completed form E10.

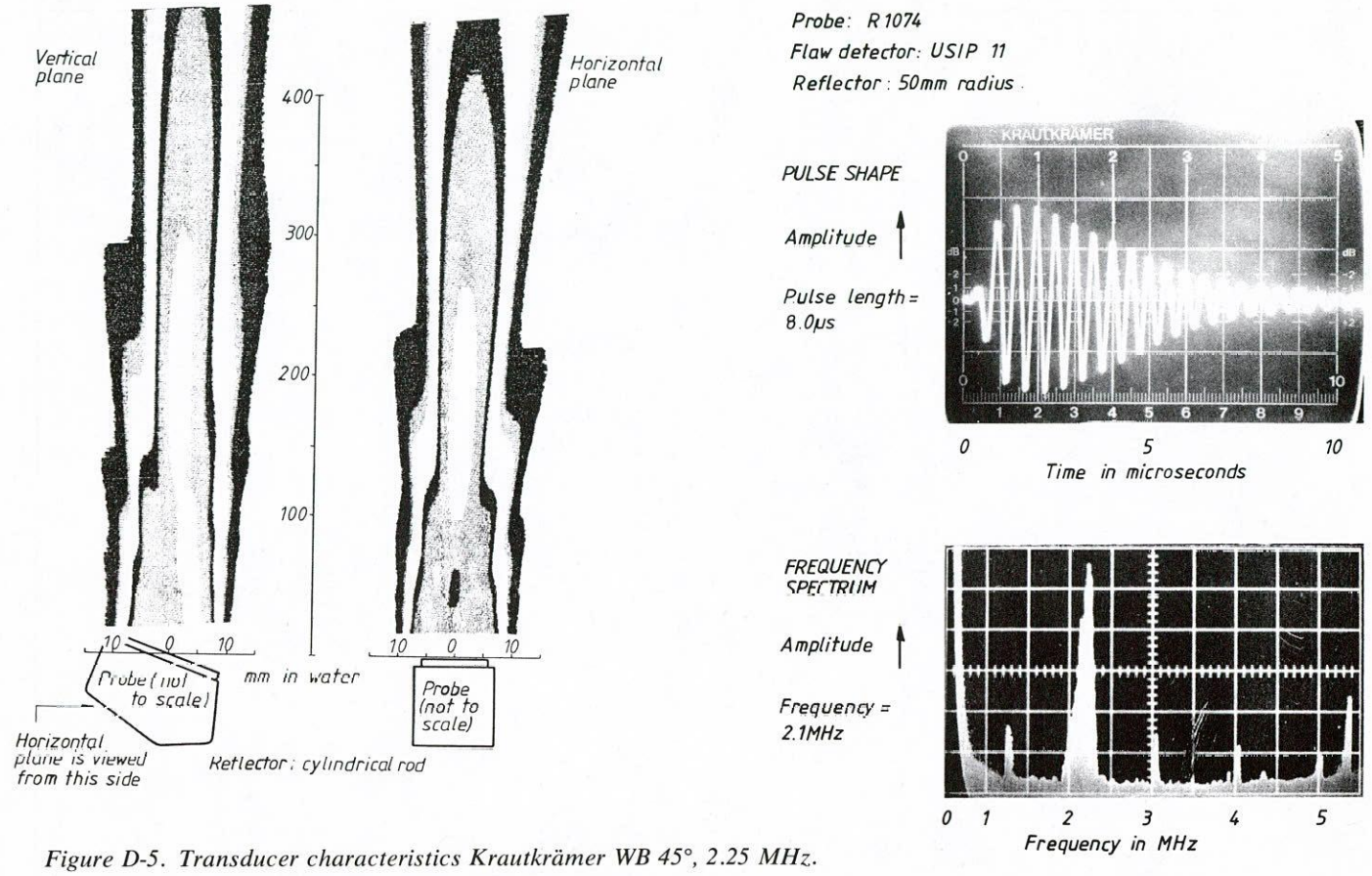

Figure D-5. Transducer characteristics Krautkrämer WB 45°, 2.25 MHz.

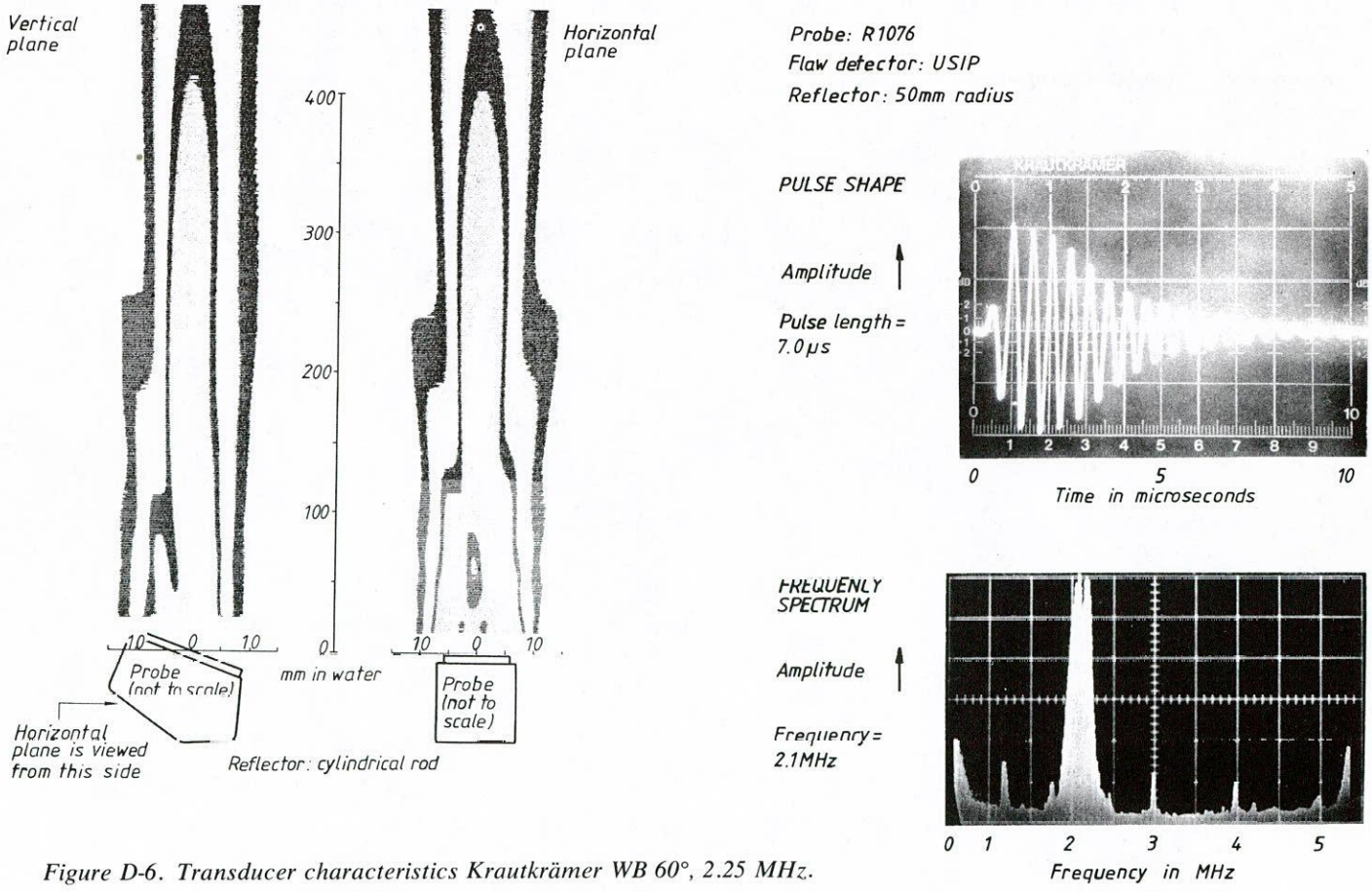

Figure D-6. Transducer characteristics Krautkrämer WB 60°, 2.25 MHz.

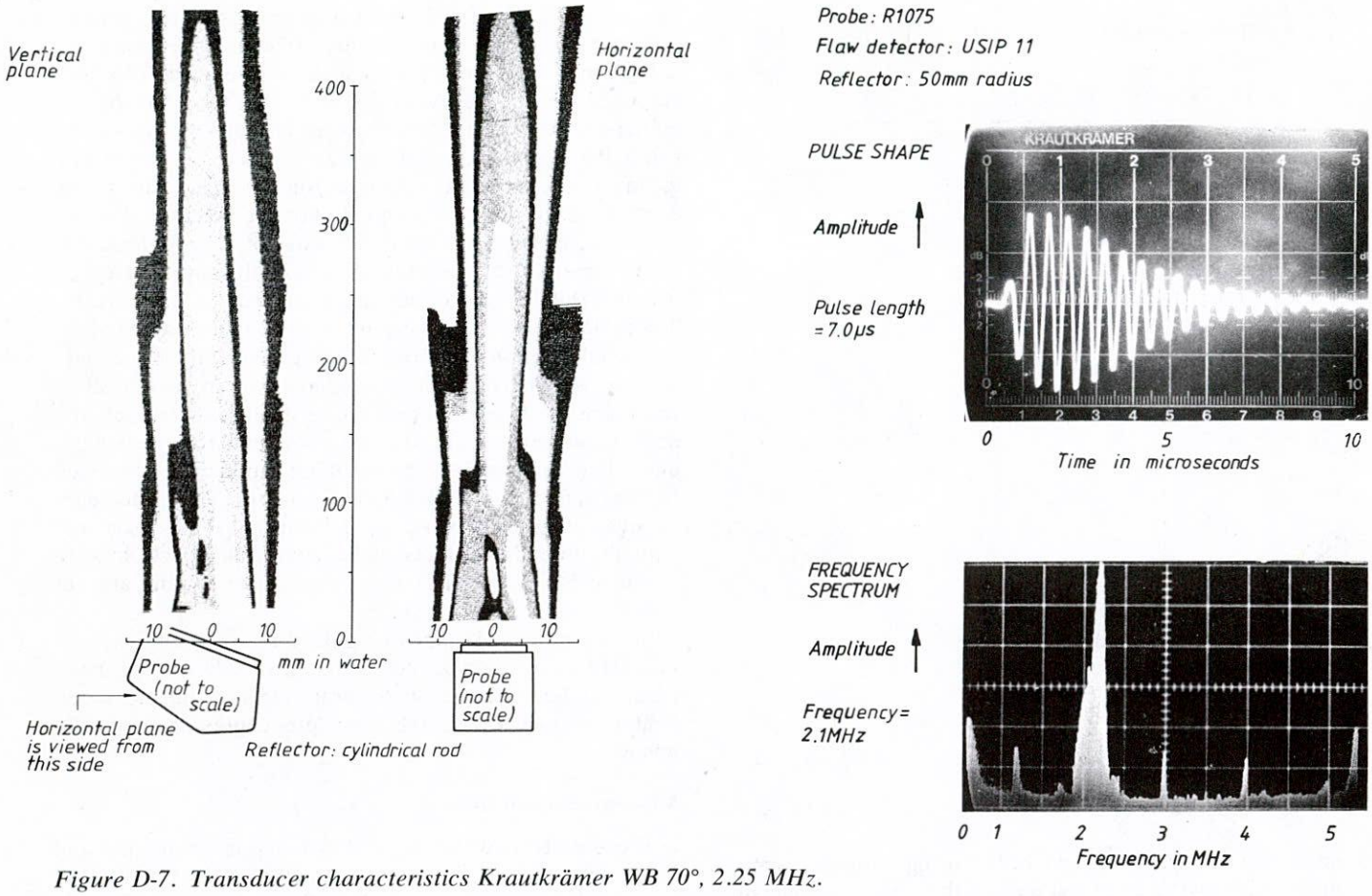

Figure D-7. Transducer characteristics Krautkrämer WB 70°, 2.25 MHz.

APPENDIX E

DETAILS OF EXPERIMENTAL EVALUATION OF AWS D1.1 ULTRASONIC TESTING PROCEDURES

This Appendix is based on the interim report: "An Experimental Evaluation of the Ultrasonic Testing Requirements of the AWS D1.1-80 Structural Welding Code, as Related to Welds in Steel Bridges," submitted to the NCHRP in July 1980. The report is not reproduced verbatim because additional information now available on the actual defect sizes and types enabled some revisions and additional analysis.

EXPERIMENTAL PROCEDURE

All tests were carried out in accordance with the Code. The relevant parts of the Code were summarized in a separate document that was used as a working document by all operators for testing. This document was submitted to the NCHRP early in the project and is included herein as Document E1, "Procedures for Testing Plates J201 to J213."

The major factors under study were:

1. The performance of AWS D1.1 techniques for detection and assessment of defects in welds.
2. The effect and significance of operator variability on results.
3. The effect and significance of equipment variability on results.

Item 1, the laboratory tests, were accomplished using the scanning frame discussed in Appendix D and shown in Figure D-2. This ensured that measurement errors and coupling variability were minimized, thus enabling a thorough evaluation of the capabilities of the Code to detect and assess weld flaws. All specimens were tested in this way.

Item 2 was accomplished by subjecting a selection of the specimens (see Table E-1) to tests by three different operators who had no prior knowledge of the defects. These tests were performed manually (i.e., the scanning frame was not employed), and, thus, the results of such tests should represent more closely what would be expected from a site test.

Item 3 was accomplished by subjecting the same selection of specimens (see Table E-1) to a repeat laboratory test,

TABLE E-1
TESTS PERFORMED TO AWS D1.1 PROCEDURES.

Specimen number	Tests applied		
	Laboratory tests to AWS D1.1	Laboratory tests to D1.1 using borderline equipment	Three manual operators
J201	✓	✓	✓
J202	✓		
J203A	✓	✓	✓
J203B	✓		
J204	✓		
J205A	✓		
J205B	✓		
J206	✓	✓	✓
J207	✓		
J208	✓		
J209A	✓		
J209B	✓	✓	✓
J210	✓	✓	✓
J211	✓	✓	✓
J212A	✓		
J212B	✓		
J210	✓	✓	✓
J251	✓	✓	
J252	✓	✓	
J253	✓	✓	

employing the scanning device, but using ultrasonic transducers with crystal sizes just outside the Code requirements (see Appendix D). This equipment was termed "borderline" equipment.

Further details of the equipment are given in Appendix D.

RESULTS

After destructively testing the specimens to reveal the defects so that their exact size and shape could be established, the findings of the ultrasonic tests were assessed quantitatively to determine whether the accept/reject criteria given in Chapter Two (Figure 3) were indeed met.

Flaw Detection

A flaw is required to be detected before any attempt can be made to assess its severity. Not only therefore does poor detection capability preclude subsequent acceptance or rejection of defects according to the Code requirements, which are at present arbitrary in terms of fracture mechanics, but will allow potentially highly significant flaws to remain when the structure enters service with possibly catastrophic results.

Detectability of flaws may be determined with reference to Table E-2. This table summarizes the results of all tests on the 35 weld defects studied and shows that in only two cases were defects undetected out of a total of 91 separate tests, a detection rate of over 98 percent. The two cases of nondetection applied to the same defect (defect 2) which, although it has not been destructively tested, is suspected from other evidence (both ultrasonic and radiographic) to be very small.

Some variation of detection capability with testing face has been noted. Table E-3 shows that in some instances defects were not found from every required scanning direction even though they were detected by at least one scan. This discrepancy may be partly explained by the fact that the requirement for a defect to be reported depends on its position within the weld thickness. In at least one case, positioning of the maximum amplitude response from a flaw lay outside the depth zone for that scanning direction, so no result was recorded, suggesting that the defect was not, in fact, detected. Also, some defects, notably such smooth flaws as lack of fusion, exhibit highly directional responses, so some variation in detectability with testing face would be expected.

It would seem that overall scanning sensitivity is adequate to detect small defects and procedures are sufficient to allow the range of defects studied to be evaluated. In fact, the scanning sensitivities in all cases were found to be very high, and a large number of very small indications were revealed on the CRT screen. A considerable amount of time was spent on evaluating these very small inclusions, not associated with the intended defects under study, all of which were found to be acceptable minor flaws (Class D) and are not considered here.

In view of this, it appears unlikely that a potentially significant flaw of the type included in this study would remain totally undetected even if the transducer is outside specification, provided that the other procedures are correctly applied.

Diffusion-Bonded Defects

These defects (which are not included in Tables E-2 and E-3) were easily reliably detected in all cases by virtue of the strong echoes obtained from the defect extremities. Without conducting destructive tests, it can only be assumed that the echoes result from strong diffraction effects due to the sharp edges. Also in all cases the echo was large enough for the defect to be rejected (see Table E-4). Because of this behavior, which is not representative of real defects, these results were excluded from the analysis described below.

Acceptance/Rejection (A/R) Levels

Table E-2 gives the most serious "d" rating and A/R decision obtained from each test on defects 1–35 and gives a summary of all tests for each defect. It may be seen that tests using equipment within the AWS D1.1 specifications (good equipment) reject 31 defects and accept only four. However, when tests were repeated using different operators, disagreement on acceptance or rejection occurred in five cases; the possible causes are discussed in the following.

In Table E-2 it is assumed that the A/R decision for each test is based on the "worst" "d" rating (i.e., the most severe in terms of Table 9.25.3 of the Code). Comparison of these A/R decisions with defect through-wall size (projected onto the vertical or through-thickness plane) is given in Table E-4 for all tests. From the table, the likelihood of defects more than a few percent wall thickness in size being accepted would seem to be small. This is shown more clearly in Figure E-1, which demonstrates a clear trend to accept defects of a small percentage of wall thickness in size but to reject larger ones. The correlation between the proportion of total decisions to accept or reject defects in terms of their actual size is poor (see Figure E-2), and this is expected because A/R

TABLE E-2
MOST SERIOUS "D" RATING FOR DEFECTS IN WELDED SPECIMENS.

Defect number	Specimen number	Most serious "d" values from three manual operators			Most serious "d" values from tests using scanning frame		Summary of all tests		
		"Good" equipment			"Good" equipment	"Borderline" equipment	Maximum "d" rating	Minimum "d" rating	Overall decision
		1	2	3					
1	J201	+1R	+3R	0R	-1R	+6R	-1	+6	R
2		+8A	+8A	X	+6A	X	+6	X	A
3		+4A	+4A	-2R	+2R	+9A	-2	+9	A/R
4	J202	0R							
5		-2R							
6		-2R							
7	J203A	+9A	+5R	-2R	+6A	+8A	-2	+9	A/R
8	J203B				0R				
9	J204A				-8R				
10					-5R				
11	J204B				-6R				
12	J205A				+5A				
13	J205B				+10A				
14	J206	-3R	-6R	-6R	-3R	-4R	-6	-3	R
15		+3R	+5R	0R	+2R	+2R	0	+5	R
16		+11A	-7R	-8R	-2R	-2R	-8	+11	A/R
17	J207				-4R				
18					-10R				
19					0R				
20	J208				-3R				
21					-4R				
22	J209A				-7R				
23	J209B	0R	+2R	0R	+2R	+4R	0	+4	R
24	J210	-18R	-16R	-14R	-12R	-7R	-18	-7	R
25		0R	+3R	0R	+6R	+3R	0	+6	R
26		-8R	-10R	-10R	-8R	-6R	-10	-6	R
27	J211	+8R	+2R	-7R	0R	-4R	-7	+8	R
28	J212A				-2R				
29					-7R				
30					-6R				
31	J212B				-8R				
32					-9R				
33					-14R				
34	J213	+2R	+17A	-4R	0R	-2R	-4	+17	A/R
35		+6R	+14A	+3R	0R	+3R	0	+14	A/R

A = Acceptable, R = Rejectable by criteria in Table 9.25.3, X = Not detected.

TABLE E-3
THE "D" RATINGS FROM DEFECTS IN WELDED SPECIMENS FROM ALL FOUR TEST FACES ($A^+ A^-$, $B^+ B^-$ AS DEFINED IN THE CODE).

Defect number	Specimen number	"d" values from different surfaces by three different manual operators and scanning frame with "good" and "borderline" equipment																			
		1 "Good"				2 "Good"				3 "Good"				"Good" frame				"Borderline" frame			
		A^+	A^-	B^+	B^-	A^+	A^-	B^+	B^-	A^+	A^-	B^+	B^-	A^+	A^-	B^+	B^-	A^+	A	B^+	B^-
1	J201	$+1^R$	$+2^A$	-	-	$+7^A$	$+3^R$	-	$(+10^A)$	$+2^R$	$+1^R$	$(+4^R)$	(0^R)	$+6^A$	-1^R	$(+6^R)$	-	$+6^R$	$+6^R$	-	-
2		$+8^A$	$+12^A$	-	-	X	-X	-	$(+8^A)$	X	X	-	-	$+6^A$	$+11^A$	-	$(+8^A)$	X	X	-	-
3		$+4^A$	$+10^A$	-	-	$+10^A$	X	-	$(+4^A)$	-2^R	X	$(+2^R)$	$(+4^A)$	$+2^A$	$+6^A$	-	-	X	$+14^A$	$(+17^A)$	$(+9^A)$
4	J202													$+6^A$	0^R	-	$(+14^A)$				
5														$+6^A$	-2^R	-	-				
6														$+7^A$	-2^R	-	-				
7	J203A	$+14^A$	$+9^A$	-	-	$+5^A$	$+6^A$	$(+18^A)$	$(+9^A)$	-2^R	X	-	$(+8^A)$	$+6^A$	$+12^A$	-	$(+8^A)$	$+8^A$	$+16^A$	-	$(+10^A)$
8	J203B													X	0^R	$(+2^R)$	$(+10^A)$				
9	J204A													$+6^R$	-8^R	-	-				
10														-5^R	$+7^A$	-	-				
11	J204B													-	-	$+4^R$	-6^R				
12	J205A													$+7^A$	$+5^A$	$(+10^A)$	$(+8^A)$				
13	J205B													$+13^A$	-10^A	-	-				
14	J206	X	-3^R	-	-	-6^R	$+4^R$	-	-	-6^R	-6^R	-	-	-3^R	-3^R	-	(-2^R)	-2^R	-4^R	-	-
15		$+11^A$	$+3^R$	-	$(+11^A)$	$+13^A$	$+5^R$	$(+6^R)$	$(+8^A)$	$+5^R$	0^R	$(+6^R)$	$(+8^A)$	$+6^R$	$+6^R$	$(+2^R)$	$(+9^A)$	$+10^A$	$+2^R$	$(+2^R)$	$(+11^A)$
16		X	$+11^A$	$(+14^A)$	-	X	$+17^A$	(-5^R)	(-7^R)	X	X	(-3^R)	(-8^R)	X	X	(-1^R)	(-2^R)	$+14^A$	$+16^A$	(0^R)	(-2^R)
17	J207													$(+2^R)$	-	-4^R	$+2^R$				
18														-10^R	-6^R	(0^R)	$(+6^R)$				
19														$+3^R$	0^R	-	-				
20	J208													-1^R	-3^R	$(+5^R)$	$(+5^R)$				
21														-4^R	-1^R	(-3^R)	$(+1^R)$				
22	J209A													-2^R	-7^R	(-2^R)	(-3^R)				
23	J209B	0^R	$+9^A$	$(+2^R)$	$(+3^R)$	$+2^R$	$+5^R$	$(+4^R)$	$(+4^R)$	0^R	$+2^R$	$(+6^R)$	$(+4^R)$	$+6^R$	$+6^R$	$(+5^R)$	$(+2^R)$	$+6^R$	$+9^A$	$(+8^R)$	$(+4^R)$
24	J210	-	-	X	-18^R	-	-	-8^R	-16^R	-	-	-14^R	-10^R	$+1^R$	-	-12^R	-10^R	-2^R	$+14^A$	-7^R	-6^R
25		0^R	$+14^A$	-	-	$+3^R$	$+5^R$	-	-	0^R	X	-	-	$+6^R$	$+7^R$	-	-	$+6^R$	X	$+19^A$	$+3^R$
26		-8^R	-6^R	-	-	-7^R	-10^R	-	-	-8^R	-10^R	-	-	-2^R	-8^R	-	-	$+1^R$	-6^R	$+2^R$	-
27	J211	$+8^R$	$+8^R$	-	-	$+2^R$	$+5^R$	-	-	-5^R	-7^R	-	-	0^R	$+1^R$	-	-	-4^R	-1^R	-	-
28	J212A													-2^R	X	-	-				
29														-7^R	-7^R	-	-				
30														-6^R	X	-	-				
31	J212B													-4^R	-8^R	-	-				
32														-4^R	-9^R	-	-				
33														-14^R	-9^R	-	-				
34	J213	$+2^R$	X	-	-	$+17^A$	$+24^A$	-	-	-4^R	X	-	-	0^R	X	-	-	-2^R	$+10^R$	-	-
35		X	$+6^R$	-	-	$+14^A$	X	-	-	$+3^R$	X	-	-	0^R	$+7^R$	-	-	$+3^R$	$+6^R$	-	-

NOTE. values in brackets were not required to be recorded by the Code.

A = Acceptable, R = Rejectable by criteria in Table 9.25.3, - = not required to be recorded, X = not detected.

TABLE E-4
COMPARISON OF ACTUAL DEFECT SIZE AND ACCEPT/REJECT DECISION.

Defect number	Type	Approximate size		Acceptable or rejectable (worst "d" rating)				
				Operator			Scanning frame good equipment	Scanning frame borderline equipment
		Inches	(mm)	1	2	3		
1	Solidification crack	2.2 x 0.75	(55 x 19)	R	R	R	R	R
2	Solidification crack	Not sectioned		A	A	X	A	X
3	Solidification crack	Not sectioned		A	A	R	R	A
4	Slag line	2.0 x 0.1	(51 x 3)				R	
5	Slag line	2.0 x 0.1	(51 x 3)				R	
6	Slag line	2.2 x 0.2	(55 x 5)				R	
7	Crack	1.8 x 0.2	(46 x 5)	A	A	R	A	A
8	Crack	2.1 x 0.3	(53 x 8)				R	
9	Lack of fusion	Not sectioned					R	
10	Lack of fusion	Not sectioned					R	
11	Lack of fusion	Not sectioned					R	
12	Freeze-break crack	2.2 x 0.4	(55 x 9)				A	
13	Solidification crack	1.8 x 0.2	(45 x 4)				A	
14	Solidification crack	2.0 x 0.1	(52 x 3)	R	R	R	R	R
15	Solidification crack	1.9 x 0.1	(47 x 3)	R	R	R	R	R
16	Solidification crack	Not sectioned		A	R	R	R	R
17	Slag line	2.0 x 0.2	(52 x 4)				R	
18	Slag line	2.0 x 0.2	(52 x 4)				R	
19	Slag line	2.3 x 0.2	(58 x 4)				R	
20	Freeze-break crack	1.9 x 0.2	(49 x 4)				R	
21	Freeze-break crack	2.0 x 0.3	(50 x 7)				R	
22	Freeze-break crack	2.0 x 0.3	(50 x 7)				R	
23	Freeze-break crack	1.9 x 0.4	(49 x 9)	R	R	R	R	R
24	Lack of fusion	2.1 x 0.3	(54 x 8)	R	R	R	R	A
25	Lack of fusion	2.0 x 0.1	(52 x 3)	R	R	R	R	R
26	Lack of fusion	2.2 x 0.2	(56 x 6)	R	R	R	R	R
27	Freeze-break crack	2.1 x 0.2	(54 x 4)	R	R	R	R	R
28	Lack of fusion	Not sectioned					R	
29	Lack of fusion	Not sectioned					R	
30	Lack of fusion	Not sectioned					R	
31	Lack of fusion	Not sectioned					R	
32	Lack of fusion	Not sectioned					R	
33	Lack of fusion	Not sectioned					R	
34	Slag	1.9 x 0.1	(48 x 3)	R	A	R	R	R
35	Lack of fusion	2.0 x 0.1	(50 x 2)	R	A	R	R	R
Diffusion bonded specimens								
36	Square slot	1.2 x 1/8 x 0.005	(30 x 3 x 0.13)				R	R
37	Square slot	1.2 x 1/4 x 0.005	(30 x 6 x 0.13)				R	R
38	Square slot	1.2 x 1/8 x 0.005	(30 x 3 x 0.13)				R	R
39	Square slot	1.2 x 1/4 x 0.005	(30 x 6 x 0.13)				R	R
40	Square slot	1.2 x ½ x 0.005	(30 x 12 x 0.13)				R	R
41	Square slot	As for 38					R	R
42	Square slot	As for 39					R	R
43	Square slot	As for 40					R	R

decisions based on Table 9.25.3 of the Code are weighted for different wall thicknesses and do not consider absolute flaw depth in inches (mm).

An important point to note is that histograms which show the tendency to accept or reject can be distorted when a small sample of readings is presented; that is, one reject decision from a sample of one gives 100 percent likelihood of rejection according to the scales in Figure E-1 and Figure E-2, which may not be the case if a larger number of readings were considered.

For this reason it was decided to consider all A/R decisions taken from every testing angle applied to each of the defects to study trends of acceptance or rejection. These are given in Table E-3. At first sight this would appear not to represent the practical application of the D1.1 Code procedure, because the most severe "d" rating only is used for the A/R

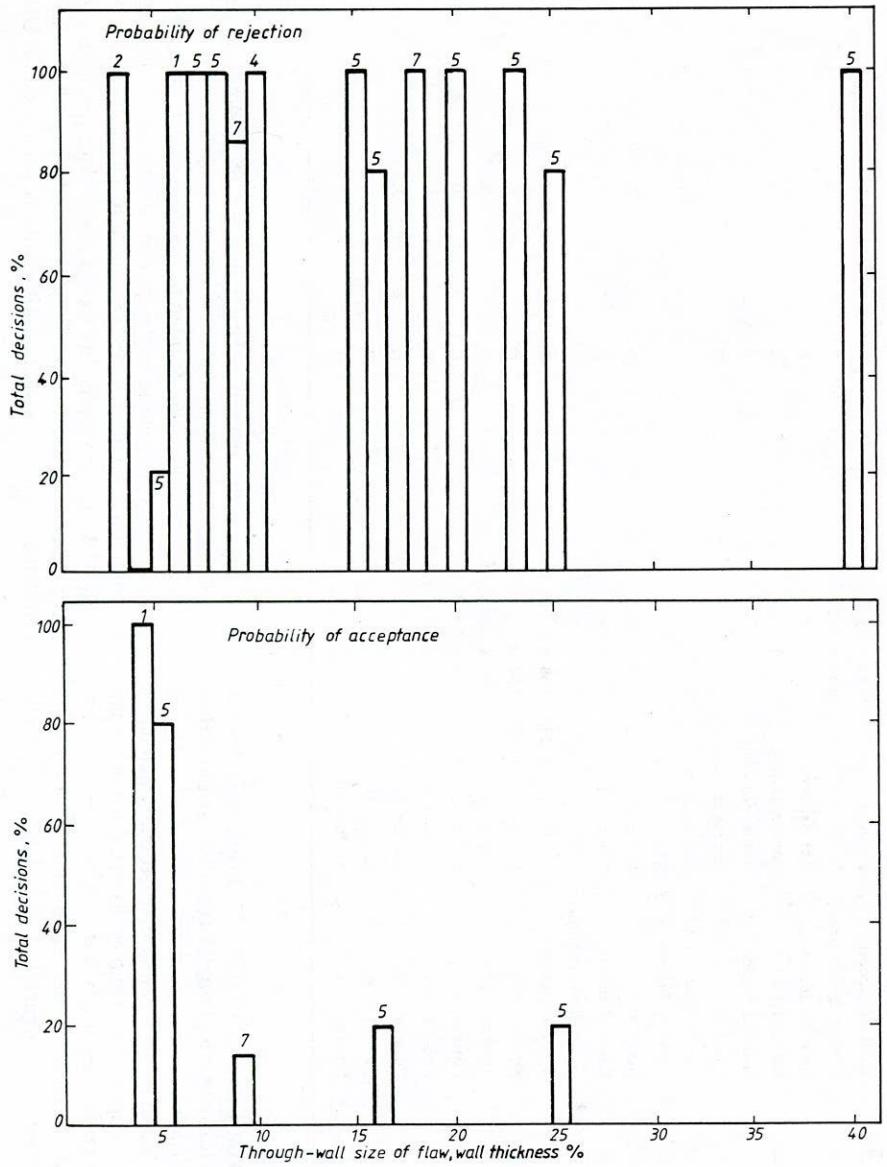

Figure E-1. Probability of acceptance and rejection of all defects according to AWS Code with percent wall thickness (most severe rating only for each defect). (Numbers above boxes show sample size.)

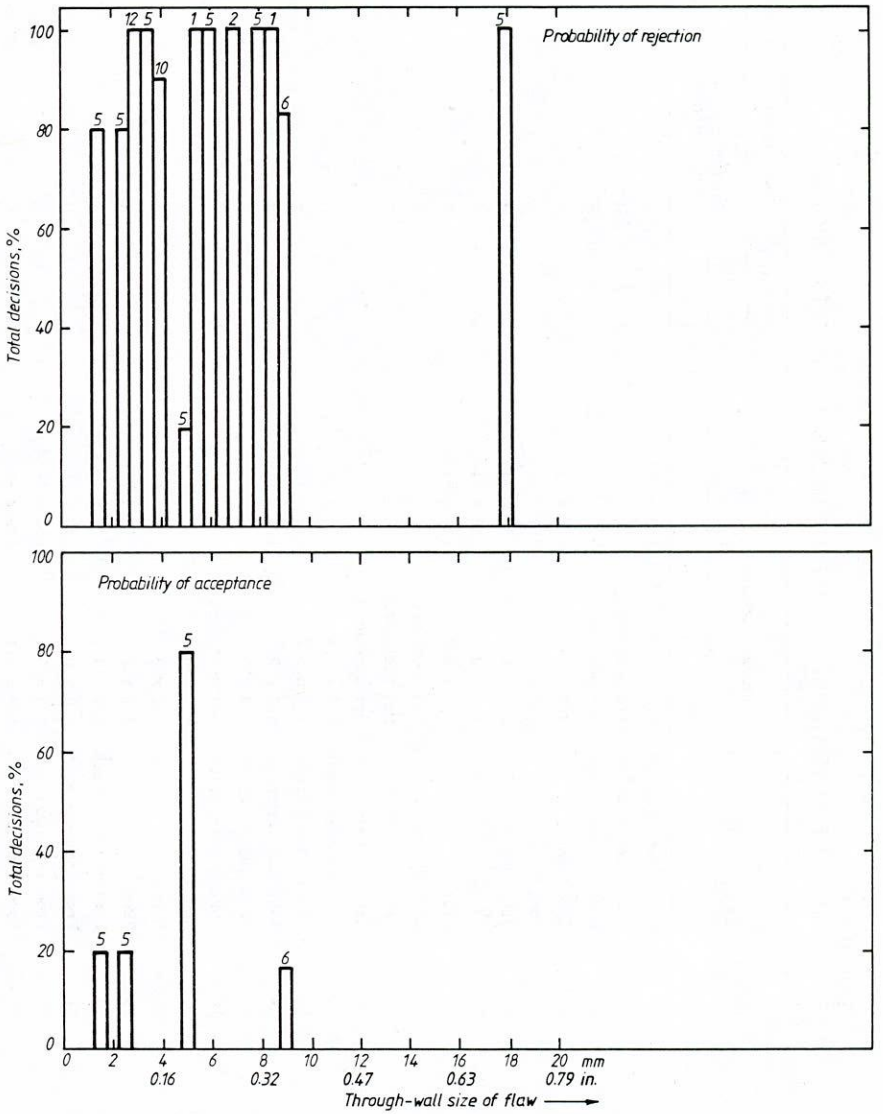

Figure E-2. Probability of acceptance and rejection of all defects according to AWS Code with actual size (most severe rating only for each defect). (Numbers above boxes show sample size.)

decision. However, when the problems of obtaining reliable amplitude information from defects (as outlined in Chapter Two) are considered, all "d" ratings and the consequent A/R decisions are of importance because it is conceivable that, in general, a given flaw might only be detected from one angle of attack from one testing surface.

The results of this approach are shown in Figures E-3 to E-7. Figures E-6 and E-7 show the overall trend of likelihood of acceptance or rejection with defect size expressed as a percentage of wall thickness and in absolute units (inches and mm), respectively. Once again there is no observable trend for acceptance or rejection with absolute size, but in terms of percentage wall thickness, flaws up to around 7.5 percent of the wall have a good chance (around 70 percent or better) of being accepted, while larger flaws have a good chance (again, around 70 percent or better) of being rejected.

It would appear that the effective accept/reject threshold for flaws, in terms of percent wall thickness, is therefore ~7.5 percent as opposed to the 2–4 percent suggested in Figure 3 (see Chapter Two).

Defect shape, and therefore type, has a profound effect on ultrasonic response amplitude and thus on acceptance or rejection by AWS D1.1 procedures. Figures E-3, E-4, and E-5 show the likelihood of acceptance and rejection of cracks, slag inclusions, and lack of fusion defects, respectively, again all expressed as a percentage of wall thickness. From Figure E-3 it can be seen that the relatively low amplitude of response from cracks allows sizes up to 7.5 percent of wall thickness to be accepted by every test, and the chance of larger cracks (up to 40 percent wall thickness) being rejected may be only around 70 percent (i.e., in 30 percent of cases these defects would be accepted).

The response from slag inclusions, which tend to have an approximately circular cross-section, is more indicative of their size. The stronger overall level of signal received from these defects permits a likelihood of rejection of defects 10 percent of the wall in size of around 90 percent (Figure E-4), but smaller inclusions, only 3 percent of the wall in size, still stand a 1 in 3 chance of rejection.

The strong signals from lack of fusion defects gave rise to a good chance of rejection (Figure E-5), with a defect 8 percent of the wall being rejected in 80 percent of cases and larger defects being rejected in over 90 percent of tests. It should be noted, however, that most of the lack of fusion defects were inclined at some angle to the through-thickness direction of the weld and their face length was therefore larger than the projected dimension on to the through-thickness plane, which is used here. This may have contributed to the larger overall chance of rejection of these defects.

The tendency to reject slag and lack of fusion reliably, and to reject vertical cracks with a far lower degree of confidence, is in direct contradiction to one of the main requirements of the AWS D1.1 Code (i.e. to ensure the integrity of welds in steel bridge structures), as the most serious form of flaw, the crack oriented at right angles to the plate surface, stands the best chance of escaping rejection, even when large.

Operator Variability

Fourteen defects were examined by all three manual operators. Eight defects, 58 percent of the total, were unanimously rejected according to the Code and one, 7 percent, unanimously accepted. In five cases, 35 percent of the total, one operator disagreed with the accept/reject decision. The variation in "d" rating from the three operators for the four testing surfaces can be seen from Table E-3 (figures in brackets refer to information recorded which was not actually required by the Code). From the table, the average variation in "d" rating from the same testing face is 8.1 dB for the A+ which showed the greatest scatter. The variation in "d" rating considering all testing faces is 6.5 dB. From Table 9.25.3 of the Code, a range of 4 dB represents the difference between class A and D defects, automatically rejectable and acceptable respectively, and therefore the operator variability measured would have a significant impact on the accept/reject decision.

Considering that one of the aims of the Code is to provide a uniform inspection level from site to site or between successive examinations of the same structure, the disagreement on defect acceptance between operators in 35 percent of cases would appear to be unacceptably high.

Two major comments were made by the operators, none of whom regularly works to AWS D1.1-80. One comment concerned the fact that the high testing sensitivity produced many indications denoting totally insignificant reflectors, which merely served to make the display more confusing. In another comment, one operator expressed considerable surprise that no means of establishing coupling or transfer losses was employed prior to testing, considering that the technique is entirely dependent on amplitude.

Such comments are further indications that the test procedure is not conducive to establishing 100 percent reproducible test conditions, thereby removing one of the reasons for which it is advocated.

Equipment Variability (Tables E-2 and E-4)

In general the effect of using a transducer of a size beyond limits set in the Code ("borderline" equipment) was small. There was little discrepancy in acceptance or rejection from the same scanning surfaces, the variation in "d" rating being less than for different operators (see Table E-3). The use of a transducer in all respects similar to those within Code specification, apart from a small size difference, probably did not alter testing conditions sufficiently to invalidate assumptions and considerations used in the derivation of procedures and acceptance levels. However, the effect which transducer size may have on response amplitudes, especially where amplitude variation with beam path is considered, may be considerable, even for the range of sizes permitted by the Code (*15*).

Other Factors Influencing Test Variability

In addition to those previously outlined, it is quite probable that minor variations in operator technique, transducer characteristics, coupling efficiency, and exact points on flaws where "d" ratings are determined will influence the overall "d" rating from a test and may change the subsequent accept or reject decision. It is worth noting that an error in positioning a defect could change the A/R decision if classified B or C and, whether or not the 4-dB root defect correction is applied (obviously dependent on defect position), could also affect whether the flaw is acceptable or rejectable.

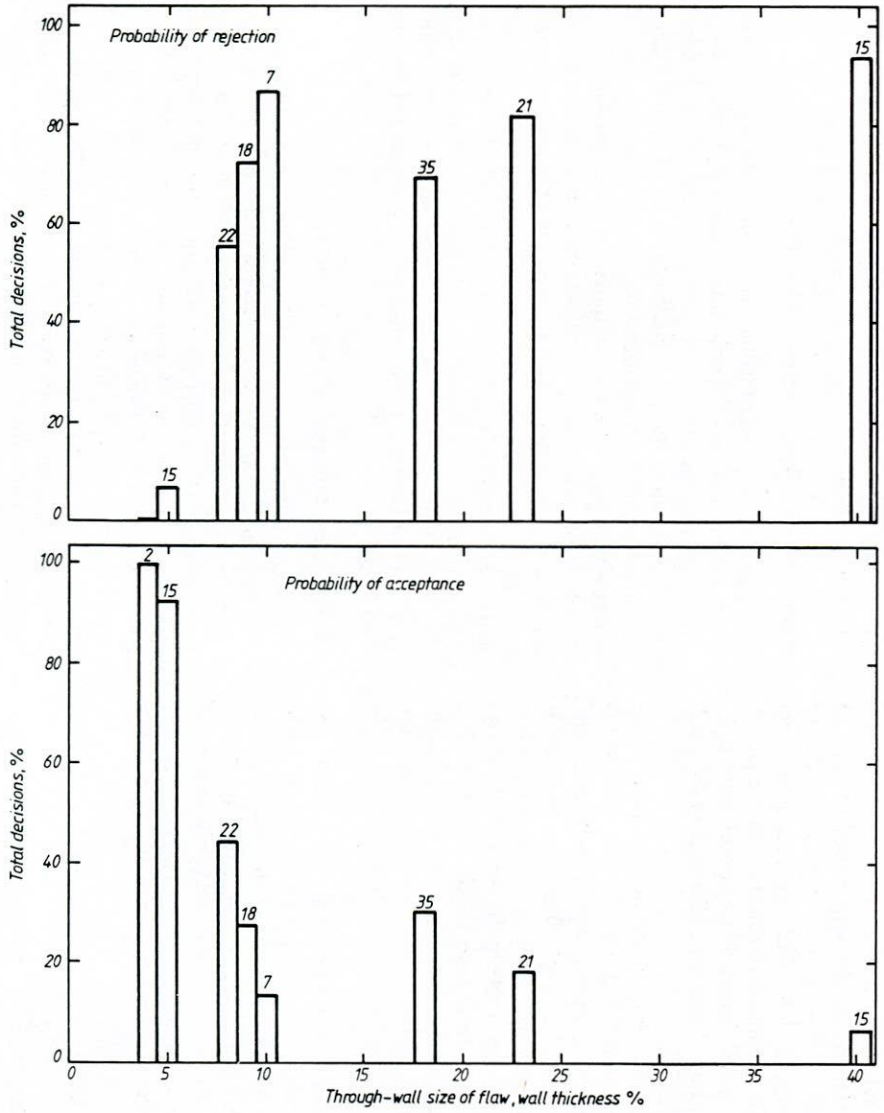

Figure E-3. Probability of acceptance and rejection of cracks according to AWS Code with percent wall thickness (all test directions). (Numbers above boxes show sample size.)

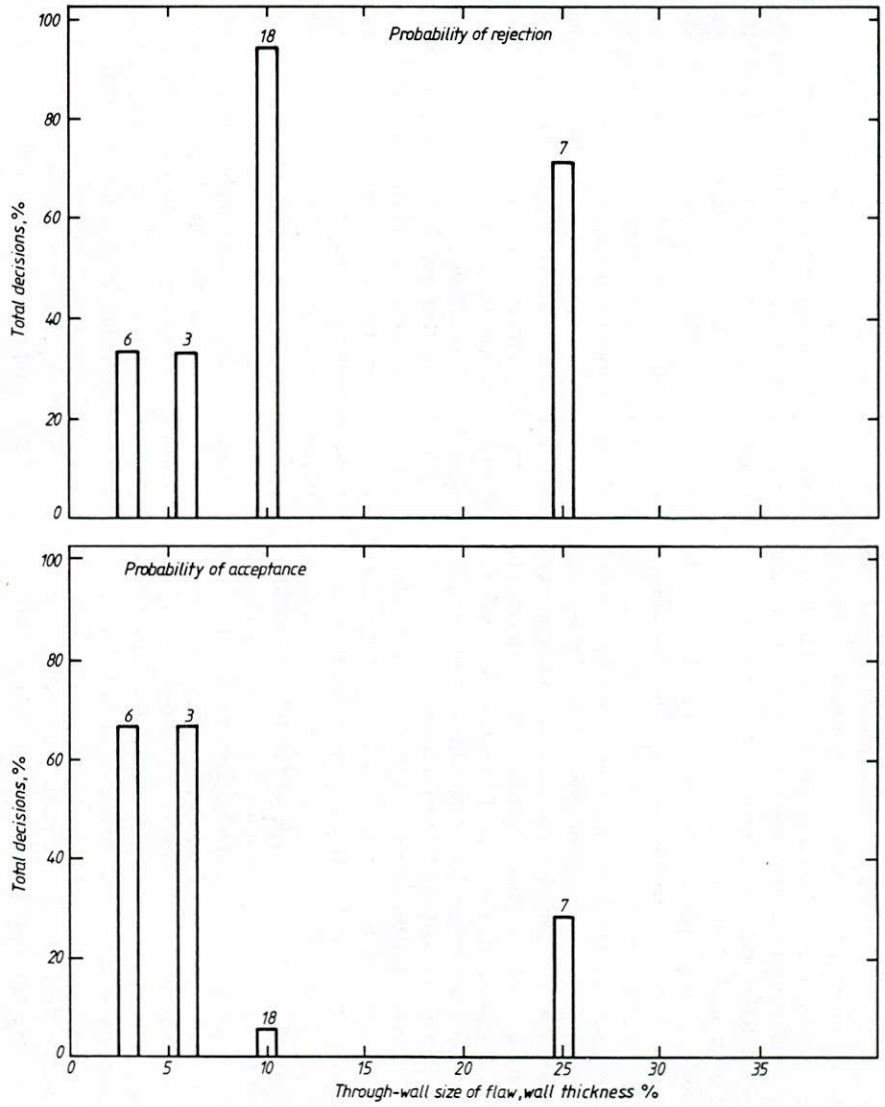

Figure E-4. Probability of acceptance and rejection of slag inclusions according to AWS Code with percent wall thickness (all test directions). (Numbers above boxes show sample size.)

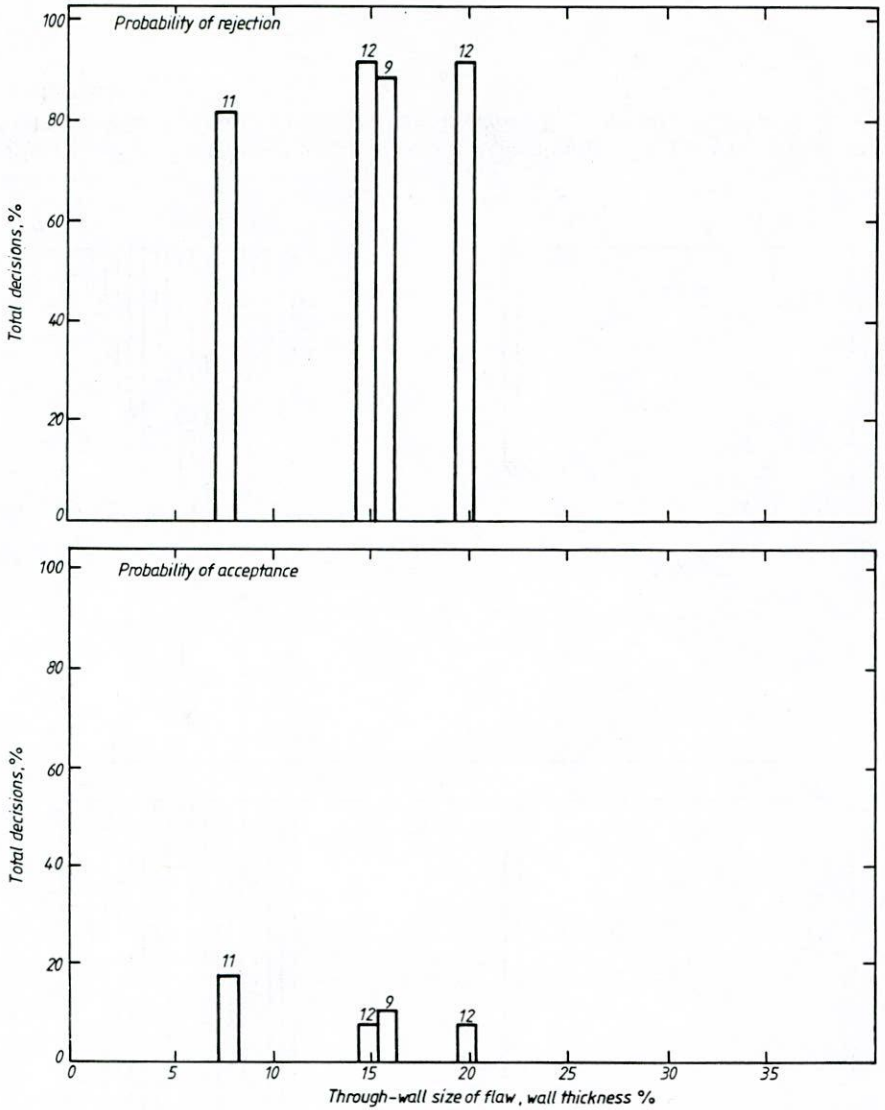

Figure E-5. Probability of acceptance and rejection of lack of fusion according to AWS Code with percent wall thickness (all test directions). (Numbers above boxes show sample size.)

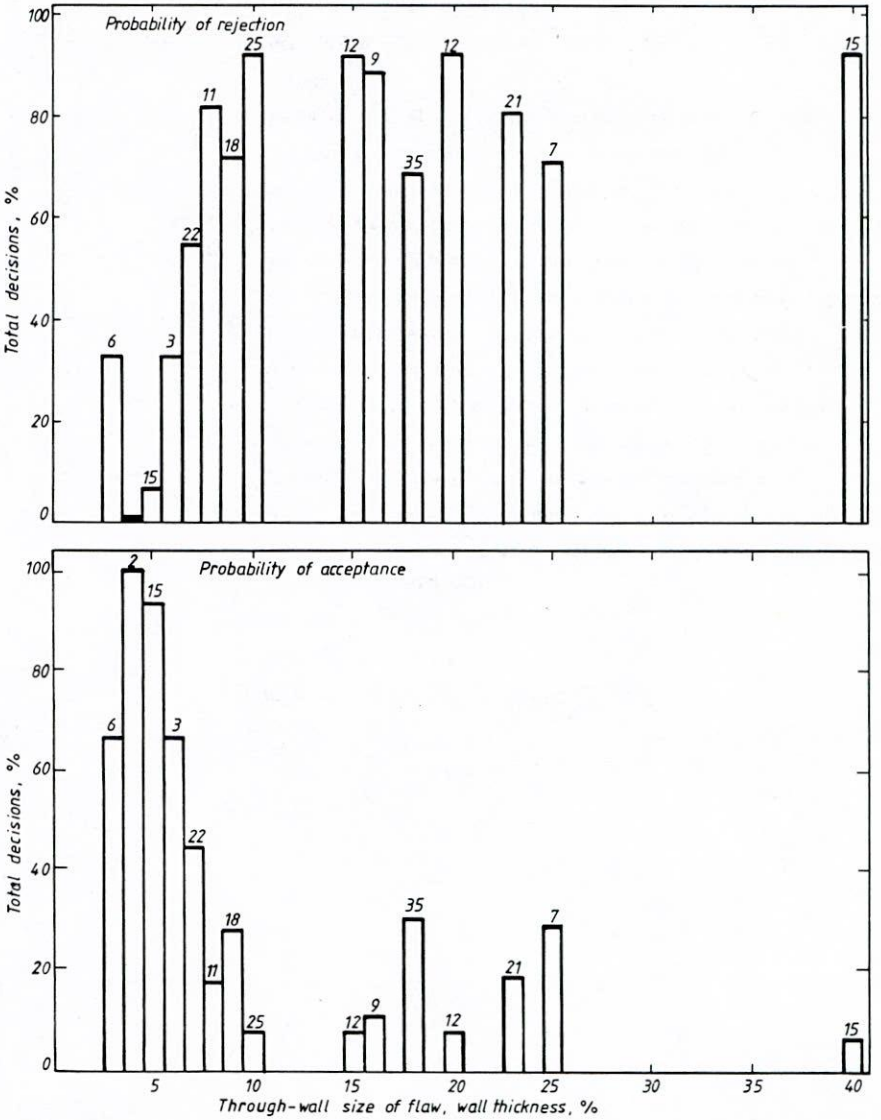

Figure E-6. Probability of acceptance and rejection of all defects according to AWS Code with percent wall thickness (all test directions). (Numbers above boxes show sample size.)

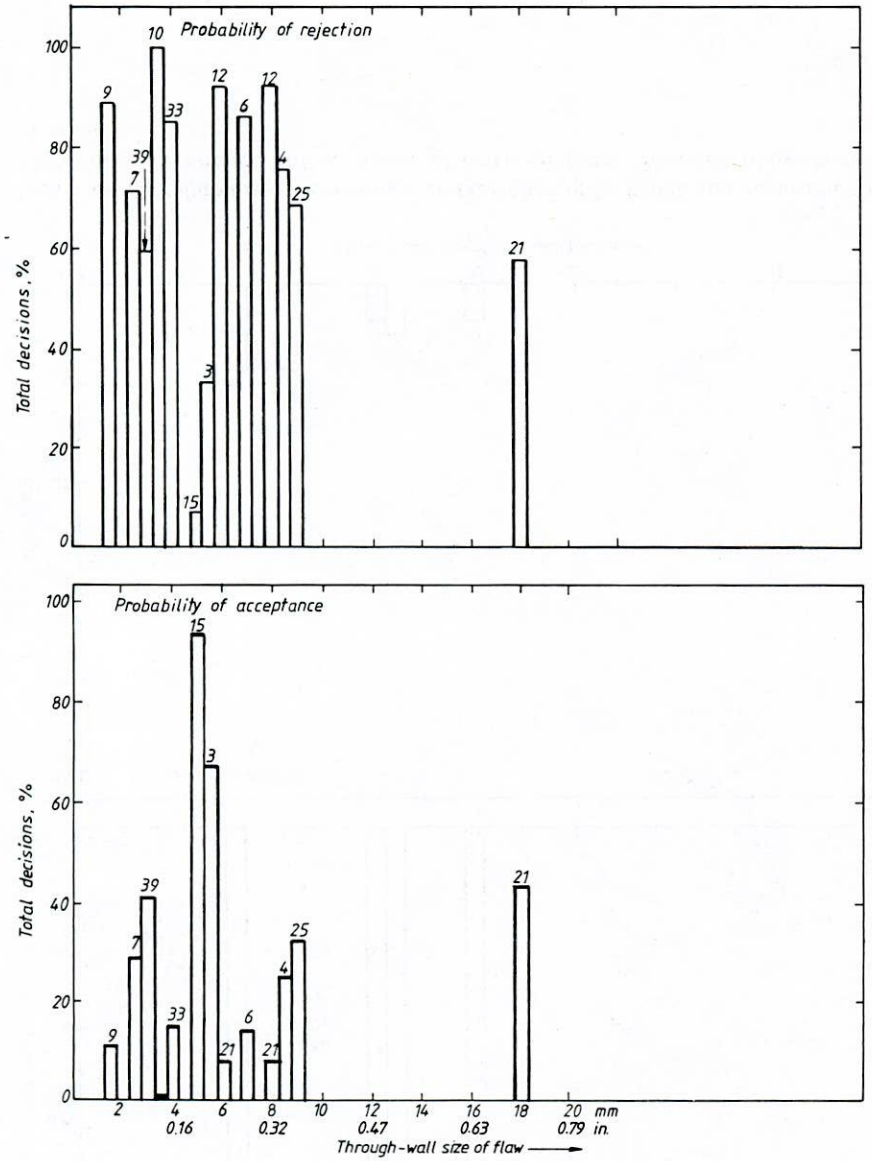

Figure E-7. Probability of acceptance and rejection of all defects according to AWS Code with actual flaw size (all test directions). (Numbers above boxes show sample size.)

Document E1

PROCEDURE FOR TESTING PLATES J201 to J213

Extracts from AWS D1.1-80

Project 3625

1. Specimens and equipment

The specimens are plain butt welds in 10, 40 and 95mm ($^3/_8$, $1\frac{1}{2}$, $3^3/_4$in.) thick mild steel plate. Information on weld preparation and process will be provided. Specimen markings are shown in Fig.1.

Use only the probes and flaw detector provided for this project. The angle probes are Krautkrämer WB series (old type) with nominal angles of 45, 60 and 70° and a nominal frequency of 2.25MHz. The compression wave probe is a 20mm ($^3/_4$in.) diameter Aerotech also with a nominal frequency of 2.25MHz. Actual angles and index points are marked on the probes. The flaw detector is a Krautkrämer USM2M. No equipment checking or characterisation is necessary as this has already been done. Beam spreads are not required.

V1 and V2 calibration blocks will be provided. The operator should use his own flaw location slide or whatever technique he prefers.

Use only the calibrated (dB) gain control on the flaw detector

Report forms, see Appendix I, will be provided.

2. Testing of parent plate (compression wave probe)

(i) Calibrate the screen such that two back wall echoes are visible and set the second back wall echo to between 50 and 75% full screen height.

Document E1 Continued

(ii) Scan the parent plate on either side of the weld such that areas to be subsequently used in angle beam testing are covered.

(iii) Record a defect only if EITHER (a) there is a complete loss of the first back wall echo, OR (b) an indication equal to or greater in amplitude than the original first back wall echo appears.

(iv) Record areas of weld which cannot be tested as a result of indications in (iii) and do not cover them in the angle beam scans.

3. Weld testing (angle probes only)

(i) Calibration for range (sound path)

Calibrate full screen width to 200mm (8in.) using V1 block.

(ii) Sensitivity setting

Place the probe on the edge of the V1 block marked with 40 to 60° graduations and point the beam at the 1.5mm hole. Maximise the echo and set it to three screen graticules in amplitude (using calibrated gain control). This is the "reference sensitivity". The dB setting on the flaw detector is the "reference level" and given symbol b.

For scanning, add dBs according to range (sound path) as follows:

Up to 63.5mm (2½in.) add 20dB

63.5 to 127mm (2½ to 5in.) add 25dB

127 to 254mm (5 to 10in.) add 35dB

(iii) Scanning procedure (refer to Fig.2)

(a) 10mm plate - 70° probe scanned on faces at A+ and A- to cover whole of weld. Upper quarter to be covered on leg II.

(b) 40mm plate - 70° probe scanned on faces A+ and A- to cover middle half and lower quarter. 70° probe on faces B+ and B- to cover upper quarter.

(c) 95mm plate - 70° probe scanned on faces A+ and A- to cover middle half.

60° probe scanned on faces A+ and A- to cover lower quarter.

60° probe scanned on faces B+ and B- to cover upper quarter.

When testing 40 and 95mm plate, any indications from the fusion boundary area which reach three screen graticules in amplitude at the SCANNING sensitivity (see 3(iii)) must be evaluated further using a beam angle closest to perpendicular to the suspected fusion face.

Scan patterns are shown in Fig.3.

(iv) Flaw classification

On finding a flaw at the scanning sensitivity, turn back to the reference sensitivity (i.e. subtract whatever was added for scanning) then add dBs until the flaw indication reaches three screen graticules. Note the dB setting (a). Note the range (sound path) in INCHES, subtract 1, multiply by two, and round to the nearest whole number (c). Then:

Indication rating, d = a - b -c.

The flaw can then be classified (A, B, C, and D) from Table 1.

(v) Length measurement (angle probes)

(a) If a relatively constant sound amplitude is maintained along the length of the defect, and if the flaw is longer than the probe crystal width, and also if flaws are separated by more than the width of the probe crystal, the 6dB drop technique shall be used.

(b) If a flaw has variable dB ratings more serious than class D level, and separations less than the search unit width, the length should be measured as described in Appendix II.

4. Recording and reporting

Using the information gained in items 3(iv) and 3(v) above, the decision can be made whether the flaw is acceptable or not from the following:

Class A (Large flaws) - Any indication in this category shall be rejected. (Regardless of length).

Class B (Medium flaws) - Any indication in this category having a length greater than ¾in. shall be rejected.

Class C (Small flaws) - Any indication in this category having a length greater than 2in. in the middle half or ¾in. length in the top or bottom quarter of weld thickness shall be rejected.

Class D (Minor flaws) - Any indication in this category shall be accepted regardless of length or location in the weld.

Notes

1. Class B and C flaws shall be separated by at least 2L, L being the length of the longer flaw, except that when two or more such flaws are not separated by at least 2L, but the combined length of flaws and their separation distance is equal to or less than the maximum allowable length under the provisions of Class B or C, the flaw shall be considered a single acceptable flaw.
2. Class B and C flaws shall not begin at a distance less than 2L from the end of the weld, L being the flaw length.
3. Flaws detected at "scanning level" in the root face area of complete penetration double groove weld joints shall be evaluated using an indication rating 4dB more sensitive.

(i.e. Subtract 4dB from indication rating "d")

The results of all rejectable flaws and those up to 6dB lower than the rejectable level should be entered on the report form (Appendix I).

Document E1 Continued

Document E1. Table 1 Derivation of flaw severity class from indication rating d.

Flaw severity class \ Weld thickness and search unit angle	10mm (3/8in.)	40mm (1½in.)			95mm (3¾in.)			
	70°	70°	60°	45°	70°	60°	45°	
Class A	+10 & lower	+4 & lower	+7 & lower	+9 & lower	+1 & lower	+4 & lower	+6 & lower	d values
Class B	+11	+5 +6	+8 +9	+10 +11	+2 +3	+5 +6	+7 +8	
Class C	+12	+7 +8	+10 +11	+12 +13	+4 +5	+7 +8	+ 9 +10	
Class D	+13 &up	+9 & up	+12 & up	+14 & up	+6 & up	+9 & up	+11 & up	

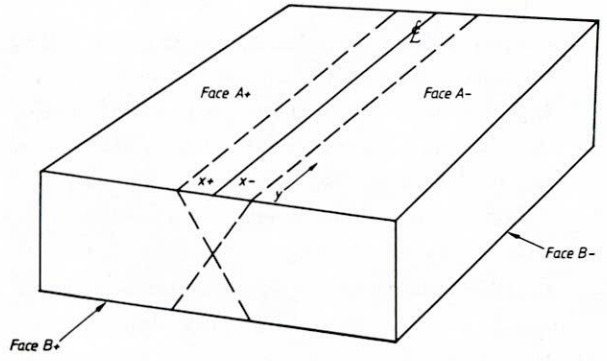

Document E1
Fig.1. Specimen markings.

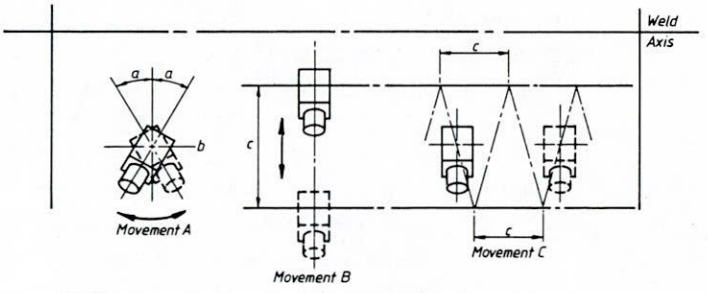

Notes:

1. *Testing patterns are all symmetrical around the weld axis.*
2. *Testing from both sides of the weld axis is to be made wherever mechanically possible.*

Scanning movement A.
Rotation angle a = 10 degrees

Scanning movement B.
Scanning distance c shall be such that the section of weld being tested is covered.

Scanning movement C.
Progression distance c shall be approximately one-half the transducer width.

Note: Movements A, B, and C are combined into one scanning pattern.

Document E1
Fig.3. Scanning patterns.

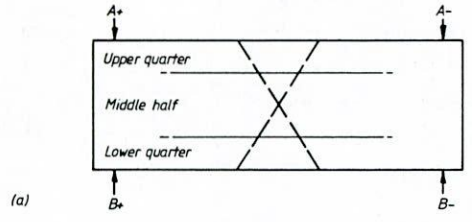

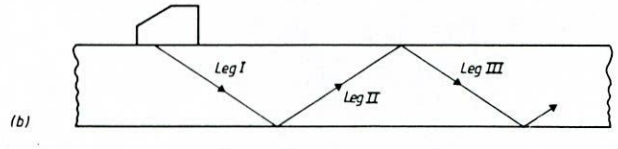

Document E1
Fig.2. Terminology:
a) thickness regions b) skip designations.

Document E1 Continued

APPENDIX I

REPORT OF ULTRASONIC TESTING OF WELDS

Project

Report no.

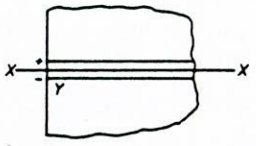

Weld identification

Material thickness

Welding process

Remarks

Line number	Indication number	Transducer angle	From face*	Leg*	Decibels				Discontinuity					Discontinuity evaluation	Remarks
					Indication level	Reference level	Attenuation factor	Indication rating	Length	Angular distance (sound path)	Depth from "A" surface	Distance			
												From X	From Y		
					a	b	c	d							
1															
2															
3															
4															
5															
6															
7															
8															
9															
10															
11															
12															
13															
14															
15															
16															
17															
18															
19															
20															
21															
22															
23															
24															
25															
26															

*See Fig.2

† = to beginning of flaw

Inspected by

Note: This form is applicable to Section 8 and 9 (Buildings and Bridges). Do NOT use this form for Tubular structures (Section 10).

Authorized by

Date

Document E1 Continued

APPENDIX II

LENGTH MEASUREMENT OF VARIABLE RESPONSE FLAWS

(See Section 3(v)(b))

1. Find the location where the most serious indication occurs and note the indication level.
2. Classify this level as being a Class A, B, C, or D flaw.
3. Adjust the calibrated gain control or attenuator to the most serious Class D level.
4. Move the search unit from the point of most serious indication level (both directions) until the indication decays to a reference level trace deflection height.
5. Mark the trailing edge locations of the search unit on the test material.
6. The distance between these marks is the indication length at Class C, B or A amplitude level(s).
7. If this distance exceeds the allowable length of Class C flaw, the indication is rejectable at this length.
8. If this length is equal to or less than the allowable Class C flaw length, further evaluation is necessary as follows:

   (a) Adjust the calibrated gain control or attenuator to the most serious Class C level.

   (b) Move the search unit toward the point of most serious indication level (Step 3) until the indication height reaches reference level trace deflection height.

   (c) Mark the locations of the leading edge of the search unit on the testpiece.

   (d) The distance between these marks is the indication length at Class B or A amplitude level(s).

   (e) If this length exceeds the allowable length of a Class B flaw the indication is rejectable at this length.

   (f) If this length is equal to or less than the allowable Class B flaw length, further evaluation is necessary.

   (g) If the flaw classification from Step 2 is Class B, C, or D, the indication is acceptable.

   (h) If the flaw classification from Step 2 is Class A, further evaluation is necessary as follows to determine the rejectable length:

      1. Adjust the calibrated gain control or attenuator to the most serious Class B level.
      2. Move the search unit further toward the most serious indication found in Step 1 until the indication height reaches a reference level trace deflection height.
      3. Mark the locations of the leading edge of the search unit.
      4. The distance between these points is the rejectable length of indication as a Class A flaw.

Examples are shown on the following two pages.

APPENDIX II contd.

Examples of length evaluation of variable amplitude discontinuities.

Three 2in. thick sections of weld are being tested to the Building Code and having discontinuity content as listed in the Example charts. The following data is constant:

1. Search unit = 70°, 2.25MHz, $^{5}/_{8}$in.H x $^{3}/_{4}$in.W.
2. Reference level = 24dB (gain).
3. 5in. Sound path (8dB attenuation factor).
4. Scanning level = 24 + 19 = 43dB.

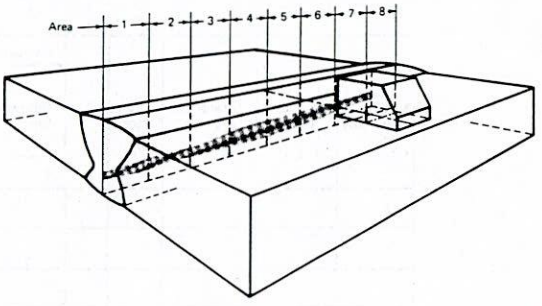

Example 1

Area	Actual length	dB rating	Class
1	2in.	+6	D
2	1in.	+4	D
3	½in.	+2	C
4	$^{3}/_{4}$in.	0	B
5	½in.	+1	C
6	$^{3}/_{4}$in.	+2	C
7	1in.	+3	D
8	1in.	+4	D

Example 2

Area	Actual length	dB rating	Class
1	2in.	+5	D
2	½in.	+4	D
3	½in.	+3	D
4	$^{1}/_{4}$in.	-1	B
5	$^{3}/_{4}$in.	0	B
6	$^{3}/_{4}$in.	+4	D
7	1in.	+5	D
8	2in.	+6	D

Example 3

Area	Actual length	dB rating	Class
1	½in.	+3	D
2	$^{1}/_{4}$in.	-2	A
3	$^{3}/_{8}$in.	-3	A
4	$^{3}/_{4}$in.	+3	D
5	½in.	+4	D
6	1in.	+5	D
7	½in.	+5	D
8	½in.	+4	D

The following data is variable in accordance with 6.19.5.7 and the Example Charts:

Step(s)	Example 1	Example 2	Example 3
1	Area 4 (0dB)	Area 4 (-1dB)	Area 3 (-3dB)
2	B	B	A
3	+3dB	+3dB	+3dB
4-6	2½in.	1in.	$1^{1}/_{8}$in.
7	Reject		
8	-	Further evaluation	Further evaluation
8a	-	+1	+1
8d	-	1in.	$1^{1}/_{8}$in.
8e	-	Reject	
8f	-	-	Further evaluation
8g	-	-	Not acceptable
8h1	-	-	-1
8h4	-	-	$^{5}/_{8}$

APPENDIX F

DETAILS OF EXPERIMENTAL EVALUATION OF PROBE MOVEMENT SIZING

The aim of these tests was to establish the degree of accuracy with which the probe movement technique can measure weld defects.

EXPERIMENTAL PROCEDURE

The procedure employed is described in Document F1, "Ultrasonic Test Procedure, Decibel Drop Methods." This is based on current UK practice (*9, 10, 11*) and on experience gained by The Welding Institute on laboratory investigations of ultrasonic testing performance (*5*). Although measurements of defect position, length, and through-thickness size were made, only the through-thickness measurements were subjected to detailed analysis.

In this study, two factors were investigated:

1. Determination of the accuracy of the technique for defect measurement using controlled equipment.
2. Determination of the variation in defect measurements likely to be encountered from the use of different manual operators.

Item 1, the laboratory tests, were accomplished using the scanning frame discussed in Appendix D and shown in Figure D-2. Forty-five and 60°, 4-MHz transducers were used for the 20-dB drop tests, and 45°, 2-MHz transducers were used for the maximum amplitude (max. amp.) tests. All specimens were subjected to the laboratory tests.

Item 2 was accomplished by subjecting a selection of the specimens (see Table F-1) to tests by two different operators who had no prior knowledge of the defects. These tests were performed manually (i.e., the scanning frame was not used). The 20-dB drop technique was employed using 45 and 60°, 4-MHz transducers.

Further details on equipment can be found in Appendix D.

TABLE F-1
PROBE MOVEMENT TESTS PERFORMED.

Specimen number	Tests applied		
	Laboratory	Operator 1	Operator 2
J201	✓	✓	✓
J202	✓		
J203A	✓	✓	✓
J203B	✓		
J204	✓		
J205A	✓		
J205B	✓		
J206	✓	✓	✓
J207	✓		
J208	✓		
J209A	✓		
J209B	✓	✓	✓
J210	✓	✓	✓
J211	✓	✓	✓
J212A	✓		
J212B	✓		
J213	✓	✓	✓
J251	✓		
J252	✓		
J253	✓		

RESULTS

Laboratory Tests

Although positional and length information has not been analyzed, a qualitative assessment revealed that they were generally of adequate accuracy considering that they are of secondary importance as far as fracture mechanics is concerned. In general, positioning was within 0.10 in. (2.5 mm), and length measurements were accurate to within ±10 percent. This is in agreement with other work (*5*).

In analyzing the through-thickness measurements, some account has been taken of the fact that when an operator makes a series of measurements on a single defect, the maximum value he obtains would normally be reported. This has been done by including in the analysis only the two highest values of defect size measured (where there are more than two) and comparing the measured value with the actual defect size in the position at which the measurement was taken. This gives a series of error values (i.e., ultrasonic measured size v. true size) for each test. Zero values (which can be obtained with both 20-dB drop and max. amp.) and negative values (which can be obtained with 20-dB drop) have also been ignored. The complete results for all defects are given in Table F-2.

For a general picture of the sizing accuracy attainable by probe movement techniques, it is necessary to average out the individual errors so that the performance of the technique can be predicted when examining an unknown flaw. To this end, the errors between actual and measured flaw size have been analyzed statistically to gain a measure of their spread. The normal or Gaussian distribution has been used throughout because this can give a readily assimilated picture of average error and degree of scatter by the mean and standard deviation, respectively. This was not always found to be a perfect fit with the data sample obtained, but nevertheless it remains a valid way of presenting the spread of data in an easily understood format.

Figures F-1 and F-2 show the spread of results for the 20-dB drop and max. amp. techniques, respectively. The diffusion-bonded defects are excluded because these are

TABLE F-2
DETAILS OF RESULTS FROM PROBE MOVEMENT LABORATORY TESTS FOR ALL DEFECTS.

Specimen number	Defect number	Defect type	Actual through-thickness size		Measured size					
					45° 20dB drop		60° 20dB drop		Maximum amplitude	
			Inches	(mm)	Inches	(mm)	Inches	(mm)	Inches	(mm)
J201	1	Solidification crack	0.413 0.433	(10.5) (11.0)	0.098 0.059	(2.5) (1.5)				
J202	4	Slag line	0.059 0.079 0.117	(1.5) (2.0) (3.0)			0.059 0.079	(1.5) (2.0)	0.118 0.118	(3.0) (3.0)
J202	5	Slag line	0.059	(1.5)					0.236	(6.0)
J202	6	Slag line	0.117 0.197	(4.5) (5.0)	0.020	(0.5)			0.394 0.197	(10.0) (5.0)
J203A	7	Freeze-break crack	0.098 0.177	(2.5) (4.5)					0.276 0.118	(7.0) (3.0)
J203B	8	Freeze-break crack	0.095	(7.5)	0.039	(1.0)			0.433 0.276	(11.0) (7.0)
J205A	12	Freeze-break crack	0.236 0.295 0.252	(6.0) (7.5) (6.5)	0.039	(1.0)	0.059	(1.5)	0.335 1.157	(8.5) (4.0)
J205B	13	Freeze-break crack	0.118	(3.0)			0.157	(4.0)		
J206	14	Solidification crack	0.098 0.118 0.138	(2.5) (3.0) (3.5)	0.059	(1.5)	0.236	(6.0)	0.098 0.118	(2.5) (3.0)
J206	15	Solidification crack	0.118	(3.0)			0.118	(3.0)	0.079	(2.0)
J207	17	Slag line	0.098 0.059	(2.5) (1.5)	0.079	(2.0)			0.138	(3.5)
J207	18	Slag line	0.138 0.157	(3.5) (4.0)	0.039 0.138	(1.0) (3.5)			0.118 0.079	(3.0) (2.0)
J207	19	Slag line	0.079 0.098	(2.0) (2.5)	0.079 0.118	(2.0) (3.0)			0.098 0.252	(2.5) (6.5)
J208	20	Freeze-break crack	0.098 0.118 0.138	(2.5) (3.0) (3.5)	0.079 0.079	(2.0) (2.0)	0.039	(2.0)	0.138 0.118	(3.5) (3.0)
J208	21	Freeze-break crack	0.236 0.252	(6.0) (6.5)	0.039	(1.0)	0.118 0.138	(3.0) (3.5)	0.217 0.157	(5.5) (4.0)
J209A	22	Freeze-break crack	0.217 0.236	(5.5) (6.0)	0.079 0.118	(2.0) (3.0)	0.197 0.138	(5.0) (3.5)	0.118 0.118	(3.0 (3.0)
J209B	23	Freeze-break crack	0.315 0.335	(8.0) (8.5)	0.236	(6.0)	0.039	(1.0)	0.252	(6.5)
J210	24	Lack of fusion	0.236 0.276 0.295 0.315	(6.0) (7.0) (7.5) (8.0)	0.039 0.138	(1.0) (3.5)	0.098 0.335	(2.5) (8.5)	0.059 0.138	(1.5) (3.5)
J210	25	Lack of fusion	0.079 0.098	(2.0) (2.5)	0.079 0.118	(2.0) (3.0)	0.098 0.177	(2.5) (4.5)	0.177 0.335	(4.5) (8.5)
J210	26	Lack of fusion	0.197 0.217 0.236	(5.0) (5.5) (6.0)	0.020 0.059	(0.5) (1.5)			0.079 0.138	(2.0) (3.5)
J211	27	Freeze-break crack	0.138 0.157	(3.5) (4.0)					0.236 0.157	(6.0) (4.0)
J213	34	Slag line	0.059	(1.5)			0.079 0.039	(2.0) (1.0)	0.059 0.098	(1.5) (2.5)
J213	35	Slag line	0.059 0.079	(1.5) (2.0)	0.079	(2.0)	0.039	(1.0)	0.098 0.098	(2.5) (2.5)
J251	36	Diffusion bonded defect	0.188	(3.0)	Results influenced by echoes from plate surface					
J251	37	Diffusion bonded defect	0.236	(6.0)	Results influenced by echoes from plate surface					
J252	38	Angled diffusion bonded defect	0.118	(3.0)	0.197 0.118	(5.0) (3.0)	0.157 0.118	(4.0) (3.0)	0.236 0.315	(6.0) (8.0)
J252	39	Angled diffusion bonded defect	0.236	(6.0)	0.197 0.315	(5.0) (8.0)	0.157 0.157	(4.0) (4.0)	0.236 0.394	(6.0) (10.0)
J252	40	Angled diffusion bonded defect	0.472	(12.0)	0.433 0.551	(11.0) (14.0)	0.315 0.315	(8.0) (8.0)	0.472 0.472	(12.0) (12.0)
J253	41	Diffusion bonded defect	0.118	(3.0)	0.197	(6.0)	0.179 0.079	(5.0) (2.0)	0.197 0.197	(5.0) (5.0)
J253	42	Diffusion bonded defect	0.236	(6.0)	0.394 0.354	(10.0) (9.0)	0.276	(7.0)	0.354 0.197	(9.0) (5.0)
J253	43	Diffusion bonded defect	0.472	(12.0)	0.472 0.512	(12.0) (13.0)	0.394	(10.0)	0.472 0.512	(12.0) (13.0)

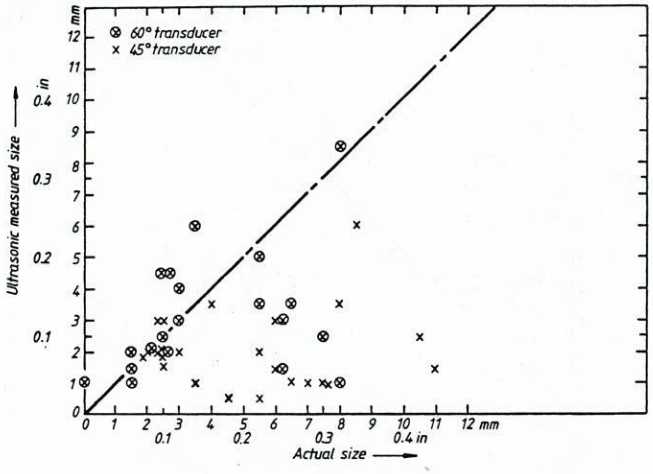

Figure F-1. Measured versus actual flaw sizes for 20-dB drop tests.

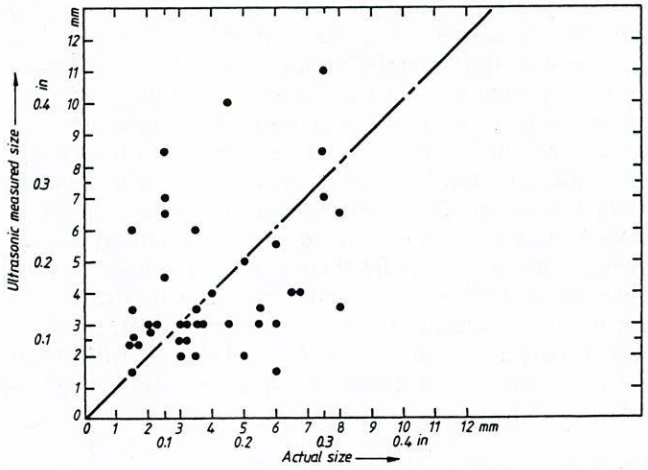

Figure F-2. Measured versus actual flaw sizes for maximum amplitude tests.

dealt with separately below. In both graphs, the 45° line represents zero error. It may be seen that there is a strong tendency for the 20-dB drop technique to underestimate defect size and a slight tendency for the max. amp. technique to overestimate. These have been quantified by extracting mean and standard deviation data (see Table F-3). This confirms the trends with regard to mean error expected from the graphs but shows that for all techniques the spread of results is similar.

From Table F-3 it can also be seen that slightly better results seem to be obtained with the max. amp. technique and with the 20-dB drop technique with a 60° transducer (when separated from the 45° transducer results). However, this trend was not found in previous work (*7*), although, overall, the values were similar to those obtained previously (see Table F-4). The latter results were obtained from tests under slightly different conditions, so strict comparisons should not be made.

The values $\bar{x} \pm 2\sigma$ (Table F-3) are the 95 percent probability limits of each distribution; in other words, 95 percent of all data will lie between these points. The 95 percent level is a standard measure which, in practice, effectively represents the limits of the data spread. The lower bound error is important because it represents the maximum amount by which a defect is likely to be undersized. This represents a nonconservative case because, as a result, a potentially significant defect could be allowed to remain in a weld. If, on the other hand, a defect is oversized, it is likely to be repaired irrespective of whether it is in fact significant; which is a "safe" or conservative condition.

It may be seen from Table F-3 that a factor varying between 0.19 to 0.35 in. (4.8 to 8.9 mm), depending on the technique used, is required to be added to the measured defect size, depending on the test, to be 95 percent certain that the new value is not less than the actual defect size. This is a large error, especially when most flaws in welds produced during manufacture would not be expected to be more than about 0.2 in. (5 mm) in depth.

The diffusion-bonded defects gave responses that were not representative of real defects, and therefore the results are treated separately. Strong echoes were obtained from points that are thought to coincide with the defect extremities (see Appendix E), and in cases where a specular reflection could not be obtained it was not possible to determine that there

TABLE F-3
STATISTICAL DATA ON ACCURACY OF DEFECT THROUGH-WALL SIZE MEASUREMENT FOR PROBE MOVEMENT TESTS.

Sizing technique	Transducer angle	Mean error ($\bar{x}$)		Standard deviation (σ)		95% probability band $\bar{x} \pm 2\sigma$		Number of measurements
		Inches	(mm)	Inches	(mm)	Inches	(mm)	
Maximum amplitude	45°	+0.088	(+0.20)	0.098	(2.50)	-0.19 to +0.20	(-4.80 to +5.20)	40
20dB drop	45° and 60°	-0.080	(-2.03)	0.115	(2.91)	-0.31 to +0.15	(-7.85 to +3.79)	45
20dB drop	45° only	-0.122	(-3.10)	0.114	(2.89)	-0.35 to +0.11	(-8.88 to +2.68)	24
20dB drop	60° only	-0.032	(-0.81)	0.096	(2.45)	-0.22 to +0.16	(-5.71 to +4.09)	21

was a defect connecting the two points. The results should therefore be treated with some caution.

In general, the larger diffusion-bonded defects were more accurately sized than the smaller ones (see Table F-2), indicating the limits of resolving power of the transducer when the two extremity echoes are close together. Difficulty was also experienced with the thinner plate when echoes from the plate surface interfered with the defect signals. The same statistical analysis as performed on the welded defects revealed a mean error of 0.026 in. (+0.66 mm) and standard deviation of 0.085 in. (2.16 mm), which is better than any of the probe movement results for the welded defects. This would be expected in view of the fact that a well-defined extremity signal is usually obtained for these artificial reflectors.

Operator Variability

Figure F-3 shows the spread of results for two operators, and Table F-5 gives the results of a statistical analysis similar to that performed for the laboratory tests. It should be borne in mind that this statistical evaluation was conducted on a small sample (~10). The results for operator 1 show a significant tendency to oversize and have a larger spread of results than obtained in any of the laboratory tests. Operator 3 followed the trend of undersizing experienced in the laboratory tests and had a slightly smaller spread of results (σ = 0.091 in. (2.32 mm)) than the laboratory tests.

The degree of variation between operators arises from differences in the subjective interpretation of the test data (the complex and sometimes ambiguous information presented on the A-scan display) and from the individual's approach to selecting and recording what he considers relevant. It is clear that differences in accuracy for different operators are likely. However, comparing these results with the laboratory tests, even the results from the operator with poorer accuracy are only marginally worse than those achieved with controlled equipment.

TABLE F-4
STATISTICAL DATA ON ACCURACY OF DEFECT THROUGH-WALL SIZE MEASUREMENT FOR PREVIOUS PROBE MOVEMENT TESTS FROM REF. *5* (PLANAR DEFECTS ONLY).

Test	Mean error ($\bar{x}$)		Standard deviation (σ)		95% probability level ($\bar{x} \pm 2\sigma$)	
	Inches	(mm)	Inches	(mm)	Inches	(mm)
45° maximum amplitude	-0.047	(-1.2)	0.134	(3.4)	-0.315 to +0.220	(-8.0 to +5.6)
45° 20dB drop	-0.091	(-2.3)	0.102	(2.6)	-0.295 to +0.114	(-7.5 to +2.9)
60° and 70° 20dB drop	-0.106	(-2.7)	0.115	(3.0)	-0.343 to +0.130	(-8.7 to +3.3)

TABLE F-5
STATISTICAL DATA ON ACCURACY OF DEFECT THROUGH-WALL SIZE MEASUREMENT FOR PROBE MOVEMENT OPERATOR VARIABILITY TESTS.

Operator	Mean error ($\bar{x}$)		Standard deviation (σ)		Number of measurements
	Inches	(mm)	Inches	(mm)	
1	-0.037	(-0.95)	0.130	(3.31)	10
3	-0.052	(-1.32)	0.091	(2.32)	11

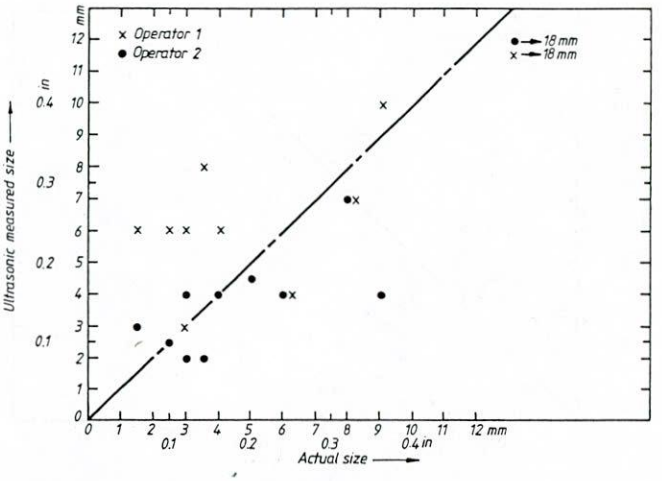

Figure F-3. Measured versus actual flaw size for probe movement operator variability tests.

Document F1

ULTRASONIC TEST PROCEDURE, DECIBEL DROP METHODS

JOB NO. 3625

1. EQUIPMENT

   Flaw detector: Krautkrämer USM2 (supplied by The Welding Institute)

   Probes: A selection will be supplied together with the necessary beam plots.

2. SPECIMEN DETAILS TO BE RECORDED (see attached form NDT/F/1)

   Identification No.

   Material

   Dimensions

   Welding process

   Edge preparation

   Surface condition

   Also note reference marks defining orientation of each plate and datum points for measurements.

3. TESTS

   The test sequence will consist of the following:

   (i) 0° compression wave scan to check for laminations, on both sides of weld from top surface only. (Faces A+ and A-)

   (ii) 4MHz shear wave scans to examine defects at 45, 60 and 70° from both sides of weld on top and bottom surfaces (A+, A-, B+, B-)

   (iii) 2MHz shear wave scans at 45° only from surfaces A+ A- B+ B-.

   Details of scans performed and tests used shall also be recorded on NDT/F/1.

Document F1 Continued

3.1. Compression wave scans

Sensitivity level: back wall echo to full screen height (FSH) + 6dB

Area to be scanned: at least 130mm each side of the weld for the entire weld length.

Record all reflectors deemed significant and plot them on a drawing. Where possible, size is to be measured by 6dB drop technique. NDT/F/3 is provided for recording of information from the scans.

3.2. 4MHz shear wave scans

This procedure is to be followed for all probe angles used. Single crystal probes are to be used, but twin probes may be used in addition if better near surface resolution if required.

Sensitivity: to be set at operator's discretion, commensurate with reliable defect detection. Levels used are to be related to the response from the 100mm radius in the IIW V1 block and recorded.

Defect assessment: The maximum amount of information obtainable from each defect is required. Therefore, defect length parallel to the weld is to be measured by the 6dB drop method and through-thickness size and depth position measured using the 20dB drop method.

For long defects a number of depth measurements are required.

Defect length	Minimum number of measurements
up to 10mm	1
10-20mm	2
20-40mm	3
40-100mm	4
100+mm	5

Form NDT/F/2 is provided for recording this information. From these scans; plan, longitudinal section and transverse section drawings of the defects found are to be produced on an outline of the weld preparation. Any relevant comments concerning defect type, orientation, etc. are to be included.

3.3. 2MHz 45° shear wave scans

The procedure and reporting requirements for these scans are the same as for 4MHz tests except through-thickness size is to be measured by the maximum amplitude method.

On completion of the tests, all forms, drawings etc. for each specimen are to be fixed together and handed to the appropriate Welding Institute investigator.

DOCUMENT F1 – FORM NDT/F/1

THE WELDING INSTITUTE

NDT RESEARCH SECTION

MANUAL ULTRASONIC OPERATOR'S TEST REPORT

This must be carried out by a qualified CSWIP operator with site testing experience.

1. Inspector:
2. Date:
3. Specimen number:
4. Material:
5. Dimensions:
6. Welding process:
7. Edge preparation:
8. Surface condition (i) weld:
   (ii) plate:
9. Flaw detection equipment:
10. Probe details:

Probe number	Size	Frequency and angle	Type and make
A			
B			
C			
etc			

11. Test details:

Scan number	Probe number	Sensitivity	Probe scan	Area tested
(1)				
(ii)				
(iii)				
(iv)				
etc.				

How sensitivity determined:

Sizing method used:

12. Results:

Condition of parent plate:

Details of defects found (drawing attached):

Test limitations:

13. Inspector's remarks:

NOTES

(3), (4), (6) and (7): Information given.

(9) Flaw detector must be typical of as used on site, (e.g. US.12) same equipment must be used throughout.

(10) Same probes must be used throughout programme.

Indicate size, (i.e. crystal size), nominal frequency, angle, type, (e.g. twin or single crystal), and manufacturer.

(11) Probe number is as designated in (10).

Document F1 Continued

Sensitivity related to 100mm on IIW block.

Probe scan — where probe was put and moved on specimen surface and which areas of the weld or parent metal were being tested.

State how sensitivity level was determined, e.g. grass level.

Sizing: All defects to be sized in length and through-thickness

Consultation will be necessary to decide if small unintended defects need sizing.

State sizing method used.

(12)Include detailed drawing indicating
- position and size of defect
- which scans found which defect
- assessment of defect type, if possible, (e.g. crack or pore)

Limitations such as poor parent plate, rough surface, etc., should be stated.

APPENDIX G

DETAILS OF EXPERIMENTAL EVALUATION OF TIME-OF-FLIGHT SIZING

The aim of these tests was to establish the degree of accuracy with which the time-of-flight technique can measure the though-thickness extent of weld defects.

EXPERIMENTAL PROCEDURE

The procedure employed is described in Document G1, "Part A: Ultrasonic time delay crack depth measurement system" and "Part B: Time delay procedure for surface breaking and embedded defects," included at the end of this appendix. This document is based on previous collaborative work with the Non-destructive Testing Centre of the Atomic Energy Research Establishment, Harwell, England, which developed the technique.

In this study, two factors were investigated:

1. Determination of the accuracy of the technique for defect measurement.
2. Determination of the variation in defect measurements likely to be encountered from the use of different operators.

Table G-1 presents the tests conducted. It proved difficult to interpret signals arising from defects in the thinnest plate (0.4 in.), therefore only a limited number of tests were performed on these. The equipment used for these tests is described briefly in Appendix D and in more detail in Document G1.

TABLE G-1
TIME-OF-FLIGHT TESTS PERFORMED.

Specimen number	Tests performed			
	"Laboratory"	Operator 1	Operator 2	Operator 3
J201	✓	✓	✓	✓
J202	✓			
J203A	✓	✓		✓
J203B	✓			
J204	✓			
J205A	✓			
J205B	✓			
J206	✓	✓	✓	✓
J207	✓			
J208	✓			
J209A	✓			
J209B	✓	✓	✓	✓
J210	✓	✓	✓	✓
J211	✓			
J212A				
J212B				
J213	✓			

RESULTS

Although it was hoped that signals from the upper and lower extremities of the defect could be analyzed simultaneously to give a "one-shot" size measurement, this proved to be difficult because of the complexity of the display. It was, however, possible to position accurately the defect extremity nearer the test surface as this signal appears first on the monitor timebase. From these data, collected from tests on both A and B faces of each specimen, the position of both edges of the flaws, and therefore their through-wall size, could be determined.

Such a correction was performed for 18 of the welded defects and 6 of the diffusion-bonded defects from those tested by the laboratory procedure. The complete results on all defects are given in Table G-2. The results on the welded defects only are presented in graphical form in Figure G-1 and in statistical form in Table G-3. In the latter, a direct comparison can be made with similar results obtained from the more sophisticated laboratory equipment described in Ref. (*5*). The comparison is favorable between the two sets of results in spite of a slightly greater tendency for the tests carried out in this study to undersize flaws. However, they indicate that provided the display can be interpreted sufficiently to obtain time-of-flight values from a flaw's extremities, a more accurate measure of through-wall depth can be obtained than with probe movement methods.

The results for the diffusion-bonded defects have again been examined separately for reasons discussed in Appendixes E and F. These are insufficient to perform a statistical evaluation, but, qualitatively, the accuracy is the best achieved for any test in this work (see Table G-2). This bears out the theoretical soundness of the time-of-flight technique. Again, the results should be treated with caution in that the responses from these defects do not represent those from real defects.

The operator variability tests confirmed the difficulty in interpreting the displays, because, in several cases, the operator did not record a value and therefore the number of results is very limited. The values recorded are plotted in Figure G-2. Apart from the values relating to defect 1 (the duplex crack, 0.71-in. (18-mm) maximum through-thickness; see Figure C-5), the results are substantially accurate, indicating that where an interpretation could be confidently made, it was usually correct. The small sample number precludes any statistical analysis.

The main shortcoming of the system employed was the absence of an intermediate display produced by the equipment to give a clearer picture of the position of defect extremities, thereby enabling the size to be determined with a minimum of operator judgment. This would appear to be necessary in order to interpret the signals satisfactorily. This is discussed in Chapters Three and Four of the main report.

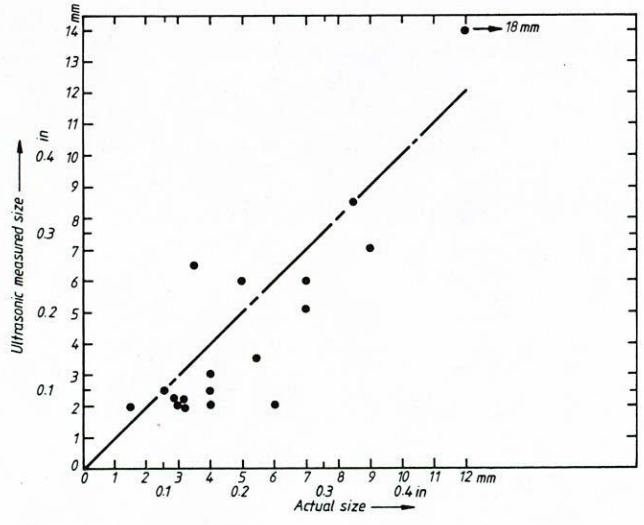

Figure G-1. Measured versus actual flaw size for time-of-flight tests.

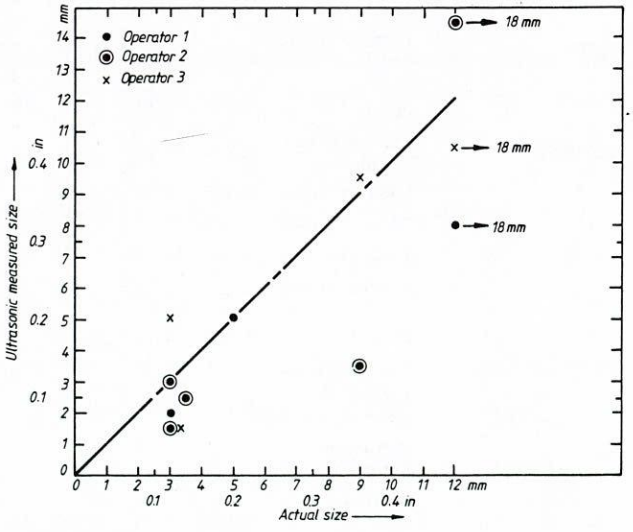

Figure G-2. Measured versus actual flaw size for time-of-flight operator variability tests.

TABLE G-2
DETAILS OF RESULTS OF TIME-OF-FLIGHT TESTS FOR ALL DEFECTS.

Specimen number	Defect number	Defect type	Actual through-thickness size		Measured size							
					Laboratory tests		Operator					
							1		2		3	
			Inches	(mm)	Inches	(mm)	Inches	(mm)	Inches	(mm)	Inches	(mm)
J201	1	Solidification crack	0.709	(18.0)	0.551	(14.0)	0.315	(8.0)	0.571	(14.5)	0.413	(10.5)
J202	4	Slag line	0.118	(3.0)	0.079	(2.0)						
J202	5	Slag line	0.118	(3.0)	0.079	(2.0)						
J202	6	Slag line	0.138	(3.5)	0.138	(3.5)						
J203A	7	Freeze-break crack	0.197	(5.0)	0.236	(6.0)	0.197	(5.0)			-	
J203B	8	Freeze-break crack	0.335	(8.5)	0.335	(8.5)						
J205A	12	Freeze-break crack	0.354	(9.0)	-							
J205B	13	Freeze-break crack	0.157	(4.0)	0.098	(2.5)						
J206	14	Solidification crack	0.138	(3.5)	0.252	(6.5)	-		0.098	(2.5)	-	
J206	15	Solidification crack	0.118	(3.0)	0.079	(2.0)	-		0.118	(3.0)	0.059	(1.5)
J207	17	Slag line	0.157	(4.0)	-							
J207	18	Slag line	0.157	(4.0)	-							
J207	19	Slag line	0.157	(4.0)	-							
J208	20	Freeze-break crack	0.157	(4.0)	0.118	(3.0)						
J208	21	Freeze-break crack	0.276	(7.0)	0.197	(5.0)						
J209A	22	Freeze-break crack	0.276	(7.0)	0.236	(6.0)						
J209B	23	Freeze-break crack	0.354	(9.0)	0.276	(7.0)	-		0.138	(3.5)	0.374	(9.5)
J210	24	Lack of fusion	0.315	(8.0)	-							
J210	25	Lack of fusion	0.118	(3.0)	0.079	(2.0)	0.079	(2.0)	0.059	(1.5)	0.197	(5.0)
J210	26	Lack of fusion	0.236	(6.0)	0.079	(2.0)						
J211	27	Freeze-break crack	0.157	(4.0)	0.079	(2.0)						
J213	34	Slag line	0.098	(2.5)	0.079	(2.0)						
J213	35	Lack of fusion	0.059	(1.5)	0.079	(2.0)						
J251	36	Diffusion bonded defect	0.118	(3.0)	-							
J251	37	Diffusion bonded defect	0.236	(6.0)	-							
J252	38	Angled diffusion bonded defect	0.118	(3.0)	0.098	(2.5)						
J252	39	Angled diffusion bonded defect	0.236	(6.0)	0.217	(5.5)						
J252	40	Angled diffusion bonded defect	0.472	(12.0)	0.394	(10.0)						
J253	41	Diffusion bonded defect	0.118	(3.0)	0.079	(2.0)						
J253	42	Diffusion bonded defect	0.236	(6.0)	0.315	(5.0)						
J253	43	Diffusion bonded defect	0.472	(12.0)	0.433	(11.0)						

- examined but no sensible result

TABLE G-3
STATISTICAL DATA ON ACCURACY OF DEFECT THROUGH-WALL SIZE MEASUREMENT FOR TIME-OF-FLIGHT TESTS.

Test	Mean error, $\bar{x}$		Standard deviation, σ		95% probability level ($\bar{x} \pm 2\sigma$)	
	Inches	(mm)	Inches	(mm)	Inches	(mm)
"Laboratory" tests on simplified equipment	-0.041	(-1.03)	0.064	(1.63)	-0.169 to 0.088	(-4.29 to 2.23)
Results from previous Welding Institute programme (5) with complex equipment	0.02	(0.50)	0.071	(1.80)	-0.122 to 0.161	(-3.10 to 4.10)

Document G1

ULTRASONIC TIME DELAY CRACK DEPTH MEASUREMENT SYSTEM

1. Principles of operation and use

One physical property of ultrasonic waves is that they may be diffracted over a wide angle by a sharp discontinuity in the material through which they are travelling. The tip of a crack is such a discontinuity and use is made of this effect to measure crack depth. If ultrasound is directed at a crack tip, it is diffracted over 360° by the tip region (Fig.1). A component of the diffracted wave is picked up by a receiver probe and measurement of the time taken for sound to travel round the crack enables the depth to be calculated by simple geometry.

The formula relating crack depth, x, and time delay δt is:

$$x = \left[\left(\frac{V \delta t}{2} + \left(d^2 + \left(\frac{s^2}{2} \right)^{\frac{1}{2}} \right)^2 - \left(\frac{s}{2} \right)^2 \right]^{\frac{1}{2}} \right.$$

where s is the probe spacing (see Fig.1)

V is the velocity of longitudinal sound waves in the material (= 5900m/sec for steel)

d is the depth of a reference notch needed to set up the system (see Section 2)

2. System characteristics

Figure 2 shows a block diagram of the Harwell modular system which uses the time delay approach and Fig.3 a schematic diagram of the front panel. The difference timer is a comparative unit so the system must be calibrated on a known notch. A series of milled notches ranging from 2 to 40mm in depth is available. The size of reference notch, probe separation, s, and angle, θ, (see Fig.1), must be chosen so the crack tip will lie within the beam. The variation of depth of intersection of ultrasonic beam axes with probe separation is shown in Fig.4. The time taken to traverse the reference notch is stored in a memory when the "set zero" button is pressed. When the probes are placed over the crack to be measured, the "measure" button is depressed and time taken to traverse the crack is recorded by the timer, the stored time to traverse the reference notch is subtracted and the difference (δt) displayed as a series of digits. Crack depth may then be calculated from the formula or determined from a calibration curve (Fig.5).

Document G1 Continued

3. Setting up and measurement

(i) Select probe angle and separation to suit cracks under examination. (Fig.4)

(ii) Connect probes Tx and Rx to socket numbers (1) and (2) respectively in Fig.3. Connect trigger (3), R.F. out (5), and strobe (4) to oscilloscope (2 channel).

(iii) Check that the system triggers correctly by placing probes over the reference notch and observing the strobe pulse. A schematic of the correct configuration seen on the CRT screen is shown in Fig.6. If system will not trigger on correct pulse, either there is insufficient gain or the strobe delay is incorrect. To adjust the latter, turn "delay" screw on the strobe unit (Fig.3). To adjust the gain, remove the connection from (4) on Fig.3 and connect (6), the gate signal. A gate will appear on the CRT as a step whose size, position and effect on signal amplitude may be adjusted by the three screws on the AGC module. After readjustment, reconnect to (4) on the strobe module.

(iv) To measure the time delay, place the probes symmetrically over a suitable reference notch as shown in Fig.1. If necessary move them slightly to minimise time of flight, observed by monitoring the CRT screen. Press the "set zero" button.

The equipment is now ready to measure a crack so place over the point to be measured, again in a manner similar to Fig.1, and making sure the strobe pulse is stable and at the correct point on the pulse (Fig.6). Press the "measure button" and δt will appear as a series of digits in micro seconds (the decimal point is marked on the display) from which crack depth may be obtained. The red LED will flash if the value is negative.

Document G1 Continued

TIME DELAY PROCEDURE FOR SURFACE BREAKING AND EMBEDDED DEFECTS

To operate time delay system using manual positioning of timing points, (i.e. not using automatic trigger)

1. Set up time delay equipment as shown in the wiring diagram: Fig.7.
2. Place probe carriage symmetrically over a suitable reference notch. Notch depth and probe separation are picked according to depth zone to be scanned: See Table (1) which refers to probes S5 and S7 with shoes W11 and W12. Beam plots are shown in Fig.8 and Fig.9.
3. As no lateral wave is available for calibration, programme calculator using P.J.M. 4.2.80 programme (Table 2).
4. Move marker on YB trace to intersect the first peak from reference notch signal on YA trace on 'scope. This is done by using the external potentiometer on front extreme right of time delay rig. (Use x5 pull on switch on front of 'scope for accuracy.)
5. Having positioned the marker on top of this peak press set zero button. Any time measurements from now on will be taken as plus or minus from this position.
6. To check all is functioning correctly place probes astride another reference notch, position marker over notch signal as before and press measure button. Punch this time in μs into the calculator and the answer should be the notch depth in mm.
7. Place probes over area to be scanned, and when defect signals are located and maximised take measurements as in Step 6. Use form NDT/F/5 to record information.
8. Calibration curves for probe separations at each depth zone are in Fig.10, 11, 12 and 13.
9. Module No. 95/0169 - 1/6 controls the range over which the marker on the YB 'scope trace may be moved for time measurements. To adjust those ranges, see Table 3.

NOTES

(i) Always use sufficient couplant, grease, Rosalex or similar to transmit the sound from probe to specimen. However, do not let couplant seep into the crack as it will render it transparent to ultrasound and this method becomes much less effective.

(ii) It is desirable to place a tensile load on fatigue cracks before measurement (up to the magnitude of the fatigue load) as these tend to close up leading to erroneous depth measurement.

(iii) If it is felt that the defect signal can be increased by changing probe separation, this may be done, but the system must then be recalibrated for the new probe separation and the new probe separation must be entered into the calculator memory.

(iv) A selection of notches of known depth are available in reference blocks No.20, 21, 22 and 24. Notch depths are given in Table 4.

Document G1 Table 1

Time delay depth zones for: Probes S5, S7, Shoes W11, W12

Probe separation	Reference notch	Depth zone	Beam center lines intersect
40mm	20mm	10-22mm	19mm
70mm	30mm	22-37mm	33mm
110mm	40mm	35-70mm	52mm
150mm	40mm	48-95mm	70mm

Document G1 Continued

DOCUMENT G1 Table 2

TITLE / TITEL / TITRE: Time Delay Analysis
PAGE / SEITE / PAGE: 1 OF / VON / DE 1
PROGRAMMER / PROGRAMMIERER / PROGRAMMEUR: P.J. Mudge
DATE / DATUM / DATE: 4.2.80

TI PROGRAMMABLE
PROGRAM RECORD
PROGRAMM-BERICHT
FICHE PROGRAMME

Partitioning (Op 17) / Speicher-Bereichsverteilung / Partition (Op 17):
Library Module / Software-Modul / Module enfichable:
Printer / Drucker / Imprimante:
Cards / Karten / Cartes:

PROGRAM DESCRIPTION • PROGRAMM BESCHREIBUNG • DESCRIPTION DU PROGRAMME

Calculate crack depth in mm from $\hat{o}t$ values for given values of d, s, and v.

Equation, crack depth, $x = \left[\left(\frac{v\hat{o}t}{2} + \sqrt{d^2 + \left(\frac{s}{2}\right)^2}\right)^2 - \left(\frac{s}{2}\right)^2\right]^{\frac{1}{2}}$

d = ref notch depth mm v = velocity ms^{-1}

s = probe separation mm $\hat{o}t$ = time delay μs

USER INSTRUCTIONS • BENUTZER INSTRUKTIONEN • MODE D'EMPLOI

	PROCEDURE / PROZEDUR / PROCEDURE	ENTER / EINGABE / INTRODUIRE	PRESS / BEFEHL / APPUYER SUR	DISPLAY / ANZEIGE / AFFICHAGE
1	Press LRN calculator enters learn mode		LRN	000 00
2	Key in programme as shown overleaf			083 00
3	Press LRN again to exit learn mode (programme now stored)			
	TO OPERATE			
4	Store d in memory 01	value of d(mm)	STO	value of d
			01	value of d
5	Store s in memory 02	value of s(mm)	STO	value of s
			02	value of s
6	Store v in memory 03	value of v(mm^{-1})	STO	value of v
			03	value of v
7	Enter value of $\hat{o}t$	value of $\hat{o}t$(μs)	A	value x
8	Calculate x (mm)			

USER DEFINED KEYS / PROGRAMM-ADRESSTASTEN / TOUCHES UTILISATEUR	DATA REGISTERS / DATENSPEICHER / REGISTRES-MEMOIRE	LABELS (Op 04) / LABELS (Op 08) / LABELS (Op 08)
A Time delay $\hat{o}t$, μs	0	8
B Crack depth x, mm	1 d, mm	1
C	2 s, mm	2
D	3 v, ms^{-1}	3
E	4 $\hat{o}t$, μs (used by programme)	4
A'	5	5
B'	6	6
C'	7	7
D'	8	8
E'	9	9

FLAGS / FLAGS / DRAPEAUX: 0 | 1 | 2 | 3 | 4 | 5 | 6 | 7 | 8 | 9

Document G1 Continued

DOCUMENT G1 Table 2 contd.

TITLE / TITEL / TITRE _____ PAGE / SEITE / PAGE _____ OF / VON / DE _____

PROGRAMMER / PROGRAMMIERER / PROGRAMMEUR _____ DATE / DATUM / DATE _____

TI PROGRAMMABLE
CODING FORM
KODEFORM
FEUILLE DE PROGRAMMATION

LOC ADR ADR	CODE KODE CODE	KEY TASTE TOUCHE	COMMENTS BEMERKUNGEN COMMENTAIRES
00		LRN enter learn mode	
1		2nd LBL	
2		A	stores ôt
3		STO	in 04
4		04	
5		NOP	
6		2nd LBL	
7		B	
8		(	
9		(	
10		(	
1		RCL	
2		03	
3		÷	
4		2	
5		)	
6		x	multiply
7		(	
8		RCL	
9		04	
20		÷	
1		1	
2		0	
3		0	
4		0	
5		0	
6		0	
7		0	
8		)	
9		+	
30		(	
1		(	
2		RCL	
3		01	
4		÷	
5		1	
6		0	
7		0	
8		0	
9		)	
40		x^2	
1		+	
2		(	
3		(	
4		RCL	
5		02	
6		÷	
7		1	
8		0	
9		0	
50		0	
1		)	
2		÷	
3		2	
4		)	

LOC ADR ADR	CODE KODE CODE	KEY TASTE TOUCHE	COMMENTS BEMERKUNGEN COMMENTAIRES
5		x^{-1}	
6		)	
7		$\sqrt{x}$	
8		)	
9		x^2	
60		-	
1		(	
2		(	
3		RCL	
4		02	
5		÷	
6		1	
7		0	
8		0	
9		0	
70		)	
1		÷	
2		2	
3		)	
4		x^2	
5		)	
6		$\sqrt{x}$	
7		x	multiply
8		1	
9		0	
80		0	
1		0	
2		=	
3		R/S	
4			
5		LRN	exit learn mode
6			
7			
8			
9			
90			
1			
2			
3			
4			
5			
6			
7			
8			
9			

LOC ADR ADR	CODE KODE CODE	KEY TASTE TOUCHE	COMMENTS BEMERKUNGEN COMMENTAIRES
0			
1			
2			
3			
4			
5			
6			
7			
8			
9			
10			
1			
2			
3			
4			
5			
6			
7			
8			
9			
20			
1			
2			
3			
4			
5			
6			
7			
8			
9			
30			
1			
2			
3			
4			
5			
6			
7			
8			
9			

MERGED CODES / KOMBINATIONS-KODES — TOUCHES COMBINEES

62			72 STO		83 GTO
63			73 RCL		84
64			74 SUM		92 INV SBR

TEXAS INSTRUMENTS

Document G1 Continued

Document G1 Table 3 Adjustment to marker on CRT for time measurements (module 95/0179-1/6)

Capacitor	Delay range	Link	Link position
390	200-350ns	1	A-B
1.00pf	300-1500ns	2	A-B
3.300pf	900-4500ns	3	A-B
0.1µf	3-15µs	4	A-B
0.033µf	9-45µs	1	A-C
0.1µf	30-150µs	2	A-C
0.33µf	90-450µs	3	A-C
1µf	300-1500µs	4	A-C

NOTES. 1. Adjustment is made by moving link pin across links 1 to 4 enabling various capacitors to be switched in.
2. Links 5 to 23 provide fine tuning for the ranges quoted above.

Document G1 Table 4 Reference notch depths

Reference block number	Notch depth (mm)
24	2
24	4
24	6
22	10
21	15
20	20
20	25
21	30
22	40

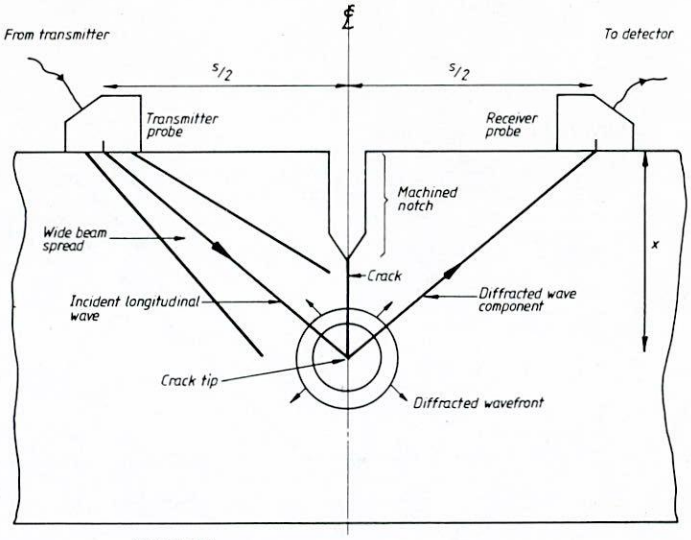

Document G1
Fig.1. Experimental setup for time of flight measurement of crack depth.

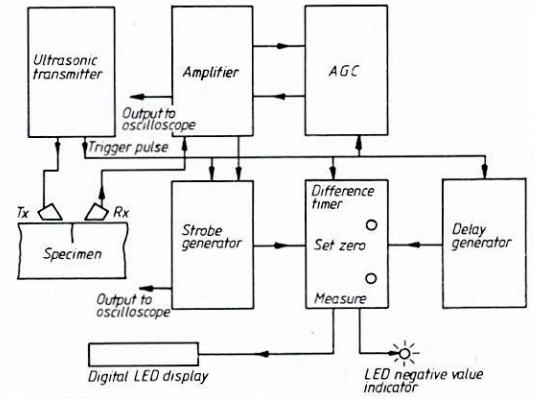

Document G1
Fig.2. Block diagram of ultrasonic time delay system based on Harwell 6000 series modules.

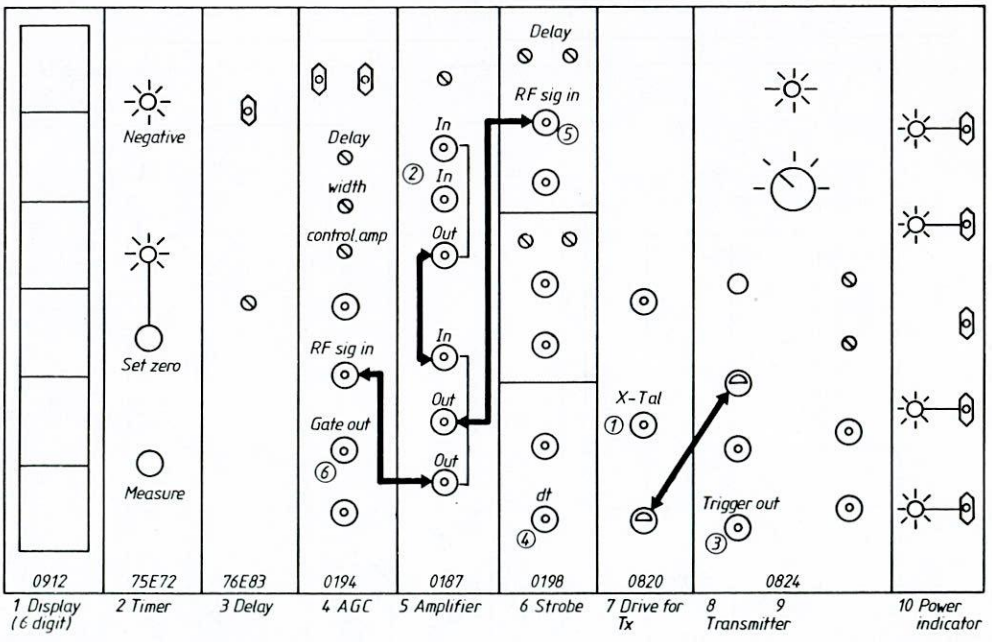

① Output for Tx (size o)
② Input for Rx (either socket, size oo)
③ Trigger out for scope (size oo)
④ Strobe pulse to scope (size oo)
⑤ RF signal output to scope (viz. oo size T-piece)
⑥ AGC gate position output to scope when required (size oo)

Key
Testpoint
Light emitting diode
Screw pots
Push buttons
LEMO socket
External connection

Document G1
Fig.3. Schematic diagram of front panel of time delay unit.

Document G1 Continued

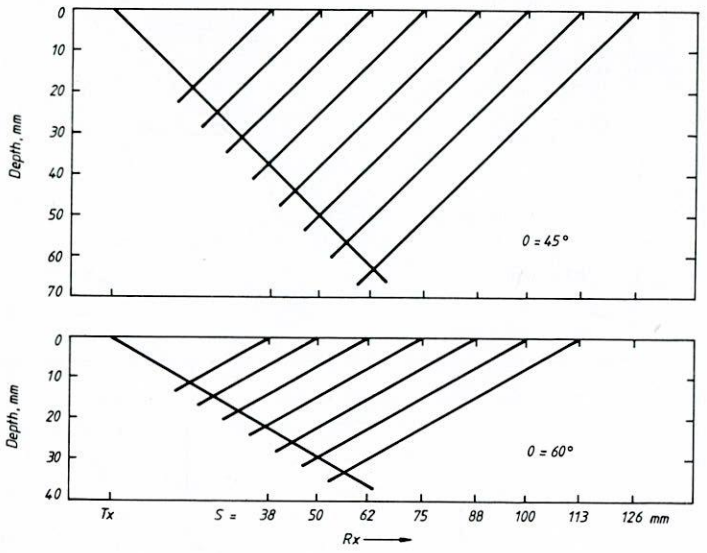

Document G1
Fig.4. Variation of depth of intersection of beam axes with separation for 45° and 60° probes.

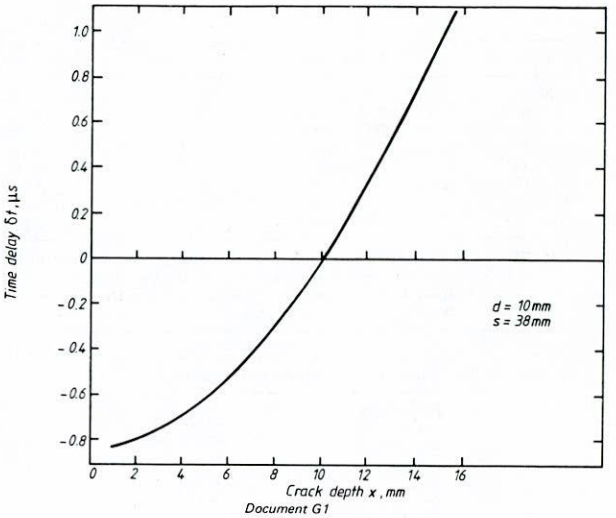

Document G1
Fig.5. Typical calibration curve.

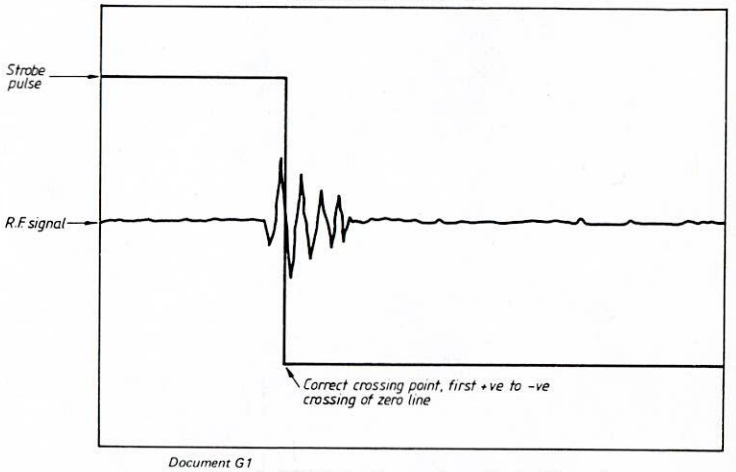

Document G1
Fig.6. Schematic of CRT display of response from surface breaking notch

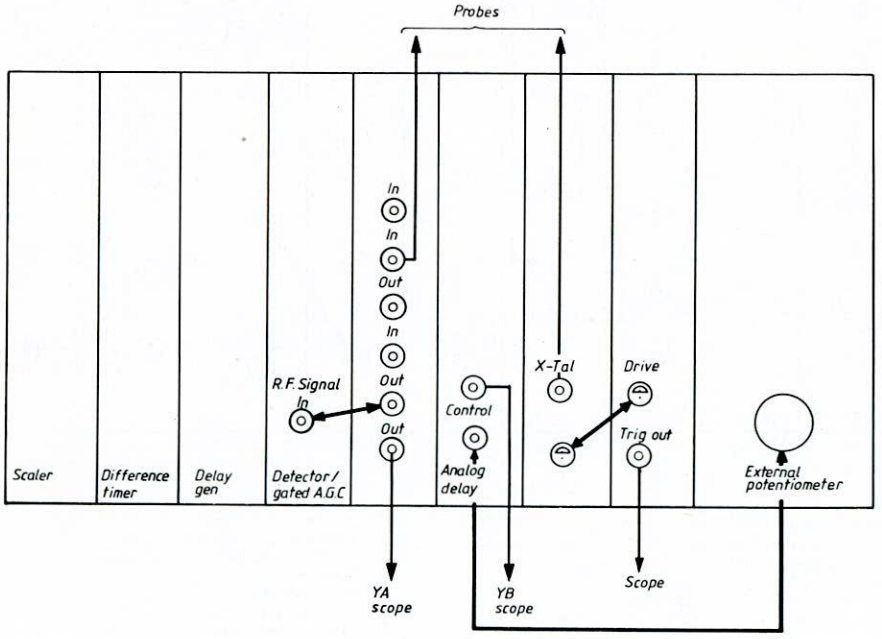

Document G1
Fig.7. Time delay unit front panel settings using 'marker' on CRT trace for time measurement. (For key see document G1 Fig.3.)

Document G1 Continued

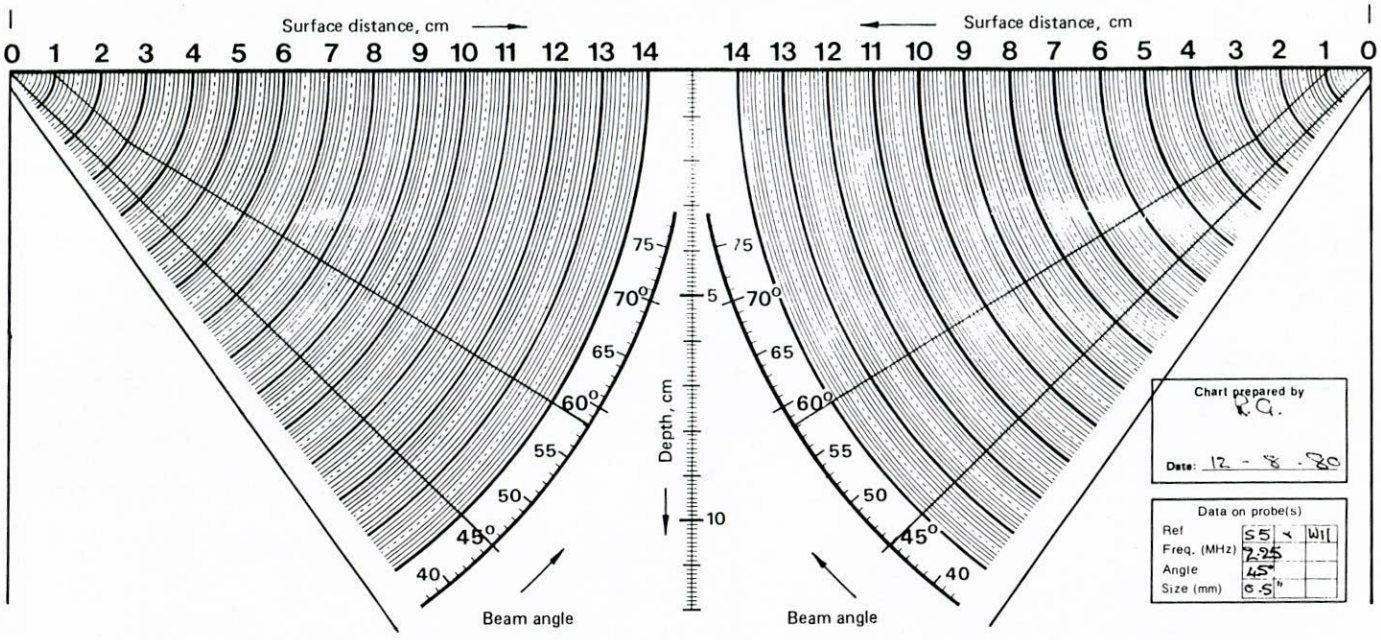

Document G1
Fig.8. Beam plots for S5/W11 transducers.

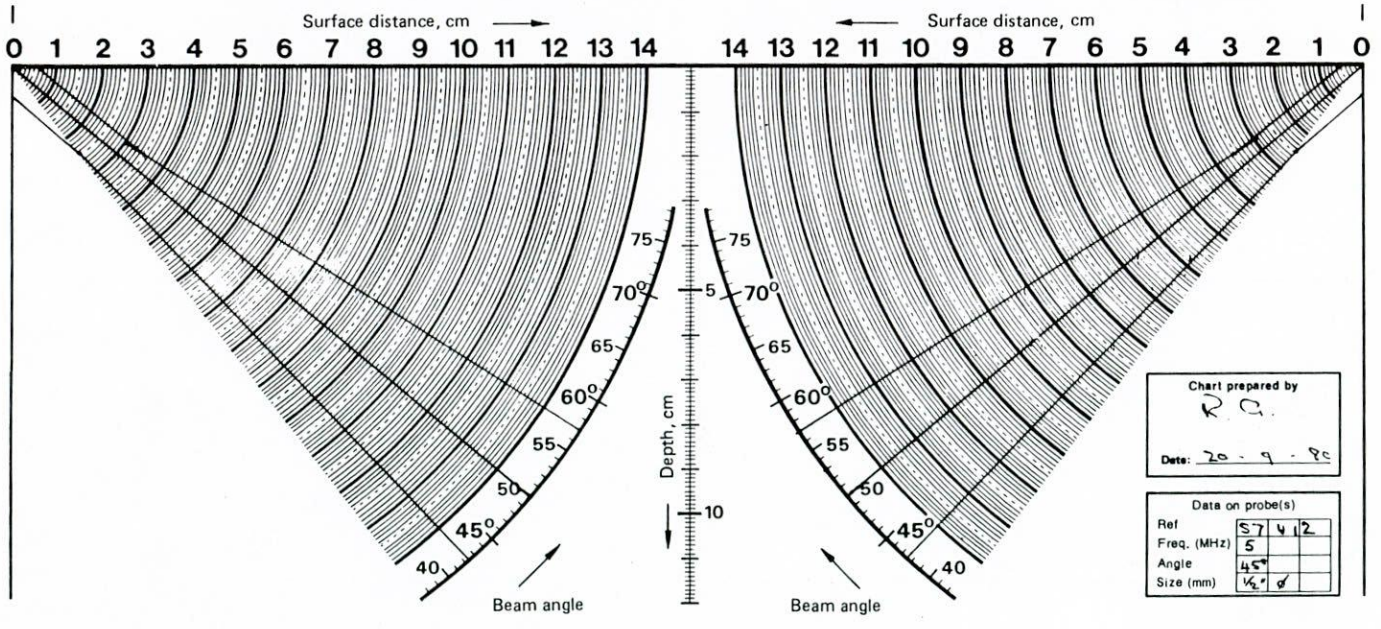

Document G1
Fig.9. Beam plots for S7/W12 transducers.

Document G1 Continued

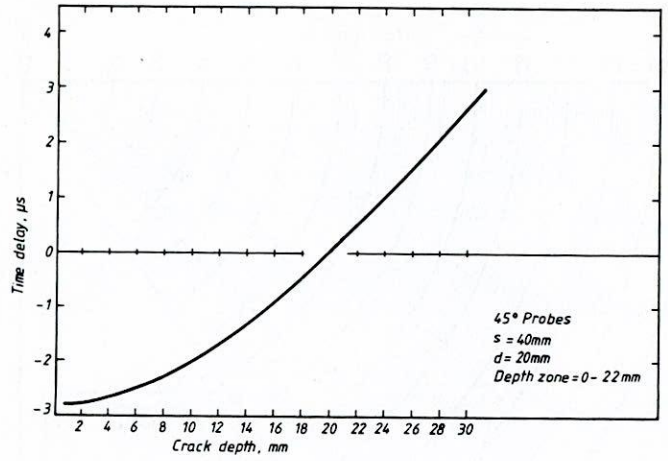

Document G1
Fig.10. Calibration curve.

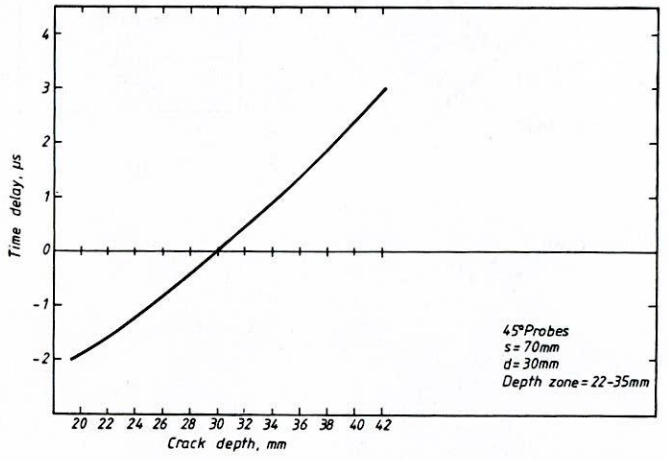

Document G1
Fig.11. Calibration curve.

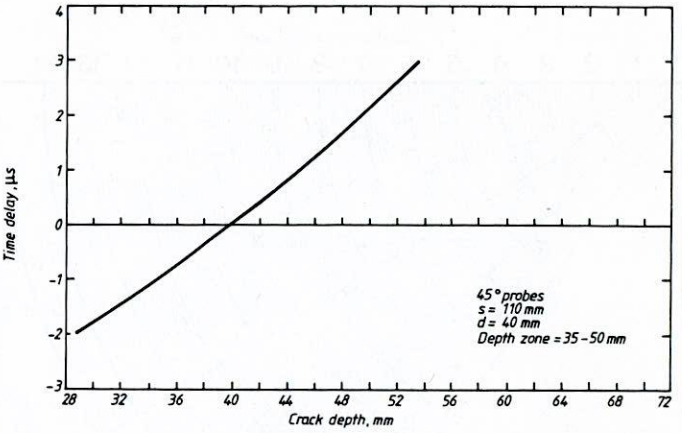

Document G1
Fig.12. Calibration curve.

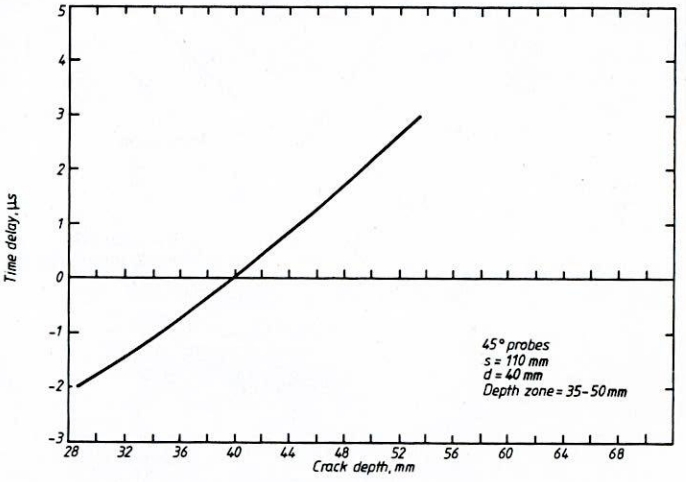

Document G1
Fig.13. Calibration curve.

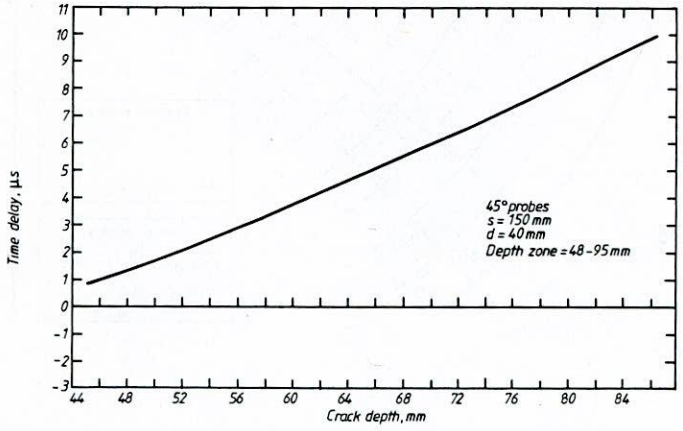

Document G1
Fig.14. Calibration curve.

THE TRANSPORTATION RESEARCH BOARD is an agency of the National Research Council, which serves the National Academy of Sciences and the National Academy of Engineering. The Board's purpose is to stimulate research concerning the nature and performance of transportation systems, to disseminate information that the research produces, and to encourage the application of appropriate research findings. The Board's program is carried out by more than 250 committees, task forces, and panels composed of more than 3,100 administrators, engineers, social scientists, attorneys, educators, and others concerned with transportation; they serve without compensation. The program is supported by state transportation and highway departments, the modal administrations of the U.S. Department of Transportation, the Association of American Railroads, and other organizations and individuals interested in the development of transportation.

The Transportation Research Board operates within the Commission on Sociotechnical Systems of the National Research Council. The National Research Council was established by the National Academy of Sciences in 1916 to associate the broad community of science and technology with the Academy's purposes of furthering knowledge and of advising the Federal Government. The Council operates in accordance with general policies determined by the Academy under the authority of its congressional charter of 1863, which establishes the Academy as a private, nonprofit, self-governing membership corporation. The Council has become the principal operating agency of both the National Academy of Sciences and the National Academy of Engineering in the conduct of their services to the government, the public, and the scientific and engineering communities. It is administered jointly by both Academies and the Institute of Medicine.

The National Academy of Sciences was established in 1863 by Act of Congress as a private, nonprofit, self-governing membership corporation for the furtherance of science and technology, required to advise the Federal Government upon request within its fields of competence. Under its corporate charter the Academy established the National Research Council in 1916, the National Academy of Engineering in 1964, and the Institute of Medicine in 1970.

TRANSPORTATION RESEARCH BOARD
National Research Council
2101 Constitution Avenue, N.W.
Washington, D.C. 20418

ADDRESS CORRECTION REQUESTED